NASA Contractor Report 4038

Development of the 15 Meter Diameter Hoop Column Antenna

A Final Report

Harris Corporation
Melbourne, Florida

Prepared for
Langley Research Center
under Contract NAS1-15763

National Aeronautics
and Space Administration

**Scientific and Technical
Information Branch**

1986

15-METER HOOP COLUMN ANTENNA DEPLOYED IN NEAR FIELD TEST FACILITY

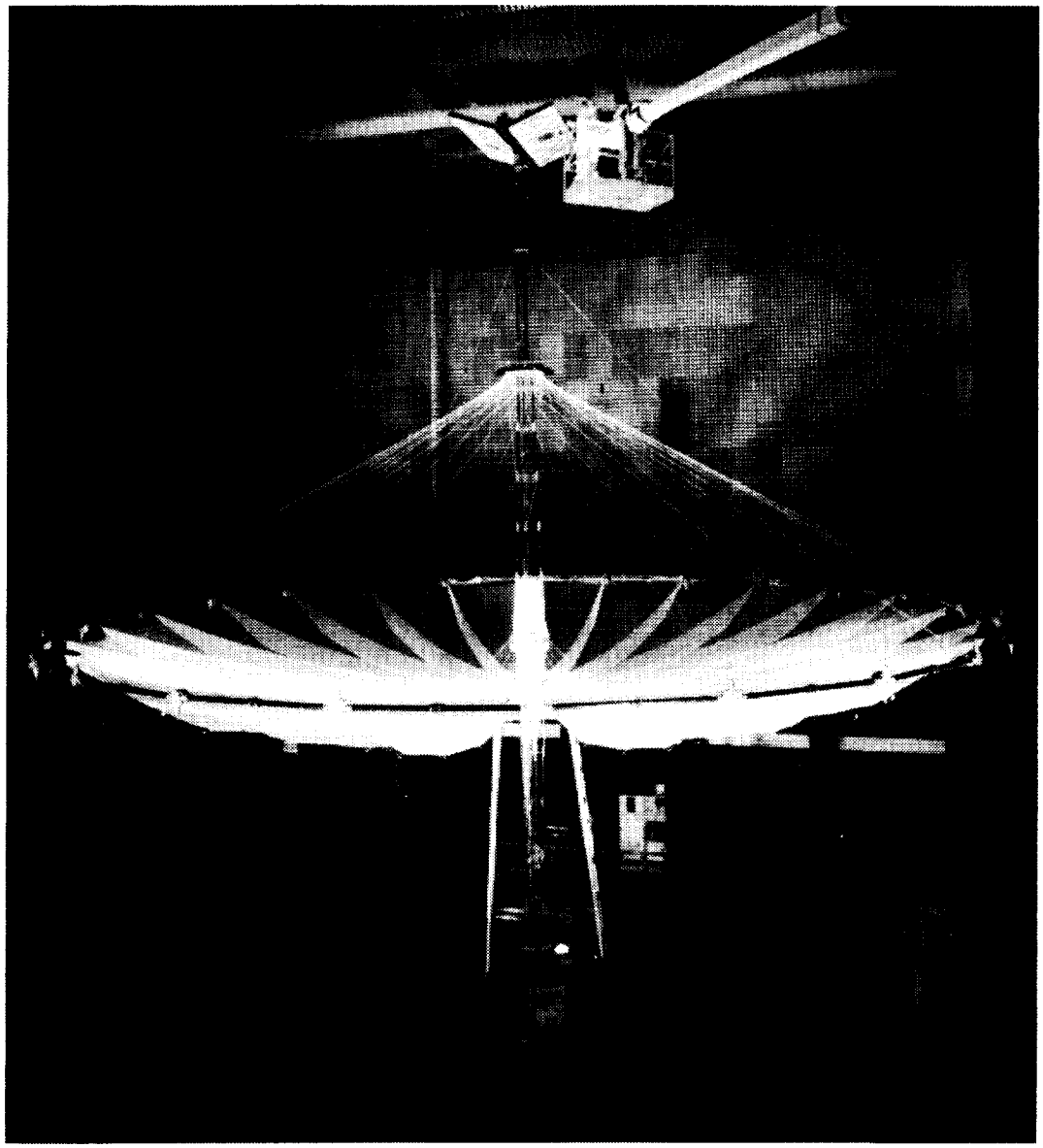

TABLE OF CONTENTS

TABLE OF CONTENTS (Continued)

LIST OF APPENDICES

1.0 INTRODUCTION

1.1 Program Background

It was recognized by the NASA community over ten years ago that many future space missions would involve large antennas. These large antennas (50-300 meters) would be utilized as earth communications devices, radio astronomers, or radiometers. For the past ten years, Harris and NASA/Langley have been working jointly on the development of the Hoop/Column Antenna. The Hoop-Column concept was chosen as baseline for this study because it possesses the following outstanding features:

- The antenna stows in a compact package.
  The 15 meter diameter Hoop-Column stows to a diameter of less than one meter.
- The antenna is lightweight.
  All structural members are tension/compression. (i.e. no bending) The 15 Meter Hoop Column weighed only 530 lbs despite being designed with high margins to withstand ground testing loads.
- The structure has zero backlash.
  All structure is preloaded subsequent to deployment and therefore there is no backlash or "dead band" in the system. This is a salient point when dealing with large structures possessing large numbers of joints.

Another key feature of the antenna is its quad aperture surface. The quad aperture concept, chosen for its RF simplicity, has the overall effect of transforming the system into one which operates as four offset antennas. The quad aperture approach was a technical as well as a manufacturing challenge because of load and geometry uniqueness of each quadrant gore.

The primary objective of the program was the development of the technology necessary to design, manufacture, deploy, evaluate and transport the Hoop/Column reflector by means of a ground-based test program. The program was consequently comprised of the following six tasks:

Task 1: Preliminary Design and Performance

The development of system level performance requirements and specifications as well as the system design, analysis, and tradeoffs.

Task 2: Materials Development

The identification, development, and recommendation of the cable/cord material to be utilized on the Hoop/Column Antenna.

Task 3: Advanced Concepts

The investigation of technical areas where study results may be used in the application of the Hoop/Column to a specific mission.

Task 4: Economic Assessment

The development of an economic system model suitable for quantitatively evaluating program size/performance/cost relationships.

Task 5: Demonstration Models and Full Scale Elements

The design and fabrication of demonstration models which verify specific technical aspects, whether mechanical or RF, of the Hoop/Column concept.

Task 6: 15-Meter Engineering Model

The design, fabrication, and testing of a 15-meter diameter model of the Hoop/Column Antenna.

All six tasks have been successfully completed. Specific results of tasks 1 through 5 may be reviewed in NASA Contractor Report 3558 as well as the "Large Space Antenna Systems Technology" publications of the annual technical reviews held since 1978. This report documents the Task 6 results.

The ground development of the 15-meter Hoop-Column Antenna marks a key milestone in the NASA Large Space Systems Program. It demonstrates that large antenna systems are feasible alternatives to smaller ones requiring higher RF power inputs for an equivalent useful output.

The primary objectives of the 15 Meter Hoop Column were to understand and verify the deployment, manufacturing, and contour analytical aspects of the generic concept.

1.2 Scope

The purpose of this report is to describe the work performed under NASA contract NAS1-15763, Task 6, 15-Meter Engineering Model. The focus of the report is to provide a detailed description of the 15 meter Hoop-Column Antenna major subassemblies and a history of its fabrication, assembly, deployment testing, and measurement results.

2.0 MODEL DESCRIPTION

The 15-meter diameter Hoop-Column Antenna is a proof of concept scale model based on the 100 meter diameter point design defined in Task 1. The 15-meter diameter was selected so that the model could be built and tested in existing manufacturing, RF, and thermal-vacuum facilities.

As shown in Figure 2.0-1, the primary structural elements of the antenna are the telescoping column which deploys from the central pedestal supported hub, and the hoop. As shown in Figure 2.0-2, the hoop consists of 24 jointed segments that support the periphery of the reflective surface. The hoop is connected to the column by cables that emanate from the upper and lower column extremities.

The reflective surface, which is also supported at the hub, is shaped by a network of cables that emanate from the lower column extremity.

The stowed antenna depicted in Figure 2.0-3, forms a compact package 2.7 meters in height and 0.92 meters in diameter. Deployment of the

15-METER HOOP COLUMN ANTENNA STRUCTURE

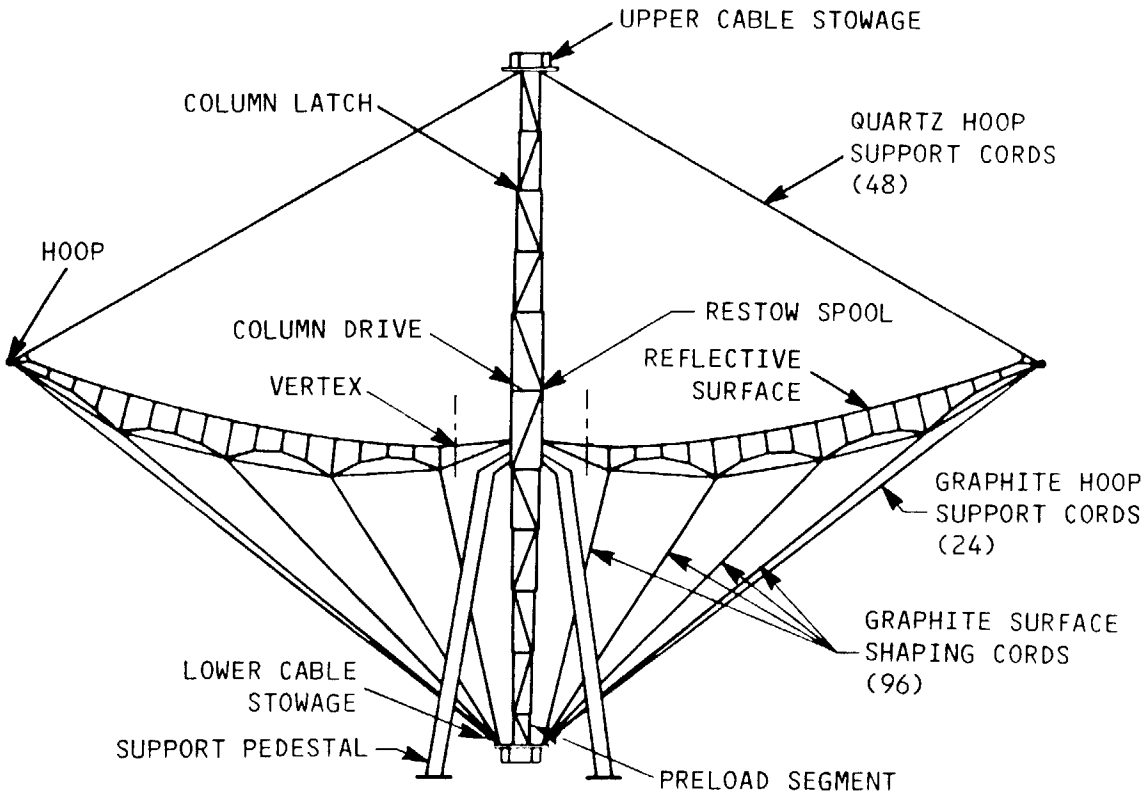

Figure 2.0-1.

The rigid Hoop-Column structure supports the reflective mesh surface.

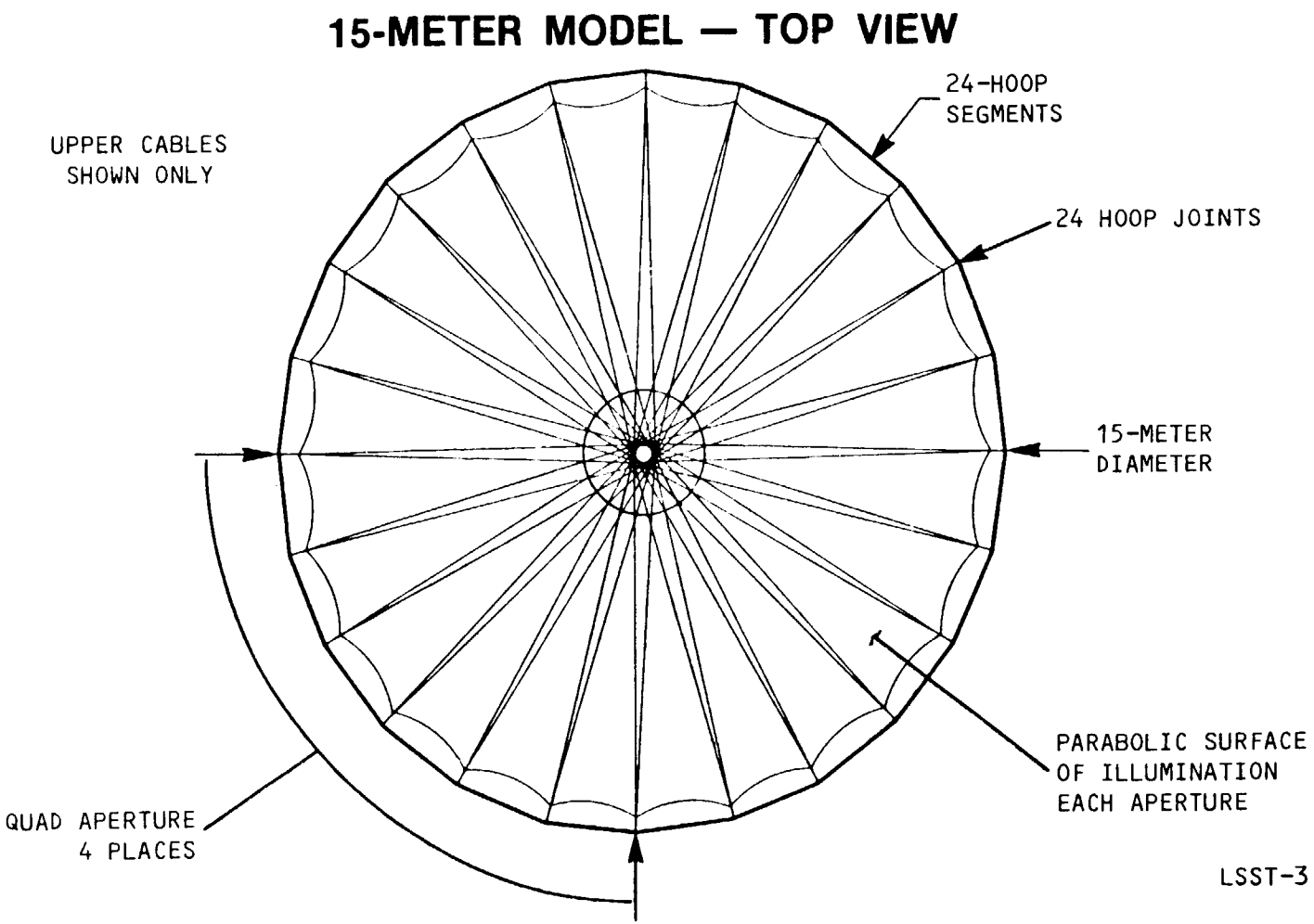

Figure 2.0-2.

Twenty-four hoop segments support the antenna surface.

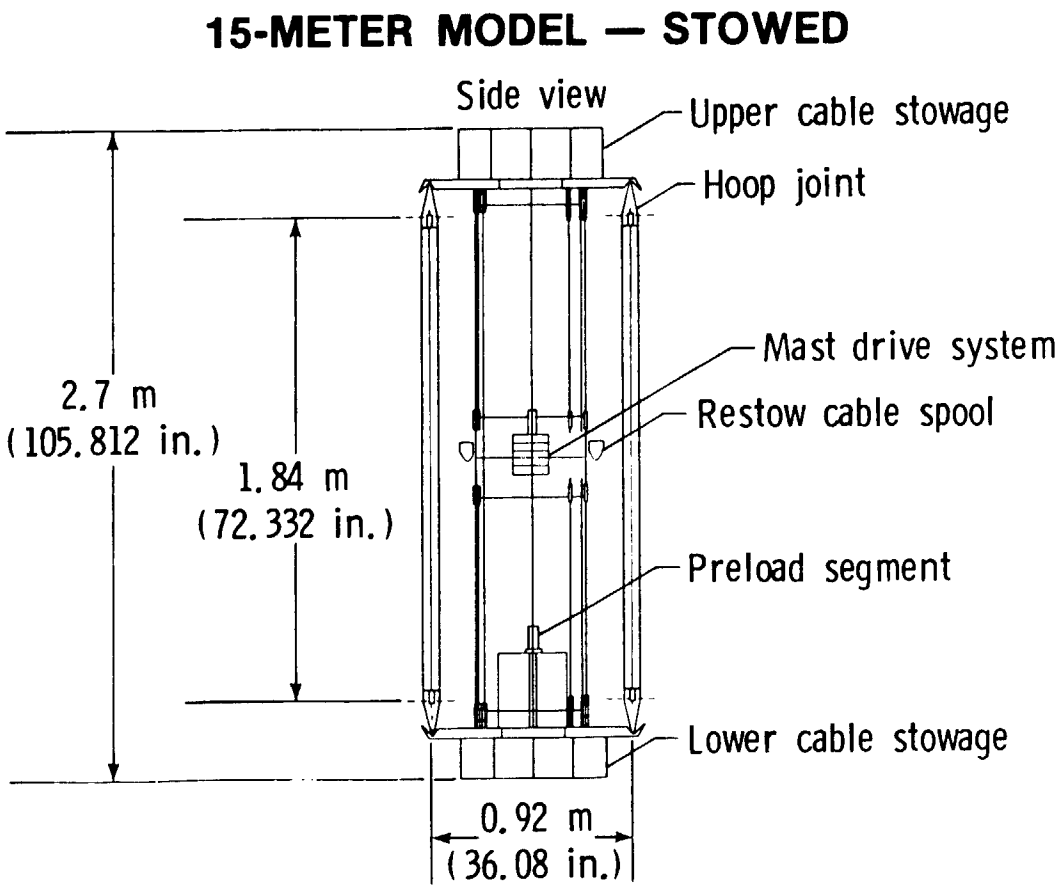

Figure 2.0-3.

The stowed hoop-column antenna forms a compact package.

antenna is accomplished in three steps: column extension; hoop-surface deployment; and extension of the preload segment, which by tensioning the cords, precisely locates the hoop and shapes the reflective surface.

All of the system deployment operations may be reversed by reversing the regulated 28 Vdc power sources in the control console. The various deploy-complete and stow-complete limit switches are "polarity smart" in that the opposite function switches are out of circuit when not in use. Switch selection is accomplished automatically by diode bridges across each switch. The electrical circuits and control panel are NASA designs. Data is available from NASA-Langley on these designs.

The following sections describe the individual components of the design and their operation.

2.1 Column

The column is a sequentially deployed, cable driven, telescoping, triangular truss unit with diagonals. The column, which is symmetrical about the center hub, extends simultaneously in both directions from the hub. This is shown in Figure 2.1-1.

2.1.1 Segments

A typical column segment is shown in Figure 2.1.1-1. The longerons, circumferentials and diagonals are tubular members. Diagonal member direction is reversed from segment to segment to minimize rotational deflections induced by compressive load.

2.1.2 Column Drive System

The Column Drive System (CDS), (Figure 2.1.2-1) consists of two large triangular plates separated by spacer brackets located directly in line with the column longerons and houses a drive motor and cable drum. This unit is located at the geometric center of the column and provides the forces necessary to deploy and stow the counter-balanced column system. The Drive System provides an additional load to the column at the final stage of deployment to assure proper column segment latching. This load is relieved upon completion of the column deployment.

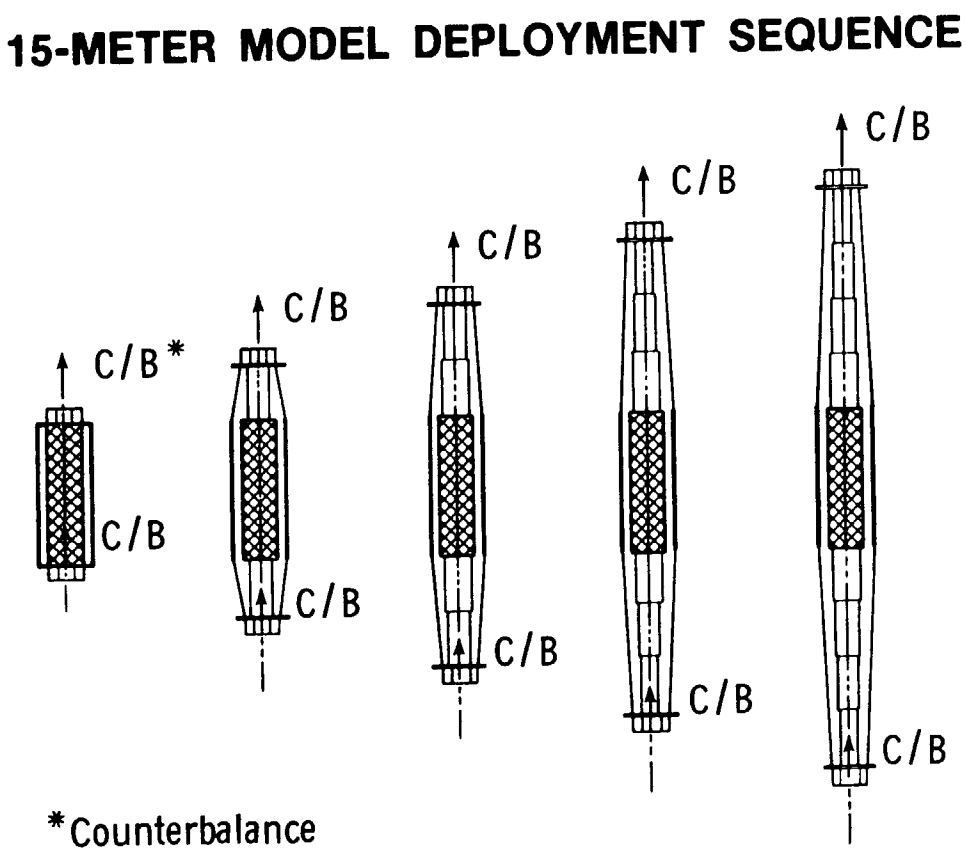

Figure 2.1-1.

The central column uses a system of cables and pulleys to pull the telescoping segments sequentially into the deployed and latched configuration.

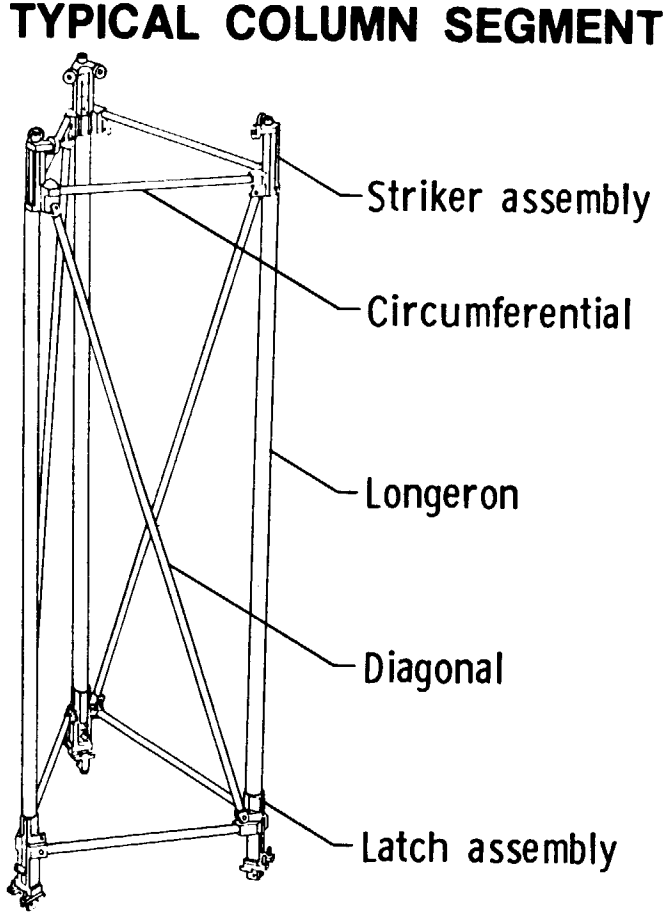

Figure 2.1.1-1.

The basic column segment is a space truss of triangular sections composed of tubular elements.

COLUMN DRIVE SYSTEM

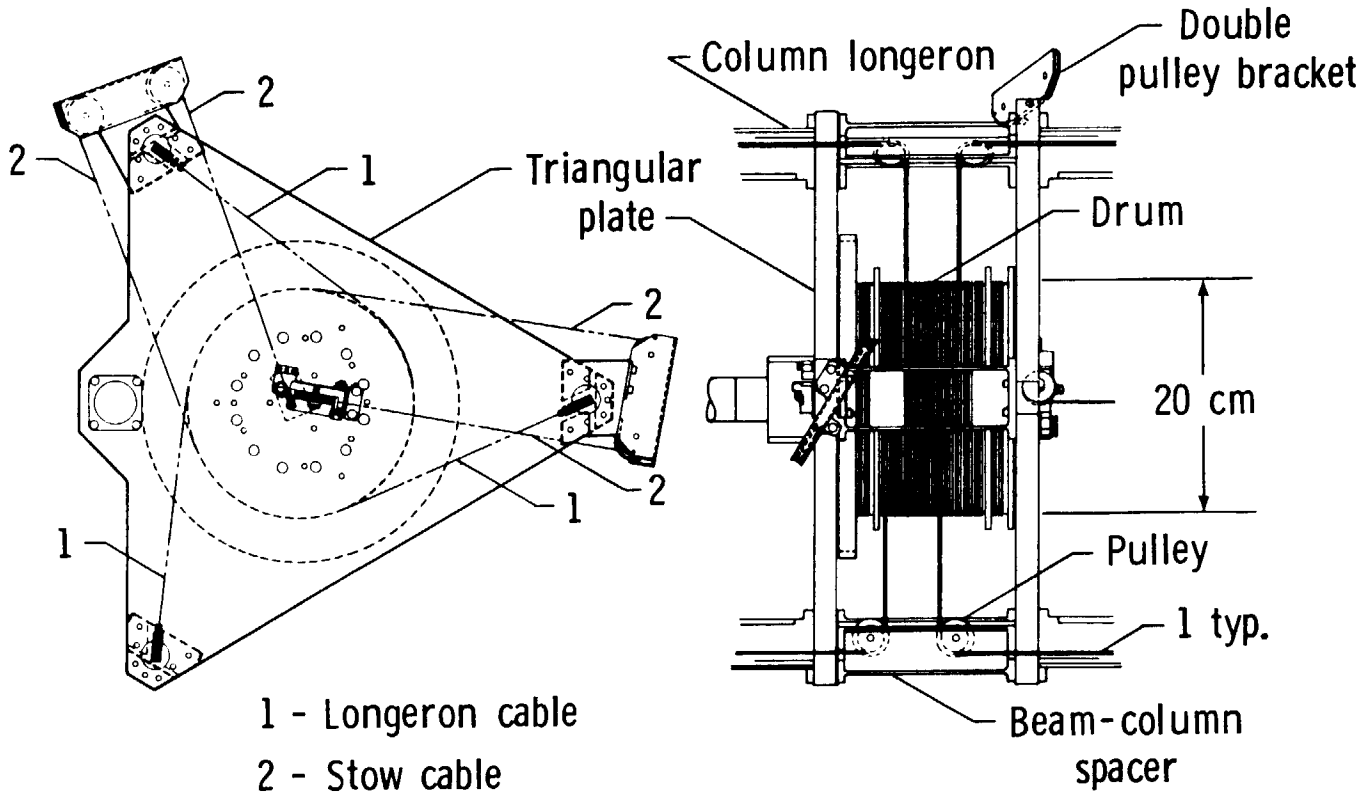

Figure 2.1.2-1.

The Column Drive System (CDS) automatically extends and latches the segments for deployment; unlatches and retracts segments for storage.

Deployment of the column is accomplished by retrieving the deployment cables onto a threaded drum. There are six (6) deployment cables which are fed through each of the longerons of each column half from the drum to a single pulley on the spacer brackets which in turn directs the cable through the longerons (Figure 2.1.2-2). When the cable reaches the end of the longeron, away from the cable drive mechanism, it turns 180° over a pulley in the striker housing and proceeds (between the longerons) toward the cable drive mechanism to the second longeron. It is then intercepted by another pulley located in the latch housing of the adjacent telescoping section and turns 180° to proceed up the inside of this longeron to the second striker housing. This pattern is repeated until the cable has been fed through all four deployable longerons on each column half. A schematic of this routing is shown in Figure 2.1.2-3.

The stow cables are attached to the latch actuation arms on the outermost telescoping sections through a bridle unit. These cables are routed down along the column centerline and through the drum to a pulley attached to the opposite triangular plate. These pulleys direct the cables to the beam spacer brackets containing dual pulleys, each turning the cable 90°. This brings the cables to the threaded drum and cam portion of the mechanism. Both stow cables have a small residual tensile load applied during the deployment and stow phases. Upon full deployment, hi-lift cams relieve the residual tension loads in the stow cables, thereby allowing them to go slack. This feature is necessary for proper latching of the outermost sections because the stow cables are attached to the latch pawl of these sections and latching cannot occur while the cables are in tension.

The cable drum is suspended between ball bearings attached to the triangular base plates. Drum rotation is accomplished by a 28 Vdc gear motor connected to a pinion and gear system mounted on the upper triangular plate. Drum backdriving is resisted by the gear motor.

2.1.3 Column Latch

The latch (Figure 2.1.3-1) is comprised of two assemblies located on the ends of the column longerons on each segment. The assembly located on the outermost end of the longeron of each telescoping segment is called the striker assembly and contains the pawl striker plate. Active latching elements are

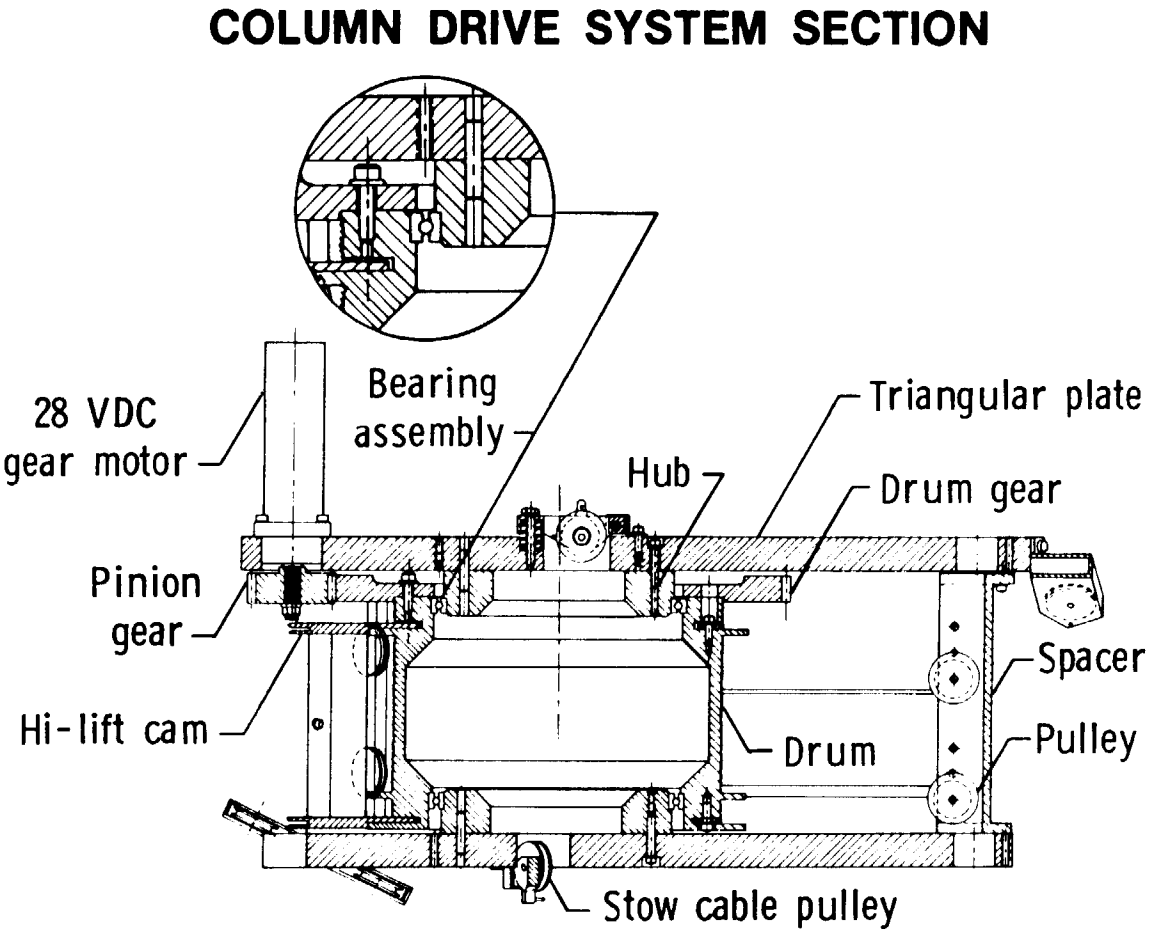

Figure 2.1.2-2.

A side view of the CDS shows the pulleys used to redirect cables between the vertically-oriented longerons and the horizontally oriented drums.

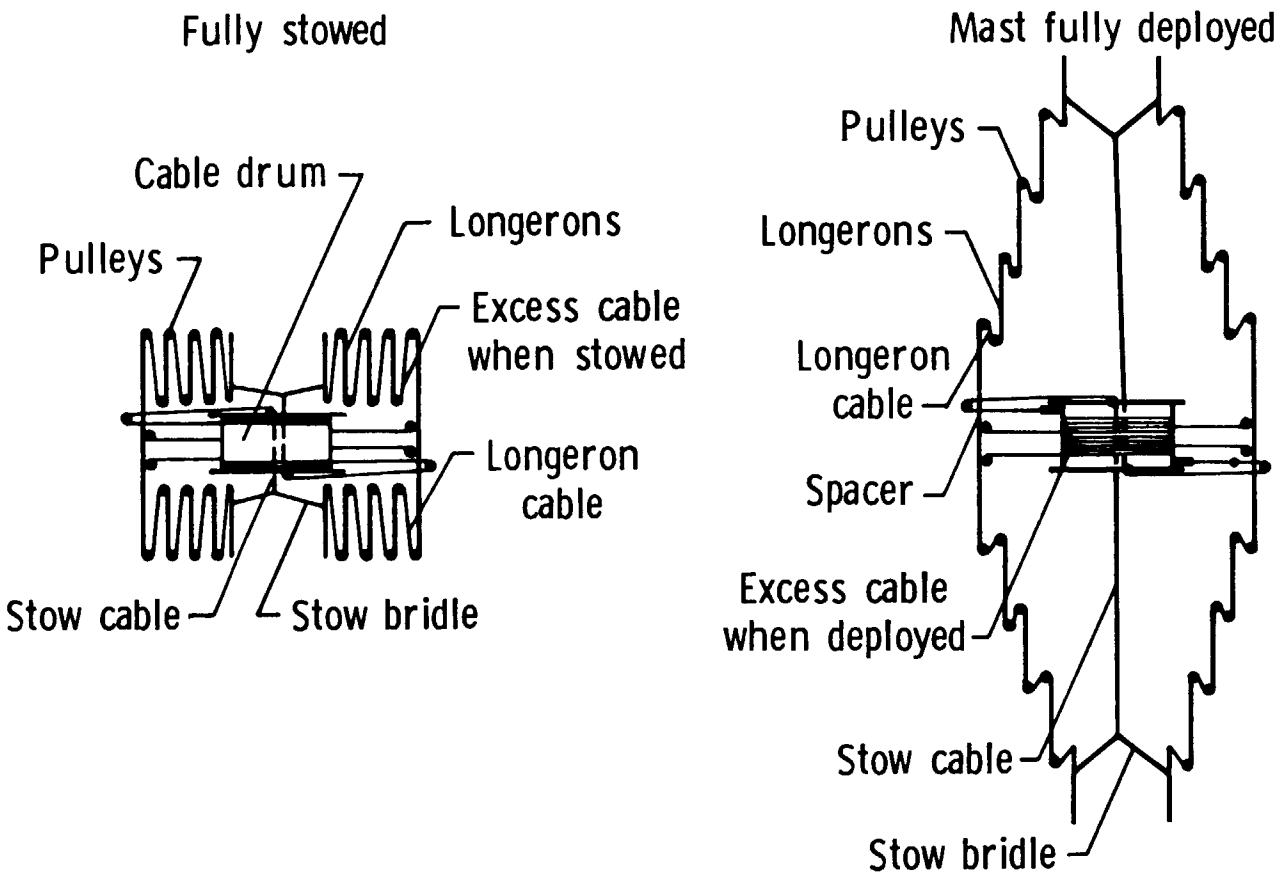

Figure 2.1.2-3.

The drive system of the column allows both deployment and storage to be accomplished with lightweight cables loaded only in tension.

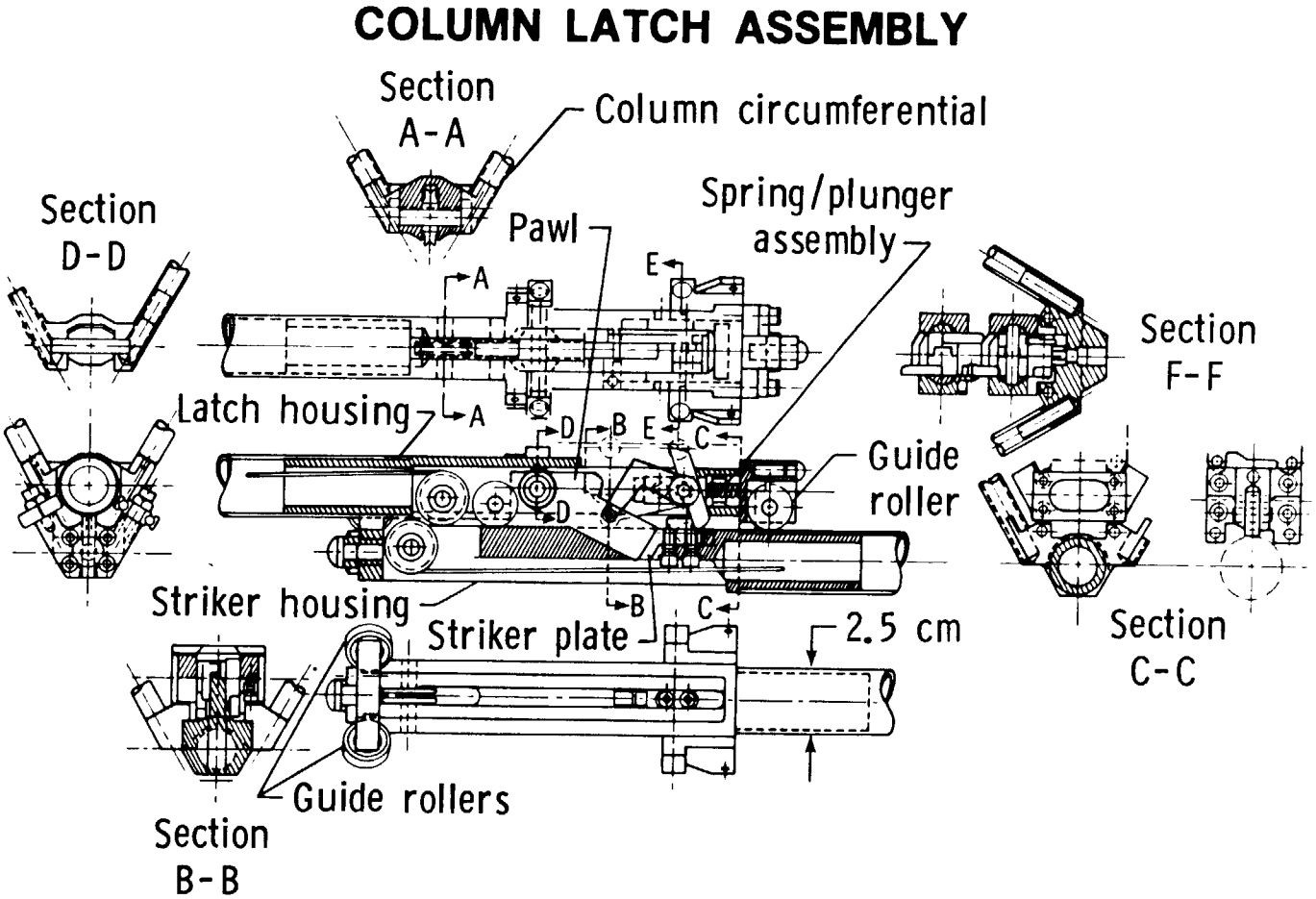

Figure 2.1.3-1.

The column latch assembly consists of a striker housing on the top of the reference longeron and a latch housing on the bottom of the next longeron to deploy.

contained in a latch housing located on the inner end of the telescoping column segments. The latch provides a continuous load path along the longerons without introducing excessive bending moments into the longerons. Both latch and striker housings contain rollers that ride on the longerons to guide the deploying segments. When deployment is initiated, the motor, pinion, and gear arrangement rotates the CDS cable drum such that the deployment cables threaded through the longerons are collected on the drum. This translates the inboard column segments away from the CDS, thereby allowing the latching actuation lever to come into contact with the deployment trip roller which trips the pawl and latches the assembly. All telescoping segments deploy as a unit because the pawl cam does not allow the stowage roller to advance until the pawl is latched into place (Figure 2.1.3-2). The next segment release begins when the pawl cam rotates away from the stowage roller (Figure 2.1.3-3). The pawl and lever arrangements are over center devices held in place by the spring/plunger assembly. It can be seen that the pawl has total control over the deployment sequence and that no additional mechanisms are required to maintain that control.

The pawl seats against the striker plate as shown in Figure 2.1.3-4 so that the normal force vector at the point of contact results in an opening moment, thus preventing binding. The cam profile also compensates for minor errors in the striker plate location. The design incorporates shims under the striker plate so that the deployed pawl angle can be adjusted prior to final column assembly. The cam feature allows the pawl to be prestressed to reduce the joint nonlinear motion by applying a large tensile force to the deployment cables located inside each longeron. The cable tension strains the latch housing and the pawl pivot to increase the distance between the latch/striker housing interface and the pawl pivot. Pawl rotation will continue because the spring/plunger assembly pushes it outward. When the cable tension is relieved, friction prevents the pawl from releasing.

2.2 Hoop

The hoop, when deployed, forms a rigid segmented ring around the column (Figure 2.2-1). It is precisely located at each of its 24 joint platforms by the hoop support cords and forms a rigid boundary to which the RF reflective surface attaches.

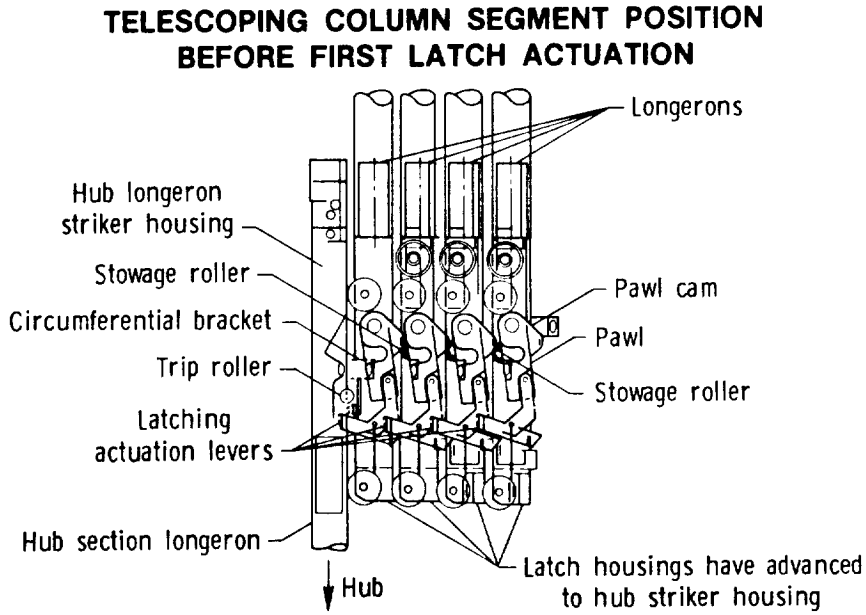

Figure 2.1.3-2. All deploying longerons move as a unit, until the outermost latch housing engages its mating striker housing and disengages from the remaining latch housings.

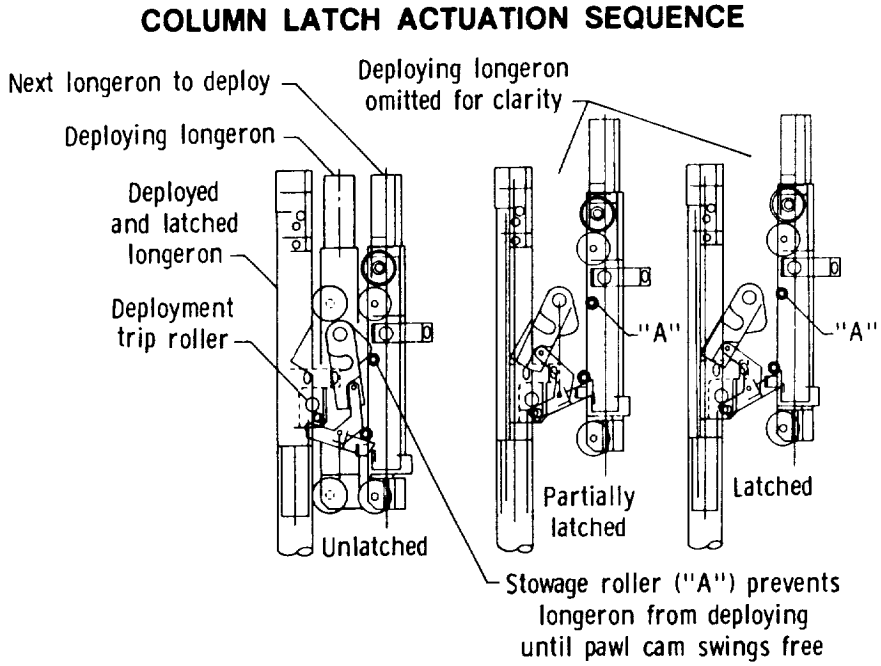

Figure 2.1.3-3. The sequential release of each longeron segment is completely controlled by the kinematic design of the rollers and levers on the striker and latch housing.

COLUMN LATCH UNIQUE FEATURES

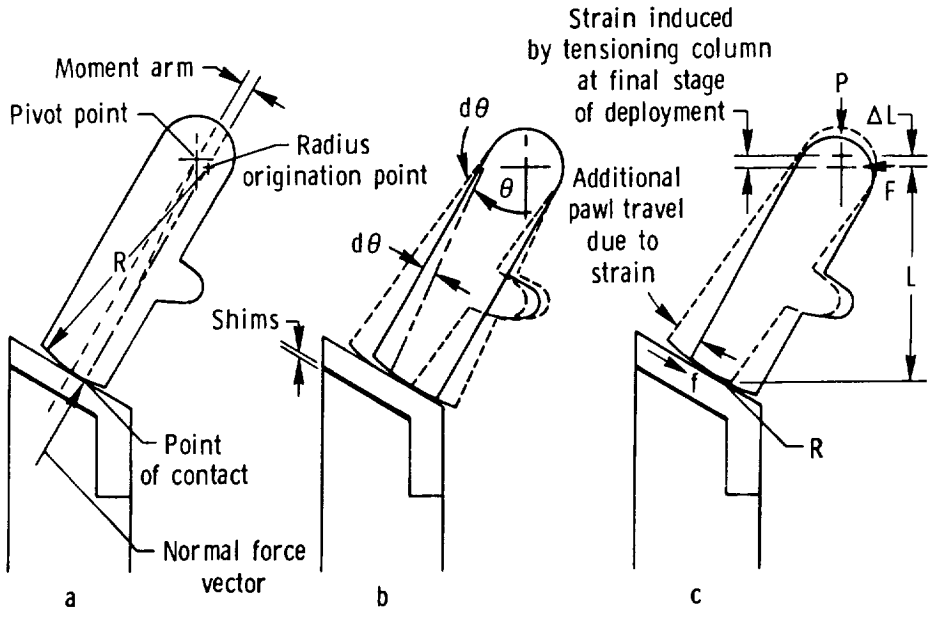

Figure 2.1.3-4.

The cam profile on the pawl seats against the striker plate, so that the normal force vector at the point of contact results in an opening moment, thus preventing binding.

To ensure a smooth and symmetrical deployment, each of the 24 joint platforms are kinematically linked to one another with synchronization rods (Figure 2.2-2) working in concert with the gears at each of the joints (Figure 2.2-3 and 2.2-4). Deployment energy for the hoop is supplied by eight 28 Vdc gear motors located 45° apart in the Hoop Joint Platforms (Figure 2.2-3). The gear motor is directly coupled to a worm which drives meshed sector gears on the ends of the hoop segments. This configuration provides a mechanical advantage of 35 to 1. During deployment, the synchronization rods, which are tension members only, maintain the joint platforms parallel to one another. Passive gears, at the 16 joint platforms without motors, transmit the necessary moment into the passive hoop segments and synchronization rods to deploy the hoop (Figure 2.2-4). The gear motors are connected through an active electronic control system which ensures symmetrical hoop deployment and stowage. Hoop deployment and stowage operations are terminated by limit switches at each gear motor location.

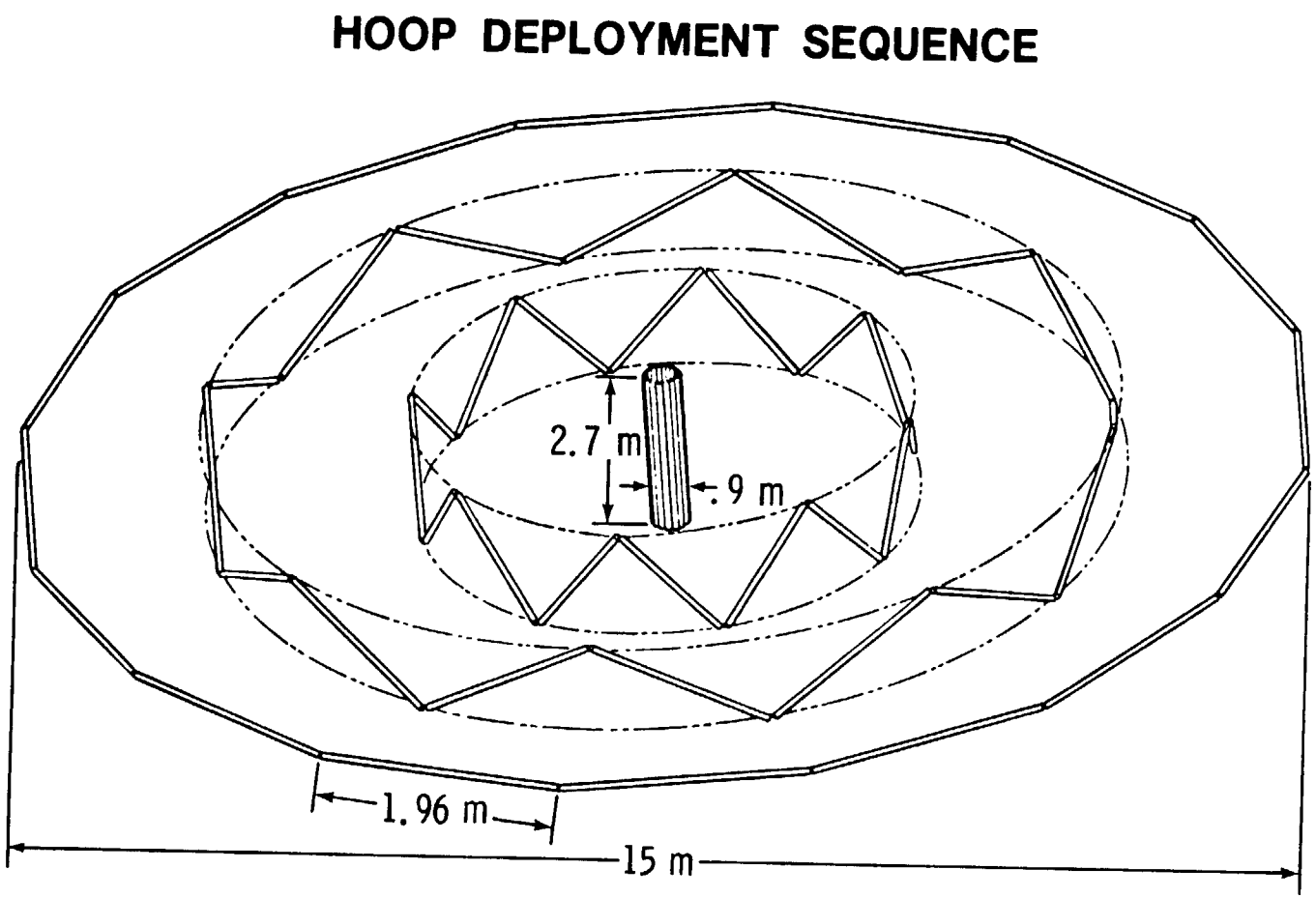

Figure 2.2-1.

The hoop deploys from the compact stowed package to its full 15 meter diameter.

HOOP SYNCHRONIZATION APPROACH

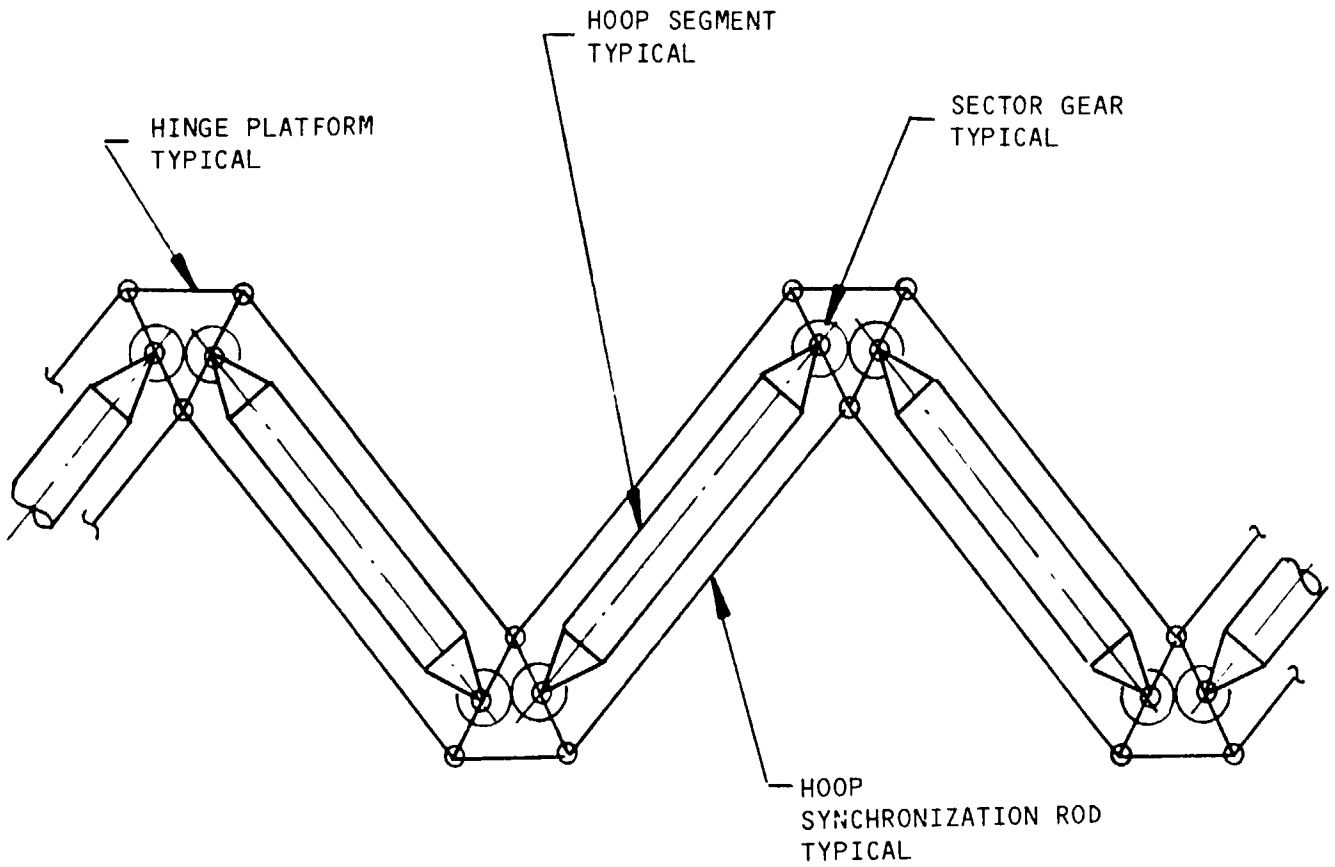

Figure 2.2-2.

Synchronization rods work in concert with the sector gears at the segment ends, providing uniform deployment.

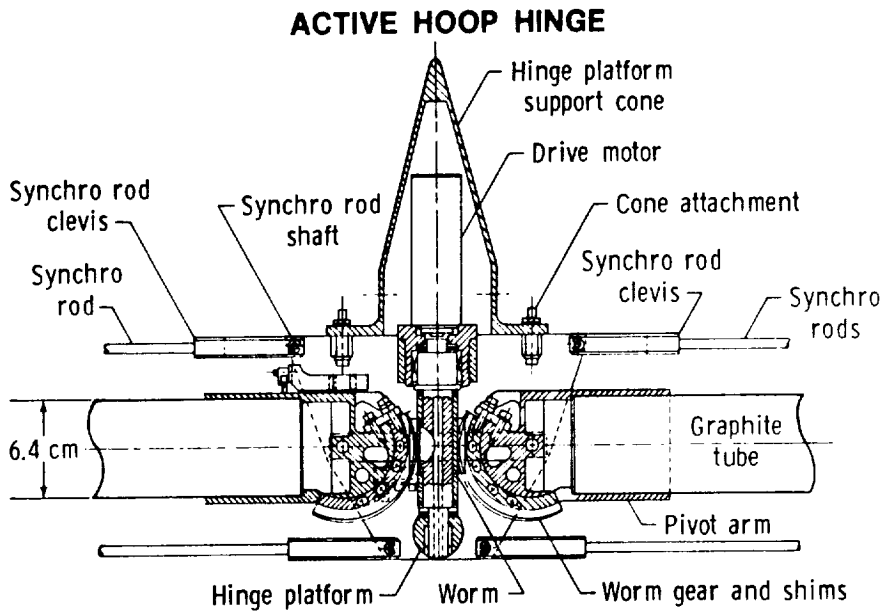

Figure 2.2-3.

Active hinges provide the energy to deploy and stow the hoop.

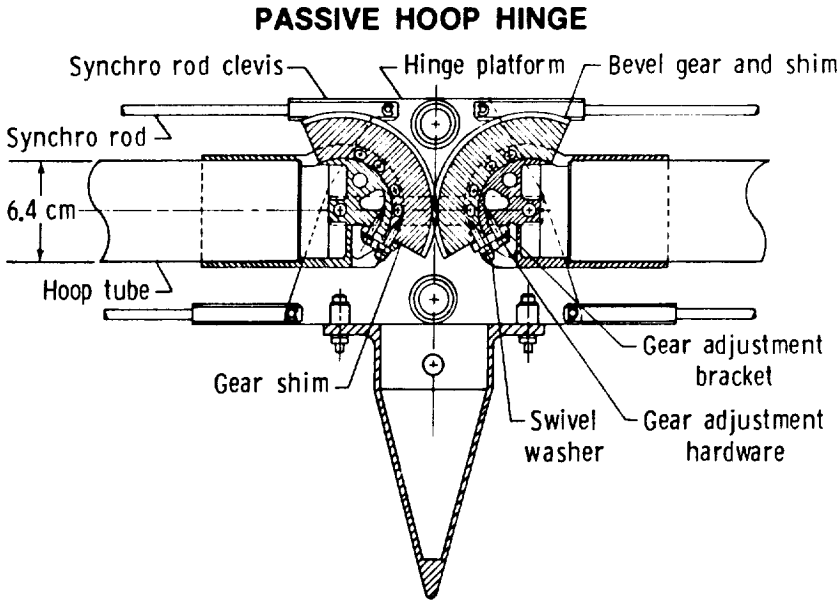

Figure 2.2-4.

Passive hinges maintain synchronization between hoop segments.

2.3 Preload Segment

The preload segment, attached to the lower end of the column, extends the column approximately 16 inches to its design length and pretensions the hoop and surface control cords (Figure 2.3-1).

A linear actuator, powered by a 28 VDC gear motor, drives the preload segment from the stowed to the deployed position (Figure 2.3-2). Screw loads are carried to the longeron through a triangular beam arrangement bonded to the inside of the longerons (Figure 2.3-3). The motor torque is translated to the column nodes through a thin flex plate. The plate is rigid in torsion, but can allow axial displacement to allow for motor mount tolerances. The screw is 0.625 inches in diameter with acme threads. Ball screws were considered but rejected because the low coefficient of friction would not prevent backdriving under load without a brake. Preload segment extension is terminated by limit switches with backup current limiting sensors.

2.4 Deployment Power Summary

Table 2.4-1 is a summary of the drive motors used on the antenna. All motors are 28VDC TRW Globe gear motors. These motors were chosen because of their availability and cost. Speed-Torque-Current curves are shown in Figures 2.4-1 and 2.4-2.

2.5 Antenna Surface

A quad aperture, parabolic surface design was selected for the 15 meter Hoop-Column Antenna. This design provides four distinct offset fed reflectors within one symmetric antenna. Each surface quadrant is illuminated by a separate feed assembly. The Hoop-Column concept is, however, capable of supporting other reflector geometries depending on individual mission requirements. Examples include center fed full parabolic, spherical, conical and flat geometries. The Hoop-Column concept allows this flexibility since the rigid hoop and column structures support the surface rather than shape it directly.

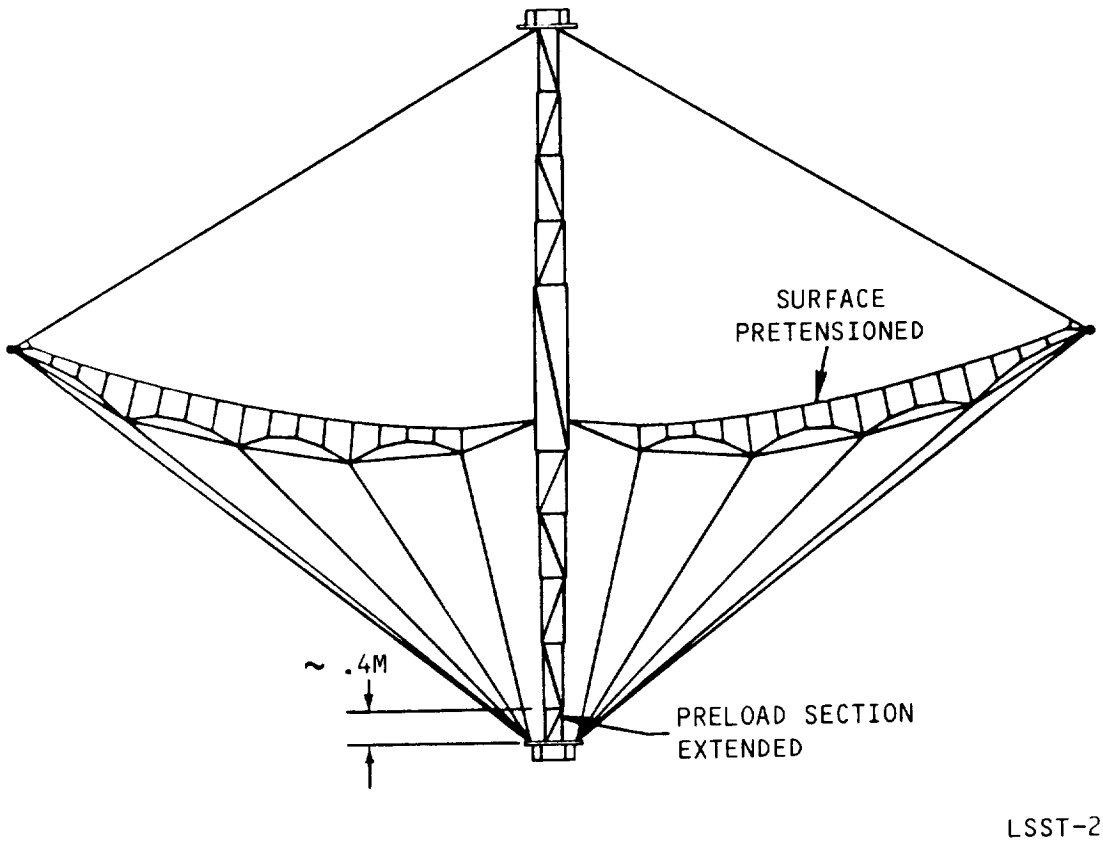

Figure 2.3-1.

The preload segment extends to tension the cord members between the hoop and column and to shape the surface.

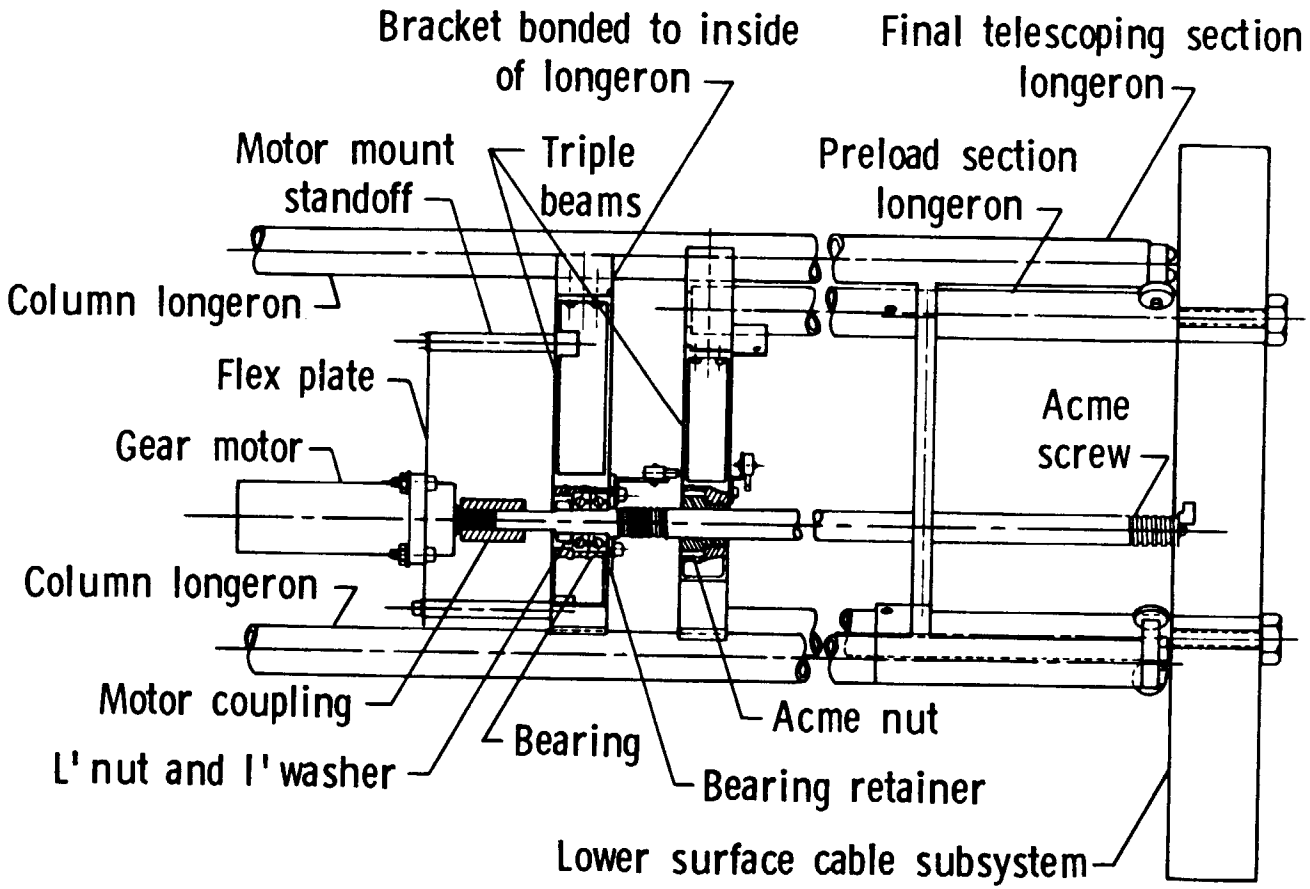

Figure 2.3-2.

The column preload segment is driven by a linear actuator which uses an acme thread and nut instead of a ballscrew to prevent back-driving under load.

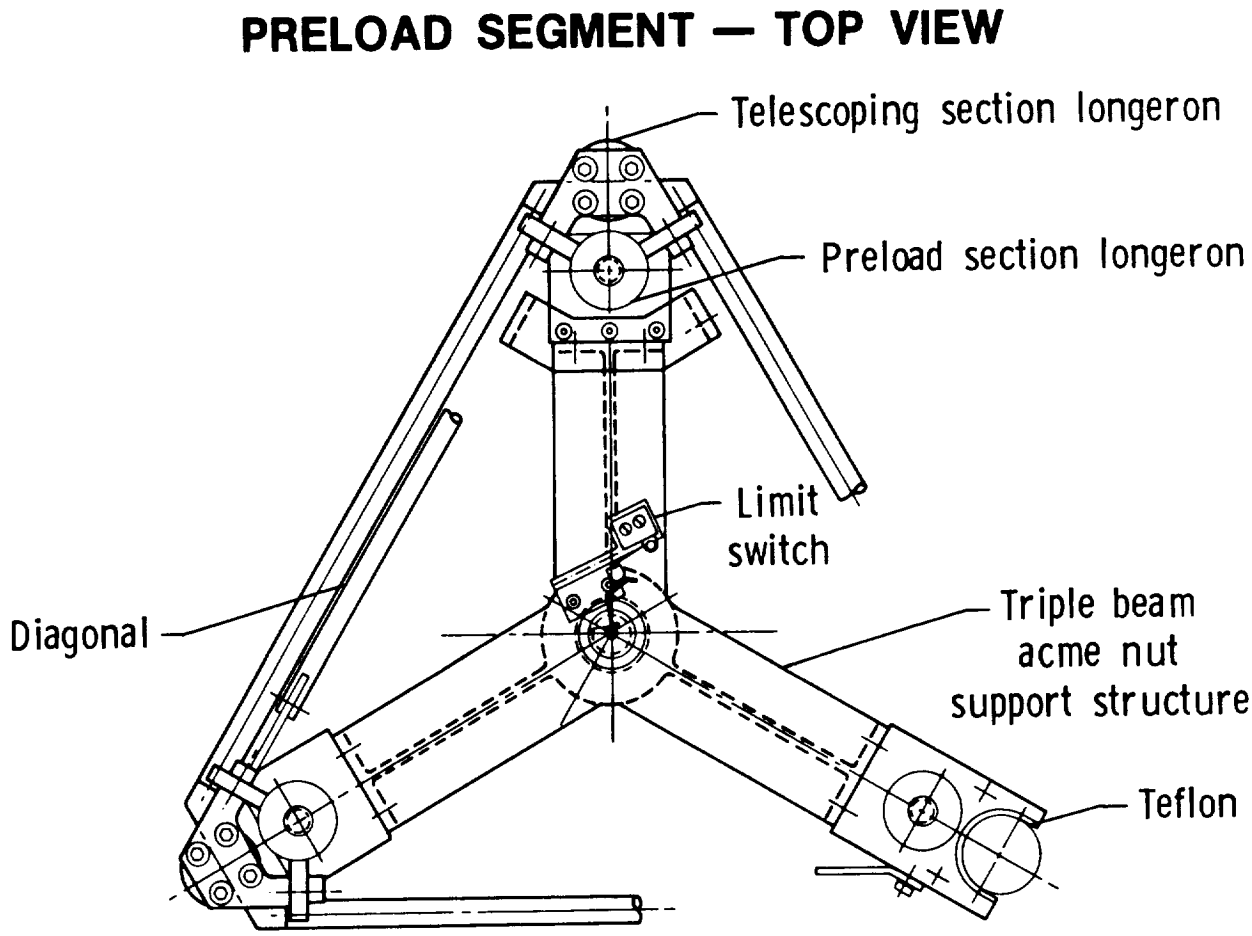

Figure 2.3-3.

Axial loads are transferred between the acme screw and the longerons through this yoke assembly.

Table 2.4-1.
Drive Motor Summary

TRW-Globe gear motors were selected for the hoop-column antenna.

FUNCTION	QTY	MOTOR PART NO.	REDUCTION	STALL TORQUE (IN LB)	STALL CURRENT (AMP)	MAX OPERATING CURRENT (AMP)
COLUMN DRIVE	1	102A202-11 TYPE BL	647/1	1015	11.8	1.5
HOOP DRIVE	8	311A228-8 TYPE JM	6621/1	854	2.8	.5
COLUMN PRELOAD	1	102A163-8 TYPE BP	170/1	243	15.0	2.8
MESH RESTOW	1	102A199-12 TYPE BL	211/1	276	7.4	.8

LSST-20

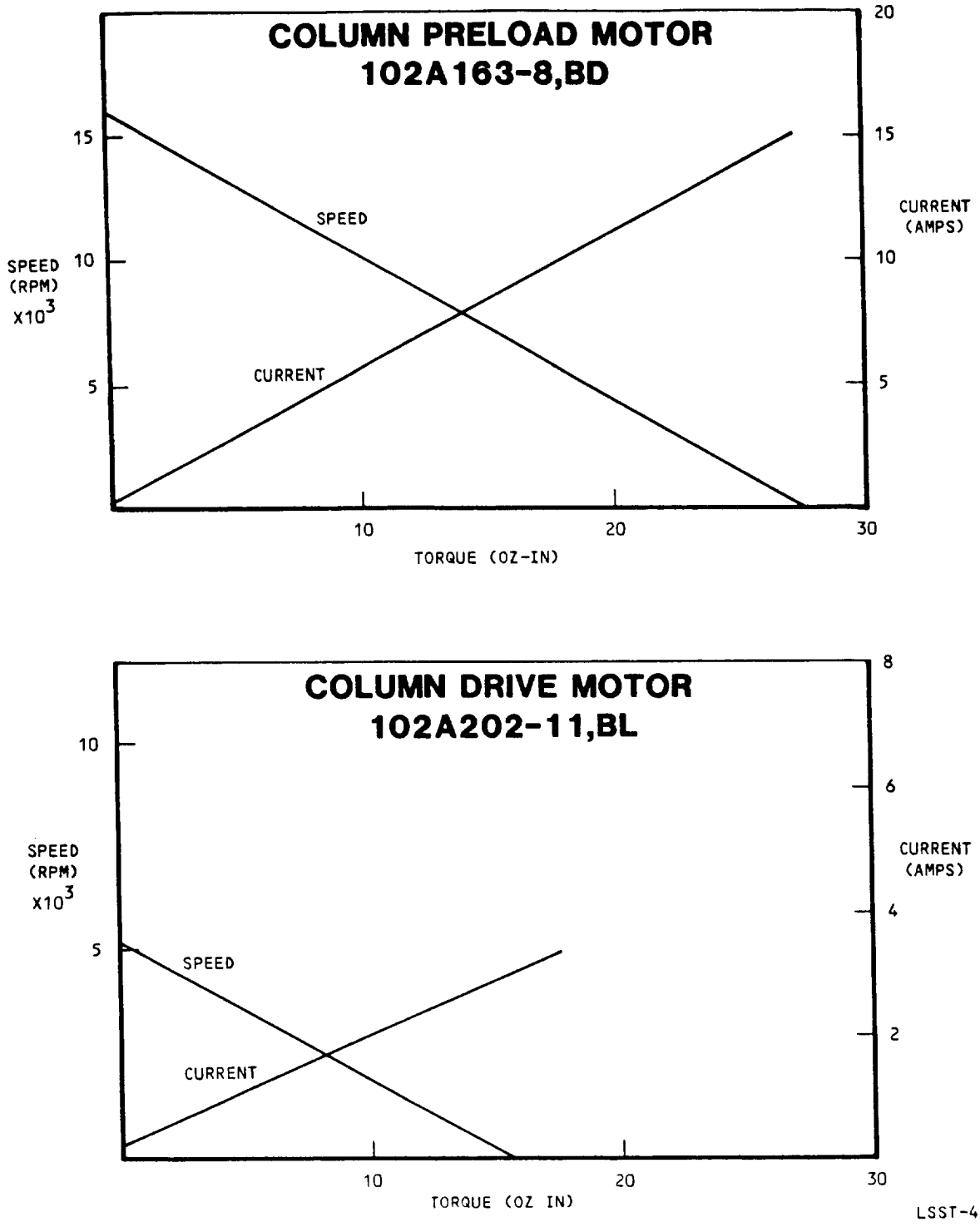

Figure 2.4-1.

The preload segment and column drive motors were selected to meet the torque requirements.

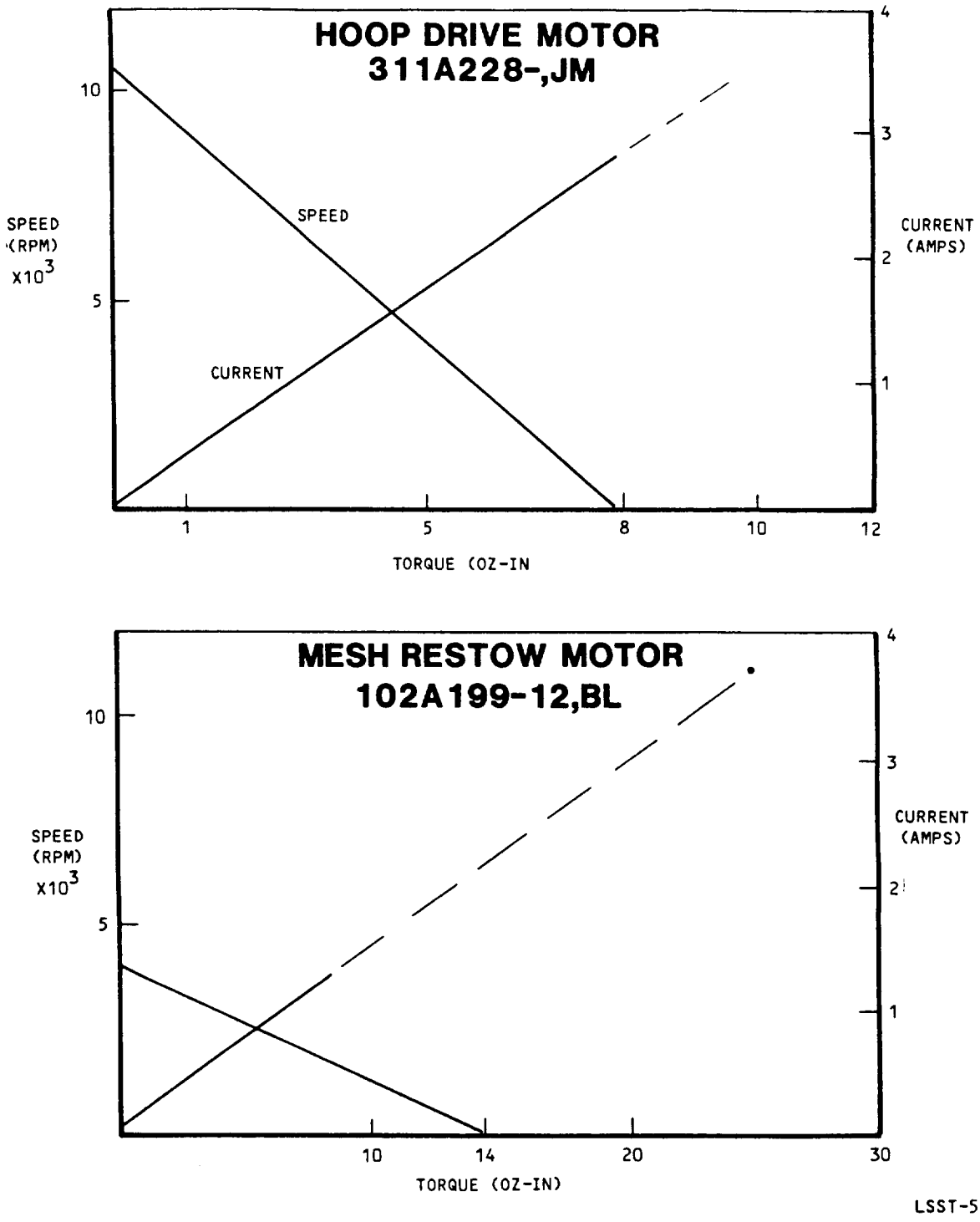

Figure 2.4-2.

The hoop and restow drive motors were selected to meet the torque requirements.

The contour of each quad aperture, shown in Figure 2.5-1, is given by:

$$Z = \frac{a^2}{2f} + \frac{r^2}{4f} - \frac{ra(\sin\theta + \cos\theta)}{2f}$$ where:

r = radius (inches)

a = 14.699 inches

f = focal length, 366.850 inches

θ = radius angle, degrees. $o \leq \theta \leq 90$

The vertex within the aperture is located at:

$r = a\sqrt{2} = 20.787$ inches.

$\theta = 45$ degrees.

During deployment and stowage of the hoop, the surface is supported by cables eminating from a drum located in the column hub. As shown in Figure 2.5-2, these cables are terminated at the hoop hinges. As the hoop deploys, additional cable is payed out off the drum allowing the tightly packed surface to unfold in a controlled manner.

Upon the completion of hoop deployment, the preload segment is extended and tensions the surface. The surface is rigidly attached to the hoop hinges but connected to the column hub through constant force negator springs.

The reflector surface is gold plated molybdenum wire tricot knit mesh and is supported and shaped by the structural elements depicted in Figure 2.5-3. These elements, being tension-only members were fabricated from flexible, thermally stable cords. Since rigid structure within the surface is not required to generate and maintain the desired contour, a considerable reduction in surface weight and bulk was accomplished. Each of the major structural elements that form the surface are described separately below.

2.5.1 Front Cord-Gore Assemblies

Each quadrant of the surface is assembled from six uniquely shaped gores. As shown in Figure 2.5.1-1, the mirror image symmetry about the mid-quadrant radial allowed the complexity of the geometry to be reduced.

SURFACE QUADRANT GEOMETRY

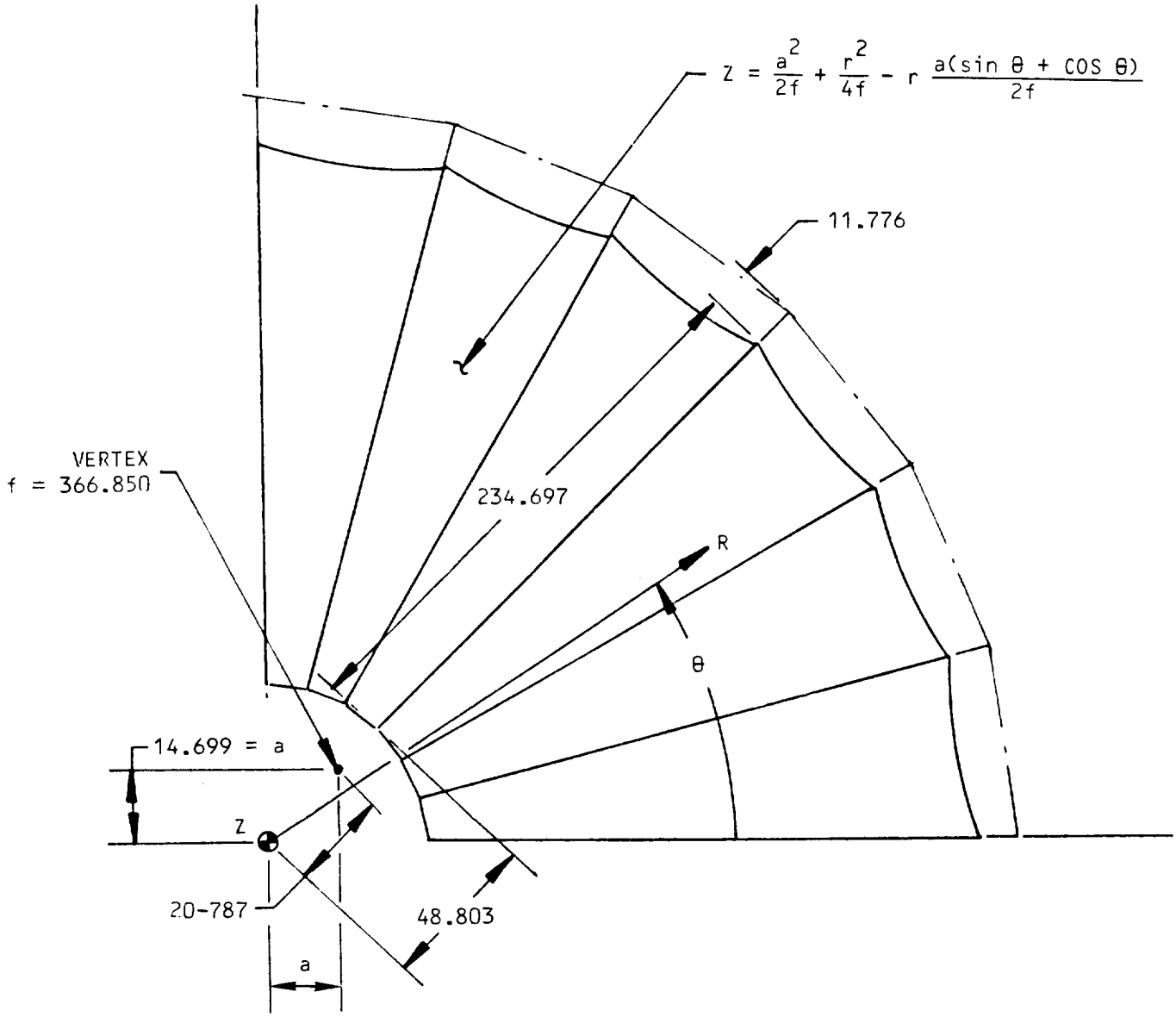

NOTE: ALL DIMENSIONS IN INCHES.

LSST-1001A

Figure 2.5-1.

The quad aperture surface geometry is described above in polar coordinates.

MESH RESTOW CORDS

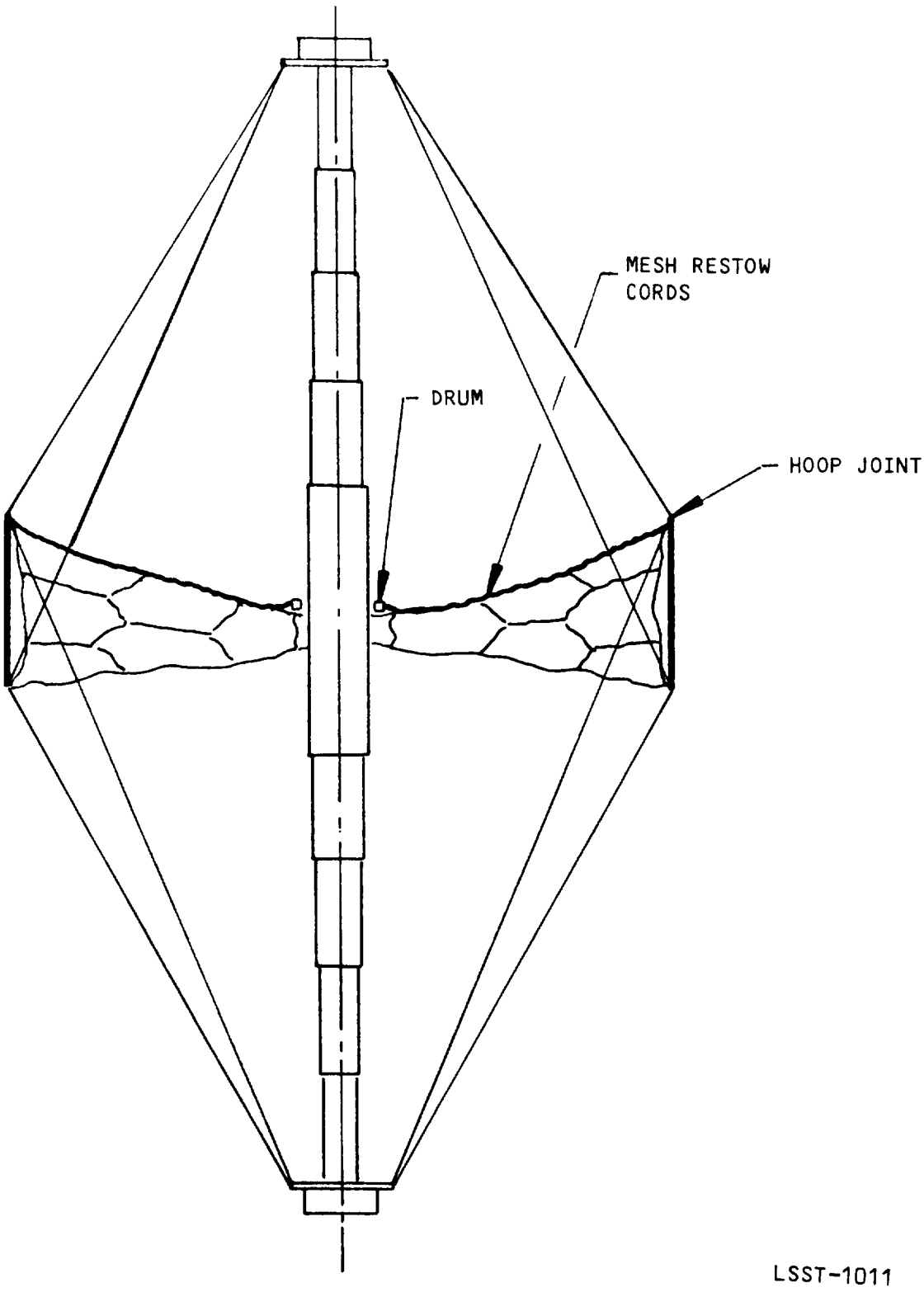

Figure 2.5-2.

The surface is supported by the mesh restow cords during deployment and stowage of the hoop.

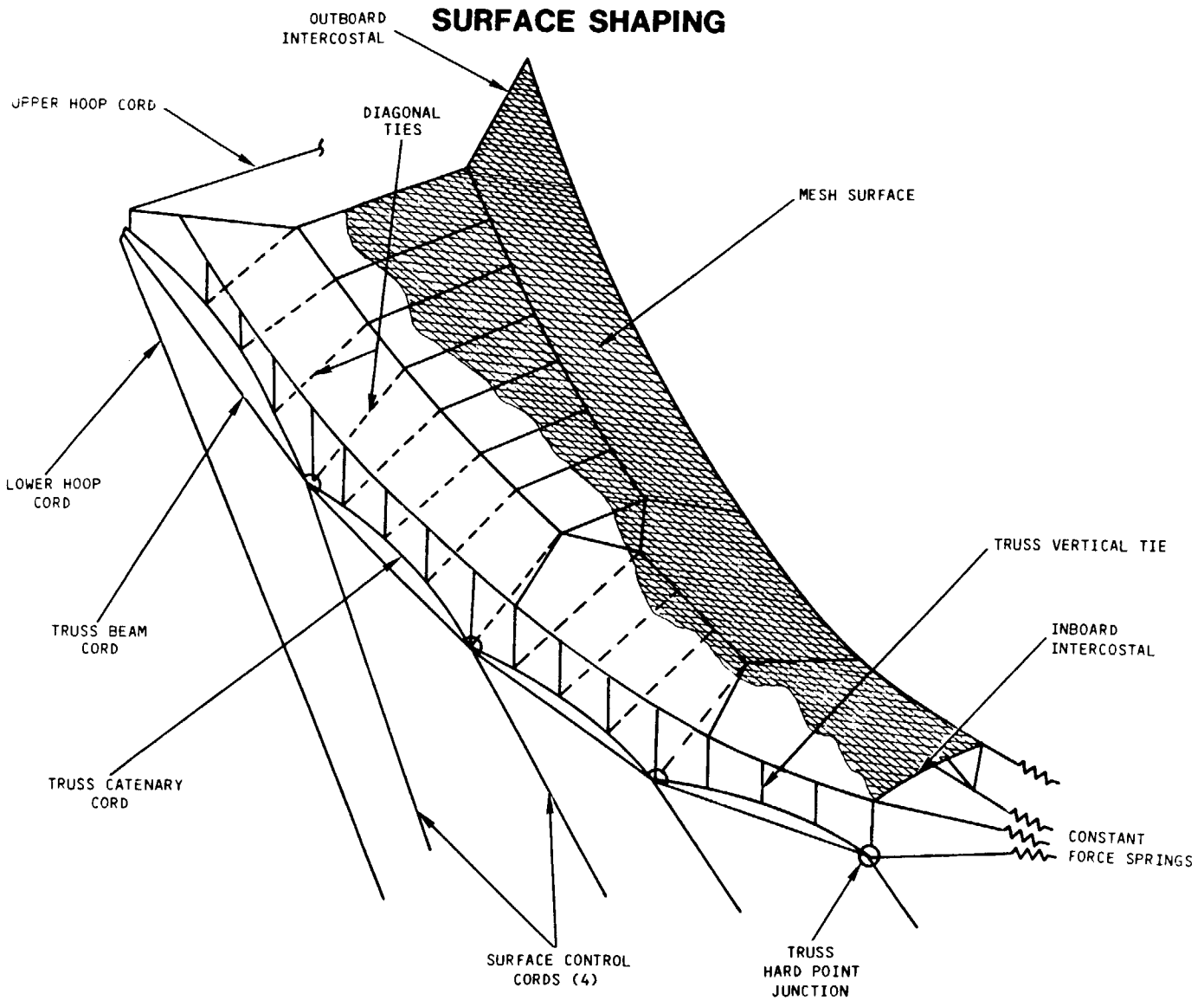

Figure 2.5-3.

The reflective mesh surface is shaped by this network of catenary cords and ties.

SURFACE GORE SYMMETRY

GORE	MIRROR IMAGE GORE
1	6
2	5
3	4

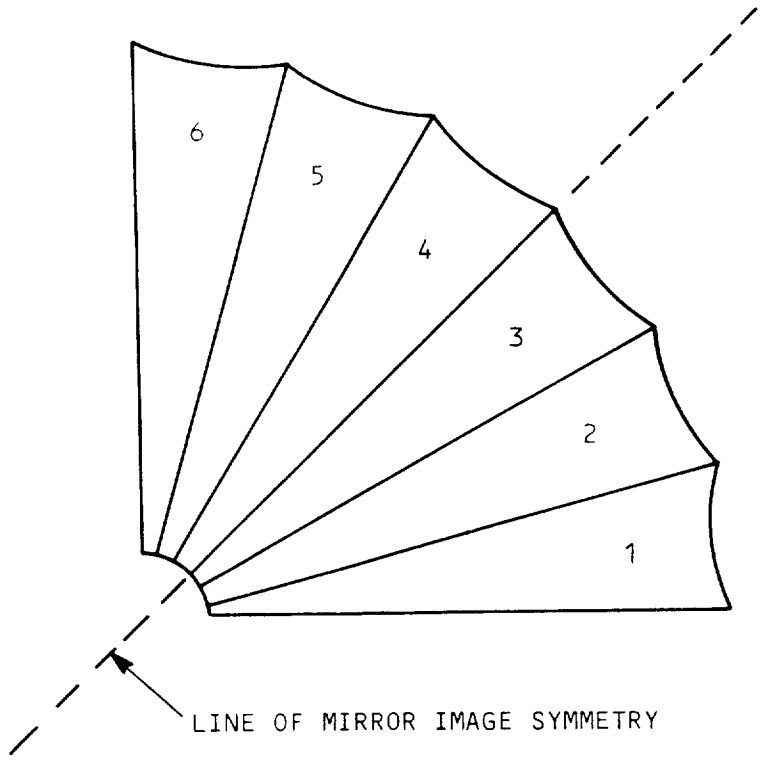

LSST-6

Figure 2.5.1-1.

Mirror image symmetry reduces the complexity of the quad aperture surface.

The reflective mesh is attached to a supporting network of tensioned cords and shaping ties. This network, shown in Figure 2.5.1-2, is on the front (feed facing) side of the reflective mesh.

Retroreflective targets of two types, secured to both sides of the surface, are used to determine the contour and surface "roughness" during theodolite and photogrammetric surveys of the antenna. Targets are located near the various cord junctions and in intermediate areas of each gore. Additional smaller targets are located on selected gores to evaluate mesh "pillow" effects.

2.5.2 Rear Truss Assemblies

The rear truss assemblies direct the loads induced by the surface control cords into the front cord-gores. The trusses also interface the surface assembly to the hoop hinge joints and the column hub segment. As shown in Figure 2.5.2-1, four unique truss geometries take advantage of the mirror image symmetry within each surface quadrant.

The rear truss is a network of tensioned catenary cords and ties covered with a woven nylon mesh shield. This shield protects the truss from snagging on itself, other surface components, and the hoop-column structure.

2.5.3 Surface Control Cords

The function of the surface control cords is to shape the reflective surface upon deployment of the preload segment. These cords pull out of stowage drums located at the lower end of the preload segment. As shown in Figure 2.5.3-1, the control cords are terminated by bead and sleeve end fittings. The sleeves interface with the rear truss hard point fittings and the beads bear against the rear side of low friction guides located on the column cap structure. Ninety-six control cords, 24 each of four lengths are used to tension the antenna surface. The effective length of each cord can be varied $\pm$.25 inches by recessing the sleeve into the rear truss hard point fitting the appropriate amount. This feature allows minor variations in control cord length to be accounted for during surface installation and permits adjustment of the surface after deployment.

FRONT CORD-GORE ASSEMBLY

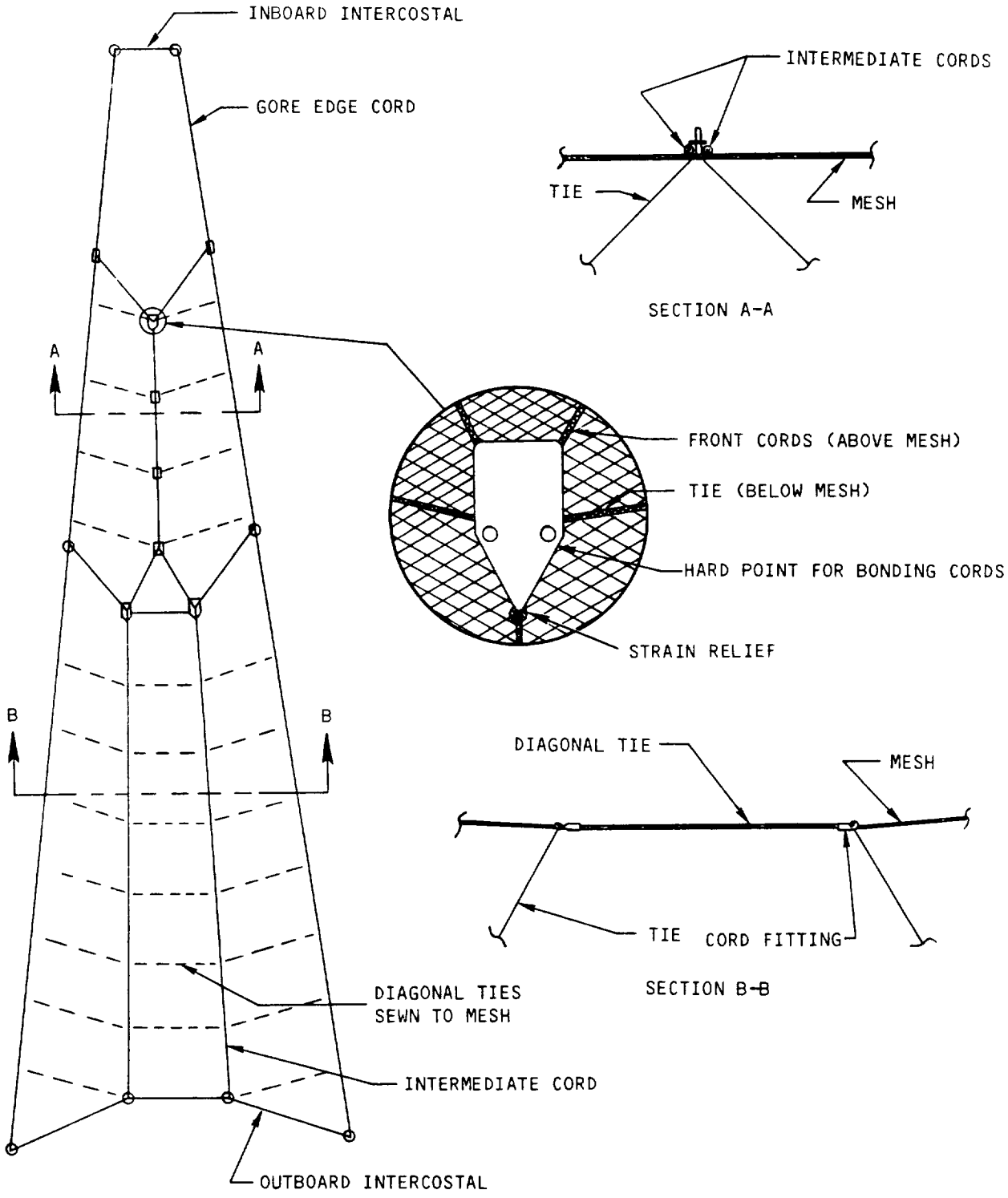

Figure 2.5.1-2.

The tricot knit mesh is supported by a network of cords on the front (feed) site of the antenna surface.

REAR TRUSS GEOMETRY

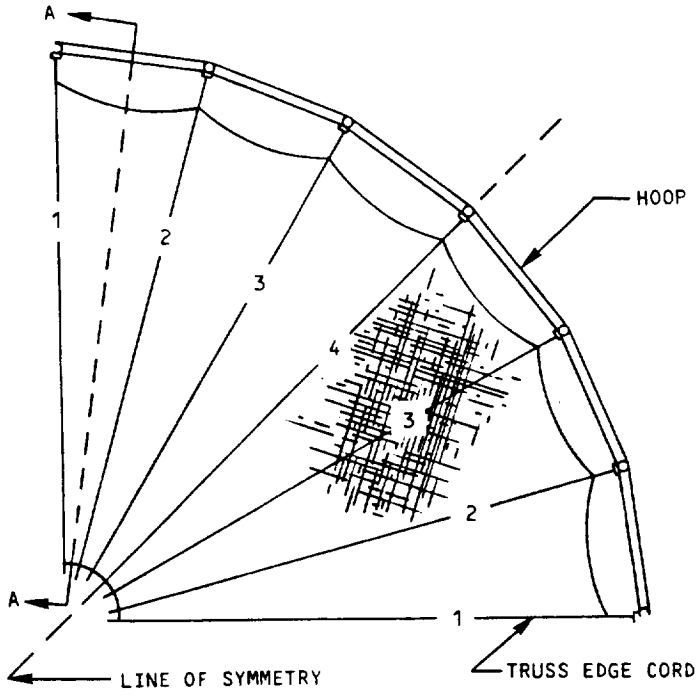

SURFACE QUADRANT (TOP VIEW)

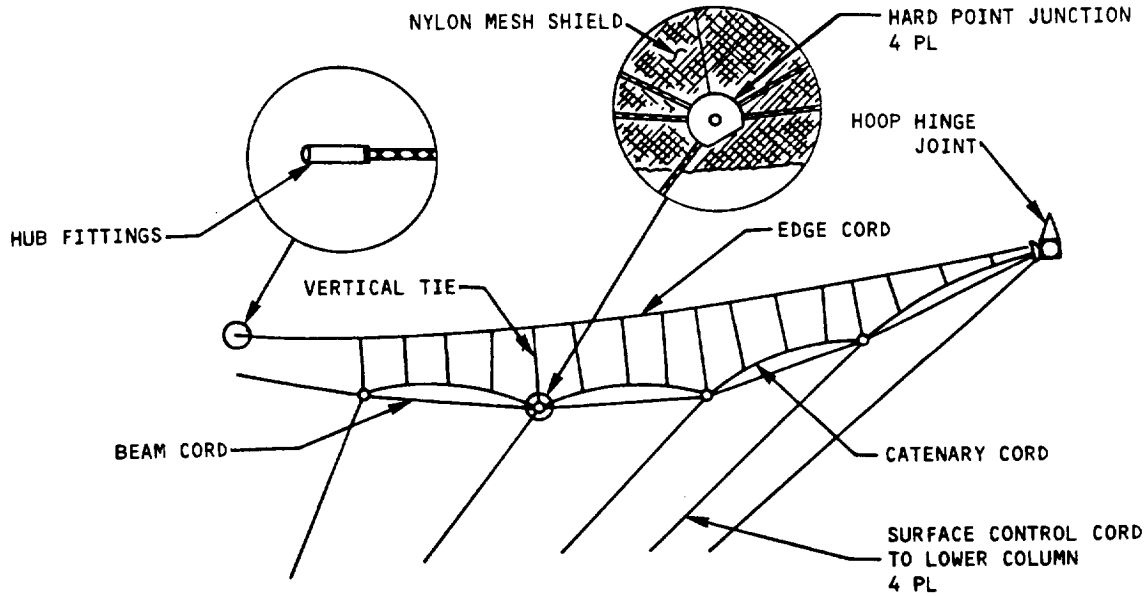

SECTION A-A

LSST-39

Figure 2.5.2-1.

Four rear truss geometries take advantage of the symmetry within each aperture, reducing complexity.

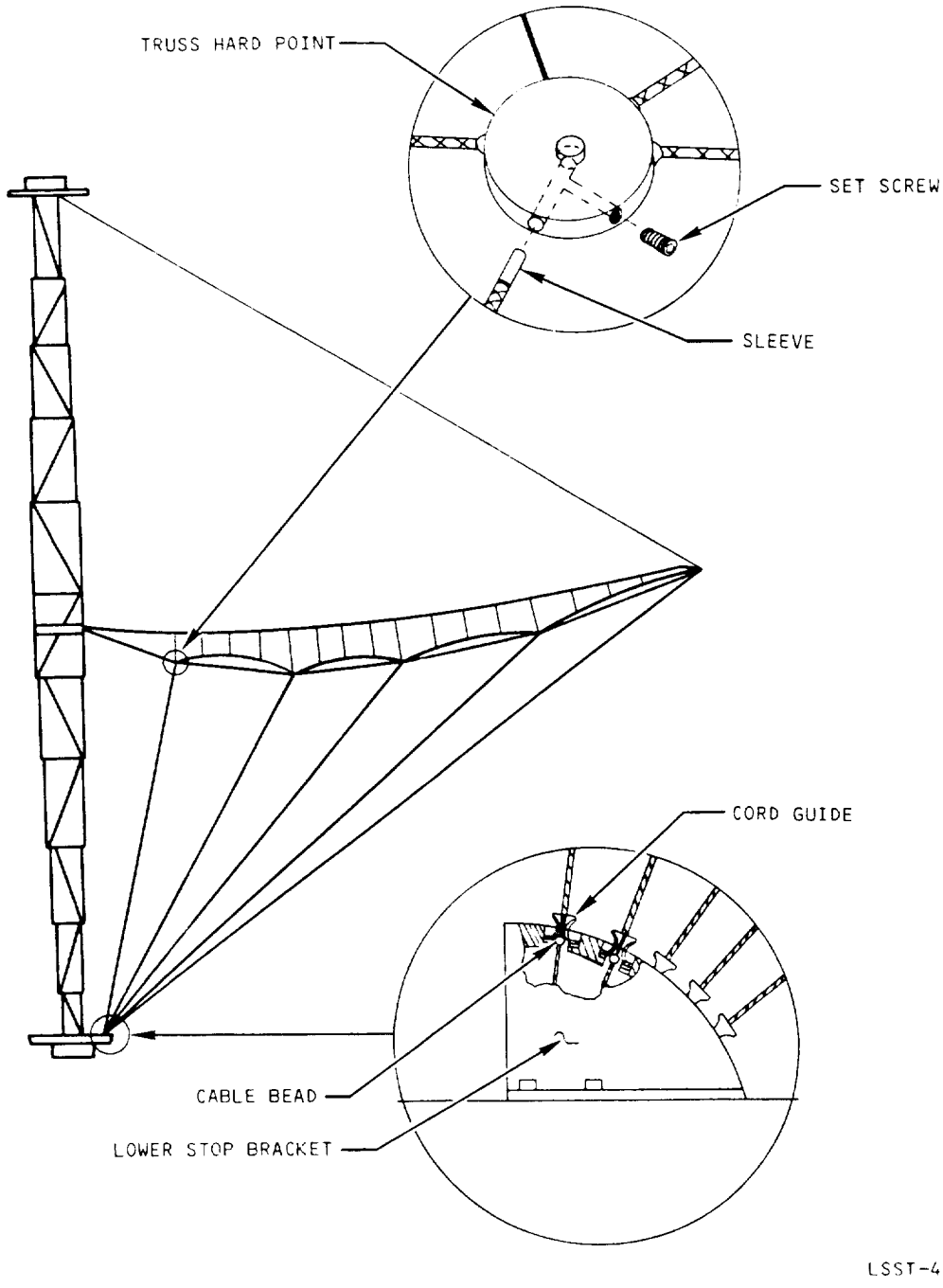

Figure 2.5.3-1.

The surface control cords are adjustable for length, allowing precise setting of the surface.

2.6 Materials

With few exceptions, materials chosen for the antenna were space qualifiable because future studies may involve a refurbishment for a flight experiment. Generally, the structural members of the antenna were sized for ground loads. Graphite was selected for the primary structure because of its relative lightness, high stiffness, and low coefficient of thermal expansion. Cords and ties were also made of graphite for the same reasons. Table 2.6-1 summarizes materials for each of the major antenna components.

2.6.1 Column

The column is primarily comprised of graphite/epoxy members. This structure was sized based on the 700 lb. load it must react in a 1-G condition.

The vertical longerons of the column are T300/948A1 graphite/epoxy tubes. They are 1.00 inch in diameter, with a 0.045 inch wall and a $\pm 15^{\circ}/0^{\circ}_{5}/\mp 15^{\circ}$ layup. A symmetrical layup was chosen to minimize in symmetrical thermal distortions and inter-laminate stresses.

Similarly, the circumferentials and diagonals are T300/948A1 graphite/epoxy tubes. They are 0.375 inch in diameter with a .045 inch wall and a $\pm 15^{\circ}/0^{\circ}_{5}/\mp 15^{\circ}$ layup.

The latch and stricker housings on the longeron ends are A356-T6 aluminum castings. Castings were chosen for this particular application because of the large number of identical parts and the consequential cost savings of manufacture.

2.6.2 Hoop

The hoop segments are 2.50 inch diameter tubes with a wall thickness of 0.045 inch. They are made of T300/948A1 graphite/epoxy layups with a $\pm 15^{\circ}/0^{\circ}_{5}/\mp 15^{\circ}$ ply orientation.

Table 2.6-1. Hoop/Column Materials Summary

System	Components	Material Description
Hoop	Segments	2.50 in. dia x 0.045 in wall Gr/E tubes (1) (2)
	Synchronization Rods	0.25 in. dia unidirectional Gr/E rods (1)
	Pivot Arms & Hinge Platforms	Machined 6061-T6 aluminum alloy
	Structural Adhesive	EA934 epoxy (3)
Column	Longerons	1.00 in dia x 0.045 in wall Gr/E tubes (1) (2)
	Circumferentials and Diagonals	0.375 in dia x 0.045 in wall Gr/E tubes (1) (2)
	Latch & Striker Housings	A356-T6 aluminum castings
	Structural Adhesive	EA934 epoxy (3)
Surface	Wire Mesh	1.2 mil dia gold-plated molybdenum wire in a tricot weaver with 10.4 spaces/inch (9)
Cords (4)	Upper Hoop Support Cords	No. 8 quartz (5)
	Lower Hoop Support Cords	No. 8 graphite (5)
	Outboard (No.4) Surface Control Cords	No. 4 graphite (5)
	Inboard (No. 1, 2, 3) Surface Control Cords	No. 2 graphite (5)
	Front Cords	No. 2 to No. 8 graphite (6)
	Vertical & Diagonal Ties	No. 1/3 and No. 1 graphite (6)
	Cord/Fitting bonds	EA956 epoxy (3)
	Cord Strain Relief and Selected Tie Bonds	Conastic AD-20 polyurethene (7)
	Stitching	EC12 Beta-Glass thread (8)

(1) Thornel T-300 graphite fibers from Union Carbide, Danbury, CT, with 948 A1 epoxy matrix from Fiberite, Winona, MN
(2) (0°/+10°/-10°/+45°/-45°/-10°/+10°/0°)
(3) Dexter-Hysol, Pittsburgh, CA
(4) For definition of cord sizes, see Table 2.7.4-1
(5) Teflon-Impregnated with Nomex cross-wrap
(6) Teflon-Impregnated
(7) Conap, Inc., Olean, NY
(8) Engineered Yarns, Coventry, RI
(9) Continental Warp Knits, Angier, N.C.

The 0.25 inch diameter synchronization rods are unidirectional T300/948A1 graphite/epoxy, while the pivot arms are machined from 6061-T6 aluminum. Because of their size the hinge platforms (6061-T6 also) were welded assemblies. Weldments were selected to minimize material and fabrication costs.

2.6.3 Surface

The reflective surface is made of a gold-plated molybdenum wire mesh. The individual strands are 1.2 mils in diameter. The tricot knit mesh has 10.4 openings per inch. This particular opening size was selected because of its excellent RF reflectivity in the 2-12 GHz range.

2.6.4 Cords and Ties

The material configurations used for the various cord members are shown in Table 2.6.4-1. All cords used on the model were made of graphite with the exception of the upper hoop support cords which were quartz (a dielectric which reduces RF interference). The cord fiber orientation was unidirectional. This enhances the cord's repeatability characteristics. For the same reason and for handling purposes, all cords were teflon impregnated. For key cord members, which see extensive movement and handling, a nomex cross-wrap was utilized to provide durability.

The No. 1 cord size is defined in Table 2.6.4-1; other sizes are based on multiples of this size. Surface control cords range from No. 2 to No. 4. Ties are No. 1 cords (3000 graphite fibers). Hoop support cords are comprised of 4 No. 2 cords and are consequently designated as No. 8 cords.

2.6.5 Adhesives

Structural bonding between aluminum fittings and graphite/epoxy elements was accomplished using an MMM-A-132, Type 1, Class 3 epoxy (EA934 from Dexter-Hysol of Pittsburg, California).

Surface cords were bonded to end fittings using Dexter-Hysol EA956 epoxy. Strain relief for surface cords and primary bonds for selected diagonal ties was done with Conastic AD-20 polyurethane produced by Conap, Inc. of Olean,

Table 2.6.4-1.

Definition of No. 1 Cord Size

	QUARTZ	GRAPHITE
PLIES/CORD	8	1
FIBERS/PLY	240	3000
FIBERS/CORD	1920	3000
FIBER DIAMETER	0.0004 IN	0.00028 IN
CORD DIAMETER	0.018 IN	0.018 IN
*DESIGN LOAD RANGE (APPROXIMATE)	0.5-1.0 LB	0.5-1.0 LB
E (MODULUS)	10.4×10^{6} PSI	33×10^{6} PSI
EA	1500-1600 LB	4000-4500 LB
TENSILE STRENGTH	15 LB	40 LB**
WEIGHT	1.482×10^{-5} LB/IN ADD 16% FOR TEFLON COATED	1.125×10^{-5} LB/IN ADD 10% FOR TEFLON COATED

*THE DESIGN LOAD RANGE IS SOMEWHAT ARBITRARILY SELECTED, BUT IS BASED ON THE MINIMUM LOAD REQUIRED TO OPERATE IN THE LINEAR RANGE OF THE LOAD/DEFLECTION CURVE OF THE CORD; THIS MAXIMIZES CORD EA (MODULUS X AREA) FOR A PARTICULAR LOAD.

**NUMBERS SHOWN ARE FOR CORDS WITH TEFLON COATING; CORDS WITHOUT TEFLON COATING HAVE ABOUT HALF THE INDICATED STRENGTH.

New York. EA956 was selected for cord bonding because of its low viscosity and consequential desirable impregnation characteristics.

3.0 MANUFACTURING HISTORY

3.0.1 One of the objectives of the program was to verify the manufacturing techniques of a very large Hoop-Column Antenna (100-300 meter diameter). To build, deploy, and test an antenna of this size on earth would be a very expensive operation. Therefore, we have developed a "build to dimension" philosophy; that is, the system is built in modular form and assembled in a stowed or semi-stowed condition, thereby minimizing facility size requirements. Because the components would be built to within specified tolerance budgets, the overall system, when deployed for the first time on orbit, would have the required surface accuracy to perform within specifications. With this philosophy in mind, the following is a description of the special manufacturing processes selected for the model.

3.1 Column

The column (shown stowed in Figure 3.1-1) is an integrated structure that contains the following subassemblies:

Column Segment Assemblies	(Dwg 627443)
Column Drive System (CDS) Assembly	(Dwg 627659)
Preload Segment Assembly	(Dwg 627445)
Upper Cable Stowage Assembly	(Dwg 627647)
Lower Cable Stowage Assembly	(Dwg 672648)

The manufacture of the Column Segments and the assembly of the Column Drive System and Preload Segment required the use of special fixtures and adjustments. Consistent with the "build to dimension" philosophy those steps were taken to ensure the precision of the completed column, and are discussed separately below.

Assembly of the upper and lower cable stowage systems did not require special fixtures and adjustments. Their precision is implied from the individual piece parts tolerancies established during the design phase of the program.

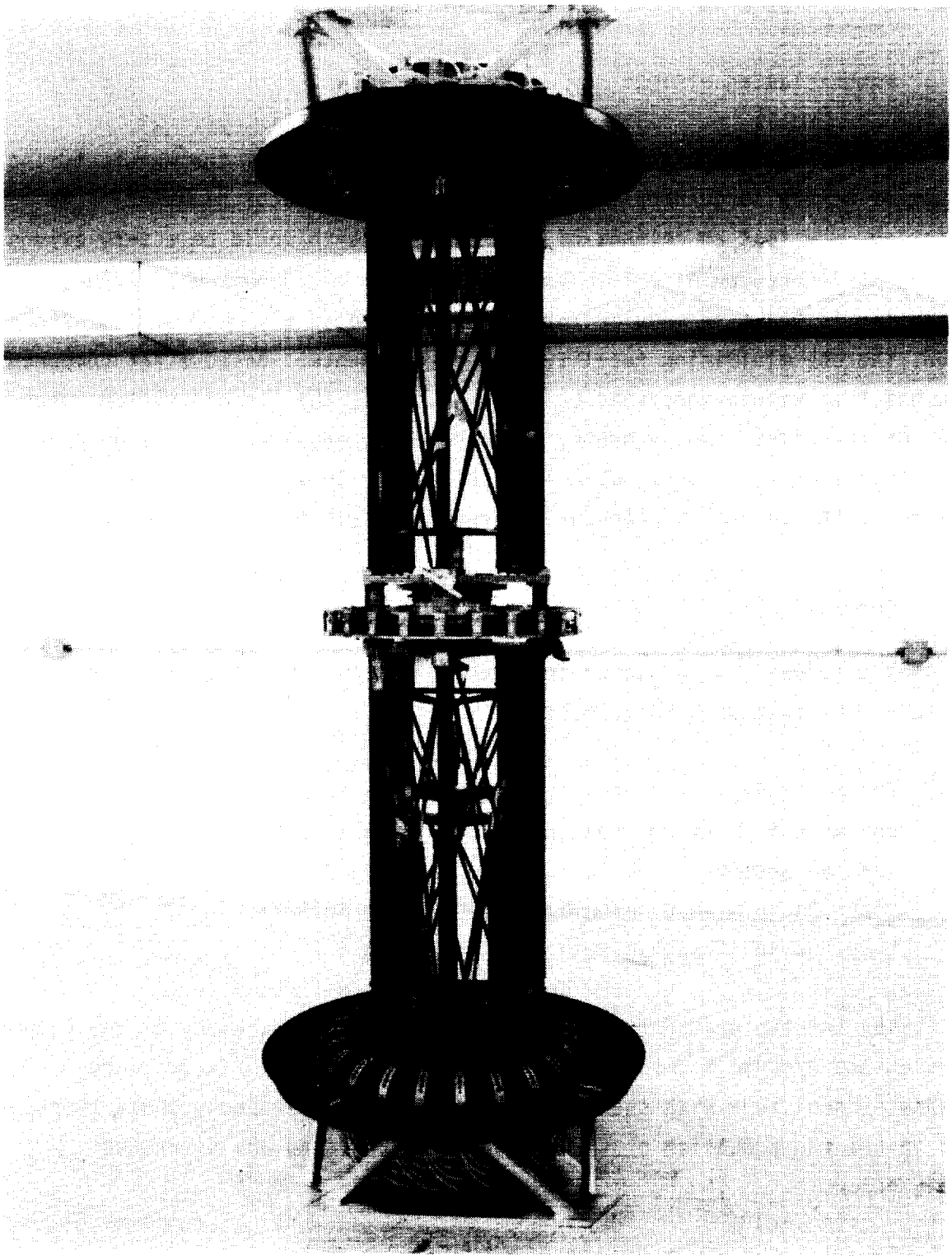

84-1060CMR-1-1

Figure 3.1-1.

The column assembly, shown in the stowed configuration, was assembled from precisely manufactured components to ensure its overall accuracy when deployed.

3.1.1 Column Segment Assembly

The column consists of eight deployable segments and two stationary segments. These segments were assembled using one universal fixture (Figure 3.1.1-1) which was aligned to an accuracy of .005 inches true position at the latch and striker housing interface points. This alignment was performed on a cordax machine.

The deployable segments (Figure 3.1.1-2) were built in stages to ensure that the epoxy pot life of 20 minutes was not violated. First, the circumferentials were bonded to the latch and striker housings using the fixture to determine the final circumferential lengths. These parts were allowed a brief cure cycle before continuing. Next, the longerons and diagonals were bonded, again allowing the fixture to set the dimensions. Because all the column members are tension-compression, there were no preloads required during buildup. All segments were assembled in a vertical attitude since this is their orientation during system requirements.

The stationary or hub segments were assembled in a similar manner after the fixture was altered to allow for differences in base fittings and longeron height.

The latch and striker piece-parts were then assembled into their respective housings, and a dummy cable was routed through each of the three longerons to facilitate the end item deployment cable installation.

Starting with the outermost segment and working inward, the segments were nestled within one another and manually translated with respect to one another to assess roller alignment. Next, the segments were manually latched and adjustments made to the striker plate to ensure proper operator. This process was repeated until each half column (one stationary segment with four deployable segments) was completed.

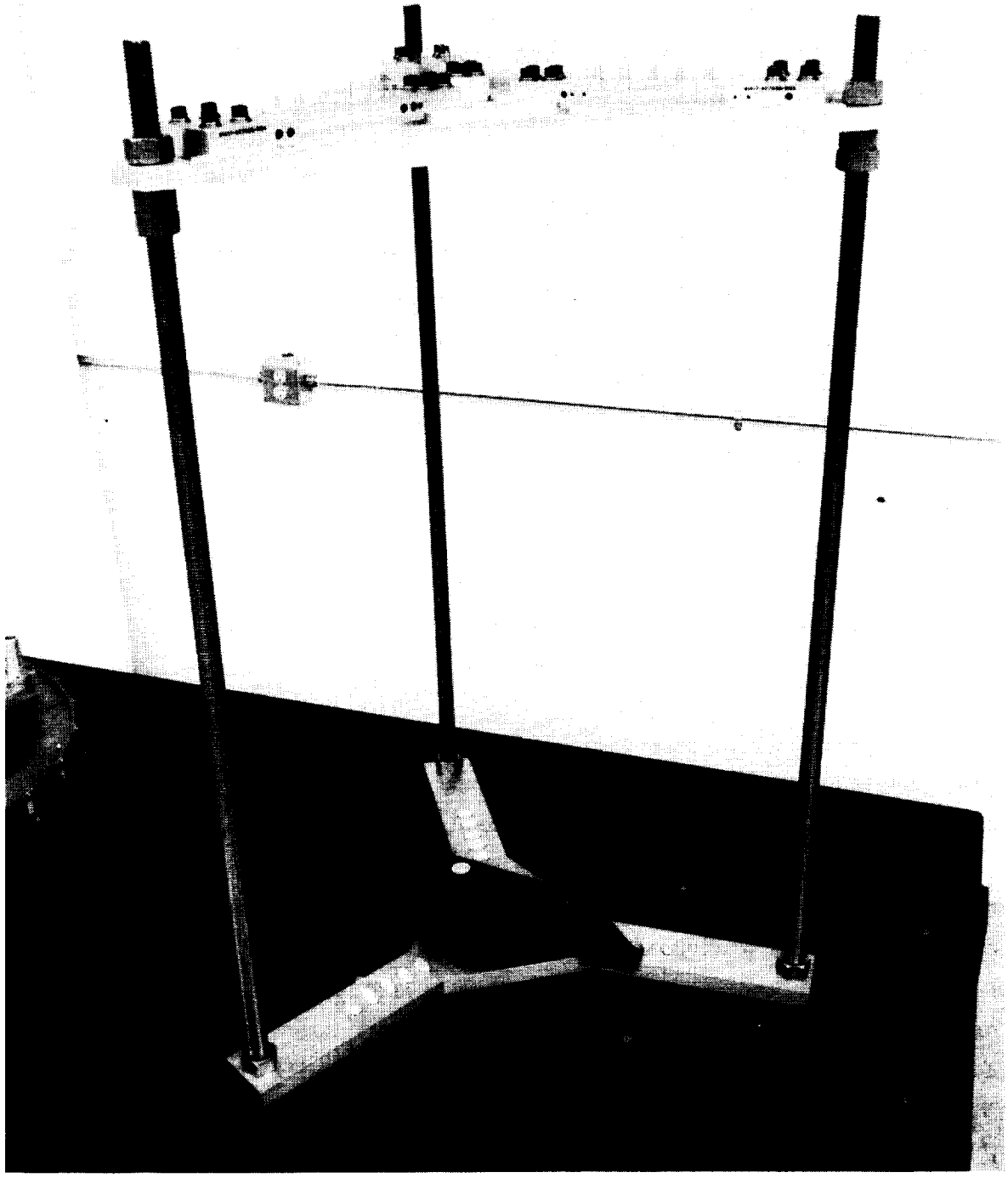

83-2122CMR-4-10

Figure 3.1.1-1.

Each of the deployable column segments was manufactured to an accuracy of ±.005 inches to minimize the overall deployed column misalignment. This fixture was used to precisely locate the segments during bonding operations.

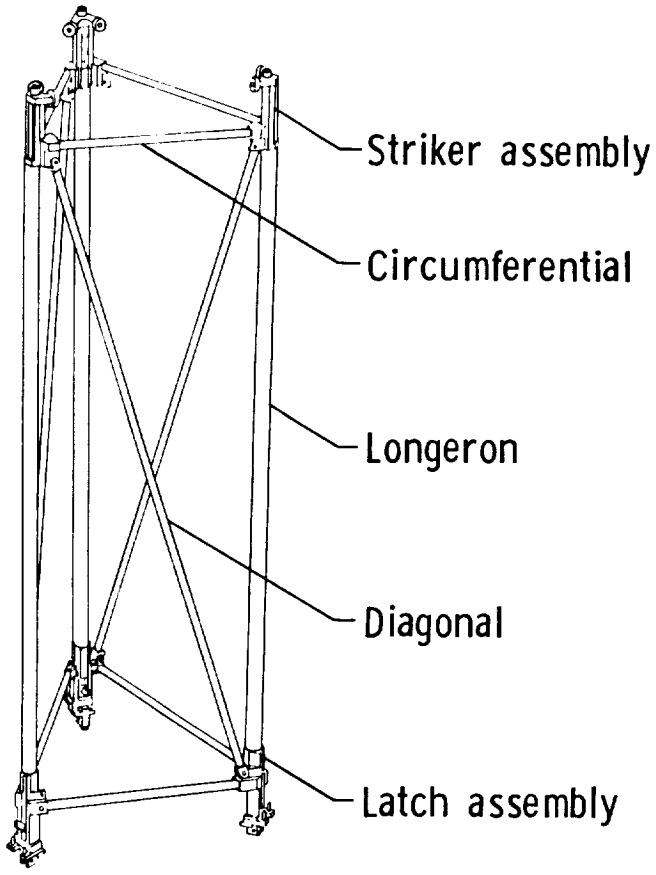

Figure 3.1.1-2.

The column segments were manufactured in stages to stay within the useful pot life of the epoxy adhesive. The diagonals and longerons were bonded to previously built latch-circumferential and striker-circumferential subassemblies.

3.1.2 Column Drive System (CDS)

The column drive system (Figure 3.1.2-1) consists of the upper and lower plate assemblies and the threaded cable drum. These assemblies were manufactured separately and bolted together at the mid hub fittings. These interfaces were shimmed to provide the proper assembly height to within .005 inches. The drive motor was then installed and the system tested to determine the deployment and backdrive torques. Installation of the Mesh Restow System completed the assembly of the CDS.

3.1.3 Preload Segment and Drive

Assembly of the preload segment drive itself (Figure 3.1.3-1) did not require special fixtures. The bearing retainer structure was bonded to the inner-most lower column segment longerons and allowed to cure. Installation of the acme screw, acme nut support structure, motor, wiring, and stow-deploy limit switches completed the drive unit assembly process. The system was then functionally checked (Figure 3.1.3-2) and the limit switches were set.

The installation of the preload segment's deploying longerons to the acme nut structure occurred during installation of the lower cable stowage system to the completed lower column structure.

3.1.4 Column Final Assembly

After proof load testing the individual upper and lower column structures, which will be discussed in Section 4.0, final assembly of the column structure was performed. This operation was limited to bolting the upper and lower column assemblies to the CDS, and installation of the end item column deployment and restow cables.

3.2 Hoop

The hoop, comprised of 24 articulating segments, was fabricated in eight-three segment subassemblies. The hoop segments and syncronization rods were bonded using fixtures that control the position of their pivot points on the hinge

83-1880

Figure 3.1.2-1.

The column drive system's triangular base plates were shimmed to within ±.005 inches of their specified height prior to installation of the stationary hub segments.

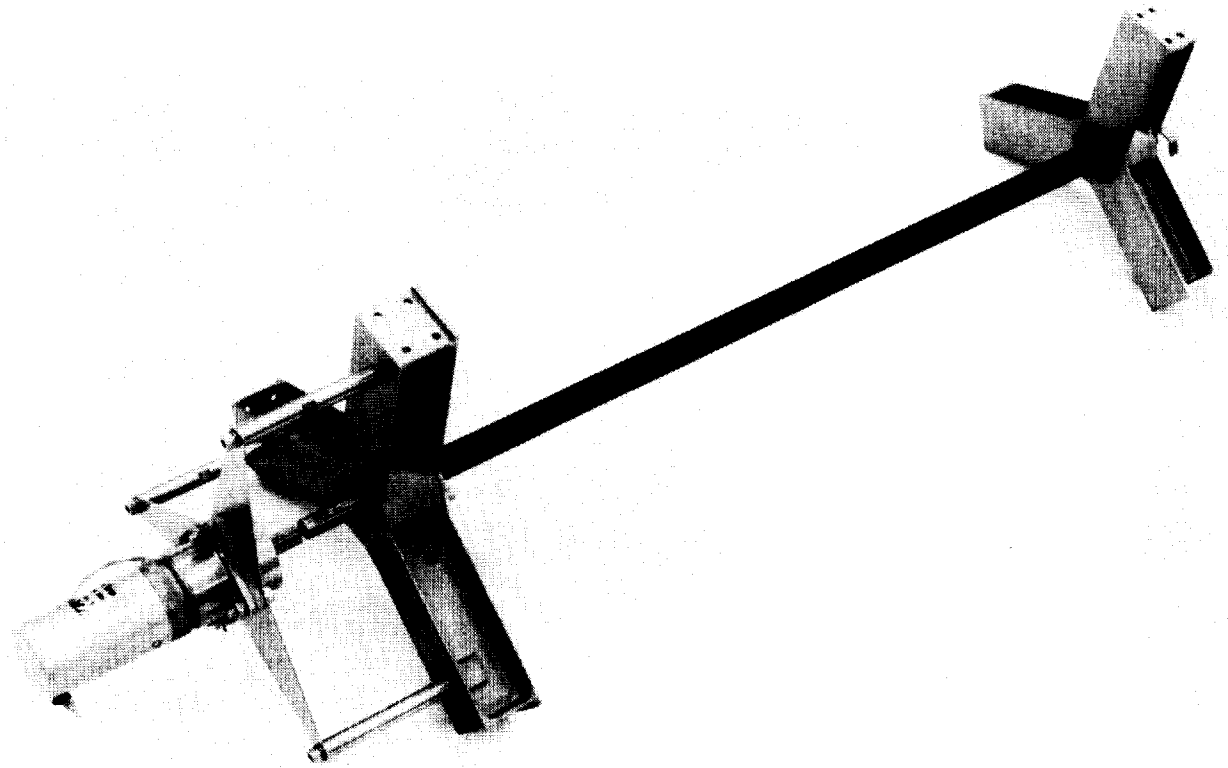

83-2122CMR-1-1

Figure 3.1.3-1.

The acme nut, acme screw, bearing, and gear motor have been installed to the preload segment triple beams. Not shown are the longeron bond and linear bearing brackets used to interface the drive unit to the column.

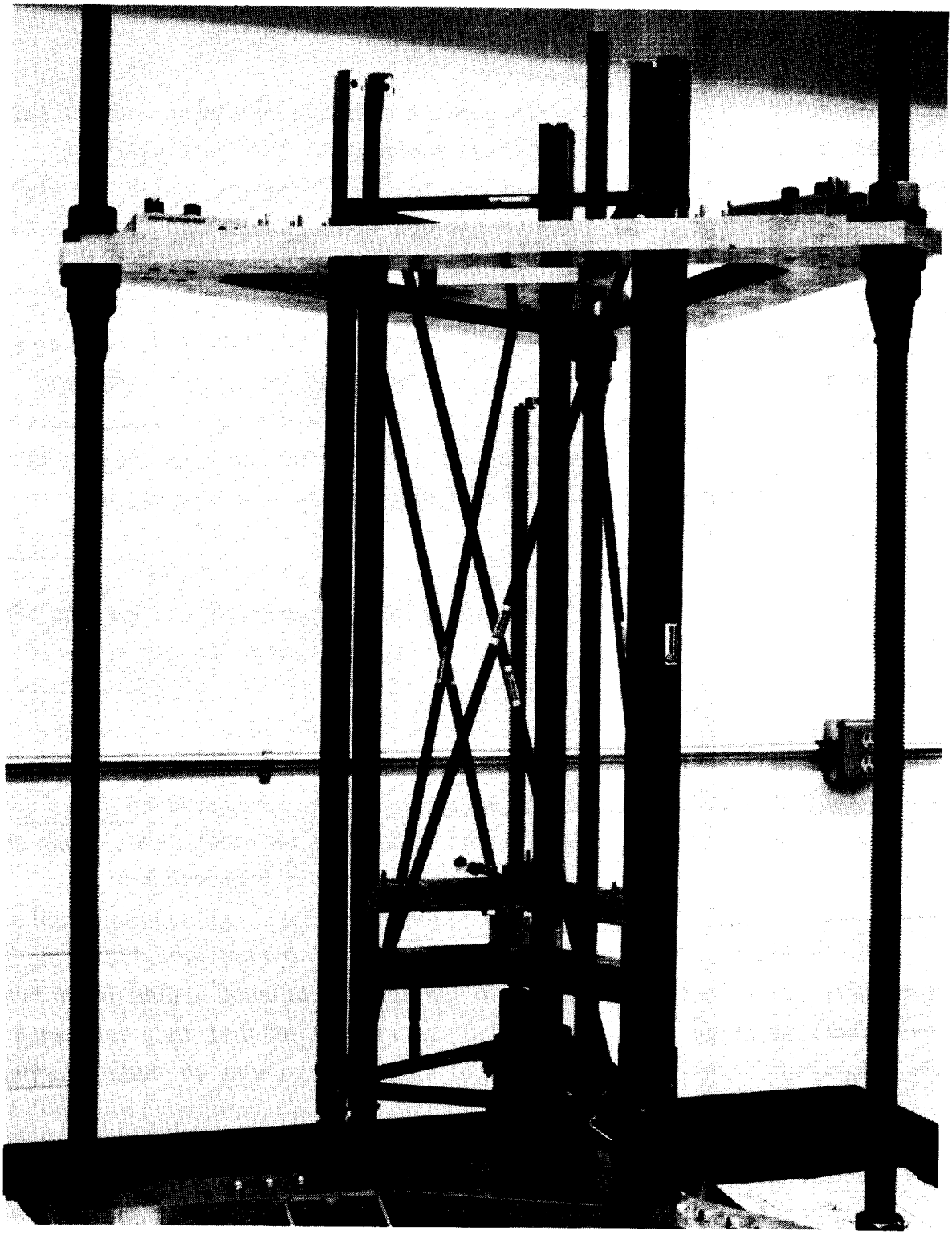

Figure 3.1.3-2.

83-2872CMR-2-6

After thorough curing of the longeron interface bonds, the preload segment drive unit was functionally tested. Setting the deploy and stow-complete limit switches, and wiring installation was performed prior to the final functional test.

platforms. These fixtures (Figure 3.2-1), which dictate hoop segment and synchronization rod lengths, were located within .020 inches true position and verified using theodolites.

To fabricate a typical three segment assembly, the hoop segment end fittings were bonded to a graphite tube and placed into the hinge platform fixture. Inserting the pivot point pins set the final segment length, as shown in Figure 3.2-2. This process was repeated two additional times, yielding the three segment assembly shown in Figure 3.2-3.

Next, the syncronization rod end fittings were bonded to the rods and installed to the hinge platforms using their pivot pins to set the final rod length as shown in Figure 3.2-4. As depicted in Figure 3.2-5, scissors jacks were used to prevent sagging in the syncronization rods during the cure cycle. It is important to note that preloads were not required during hoop segment and syncronization rod bonding.

After a brief cure cycle, the three segment assembly was removed from the floor tooling and the process repeated until all eight subassemblies were completed.

Upon installation of the platform gearing, the three segments were then reassembled in the stowed configuration as shown in the foreground of Figure 3.2-3. After all eight-three segment assemblies were completed, they were assembled to produce the stowed hoop assembly depicted in Figure 3.2-6.

Drive motors, limit switches, and electrical wiring were installed to the stowed hoop prior to its connection to the counter balance system for a brief functional check depicted in Figure 3.2-7. The results of this test indicated that the motorized hinge joints required individual alignments to their gearing.

3.3 Hoop Support Cords

The hoop support cords were manufactured to the geometry and load specified in Figure 3.3-1. These cords, which were graphite behind the antenna surface, and quartz above the surface required special processes to ensure their

HOOP TOOLING

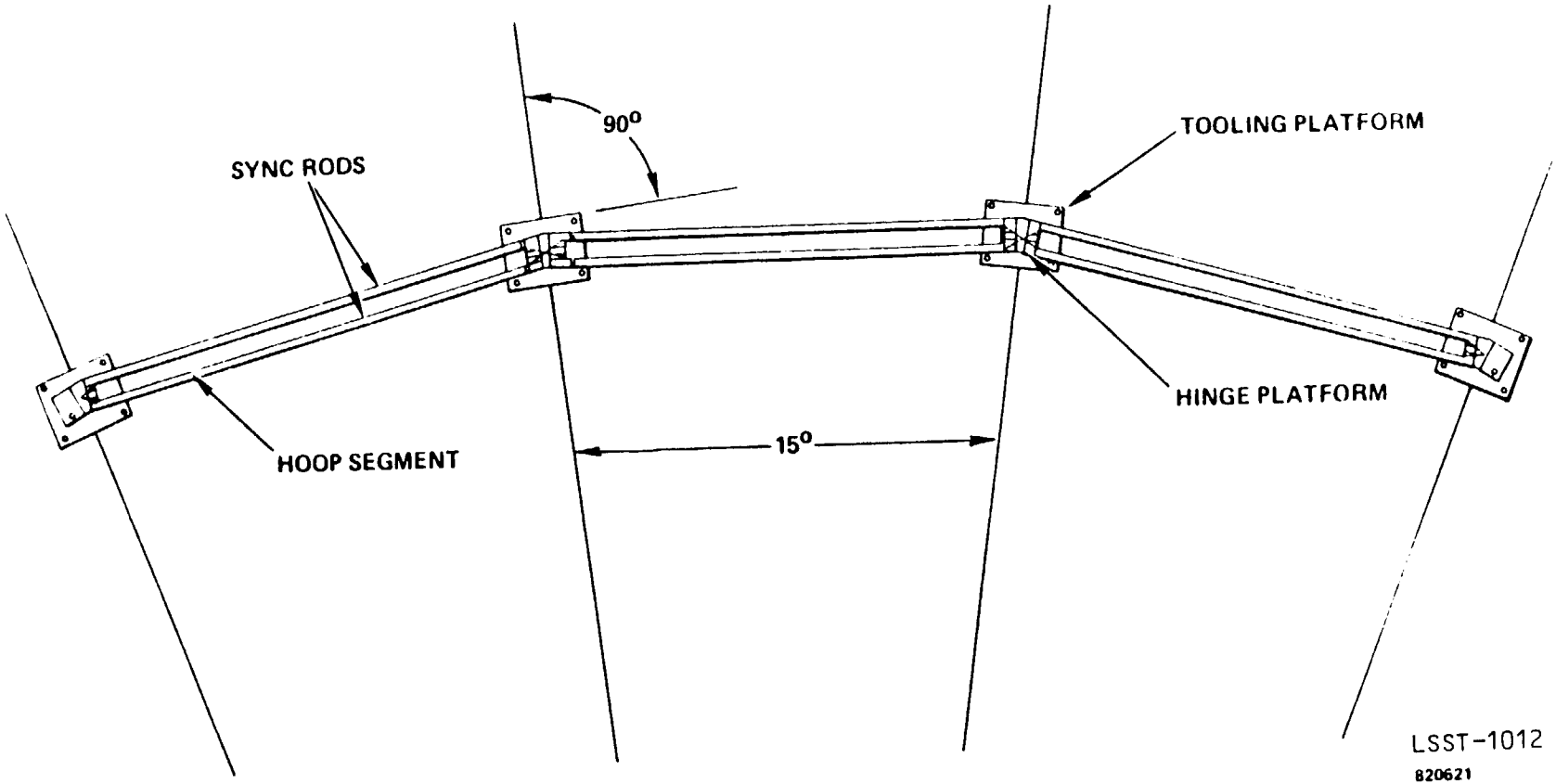

Figure 3.2-1.

The hoop fabrication fixtures were laid out on the radome floor using the rigid tooling bar to locate the fixtures to within ±.020 inches true position. The location and planer alignment of these fixtures were verified using theodolites prior to use.

83-2582CMR-1-2

Figure 3.2-2.

This hoop segment length was set by installing the pivot point pins into the fixtures prior to curing of the epoxy adhesive.

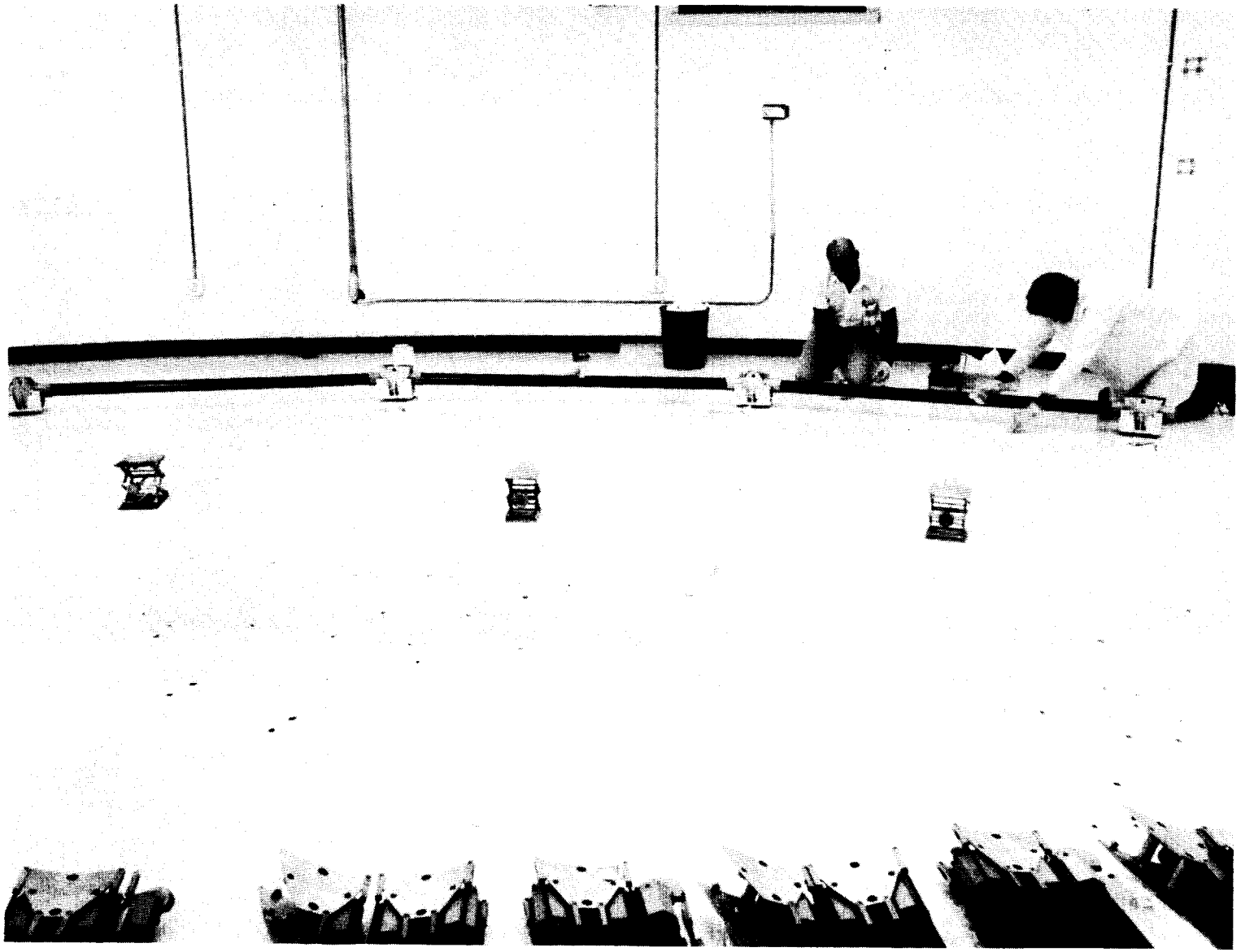

Figure 3.2-3. 83-2582CMR- -8

The hoop segments were bonded in three segment sets to minimize tolerance stackup of the completed structure. Completely assembled and stowed three segment sets can be seen in the foreground.

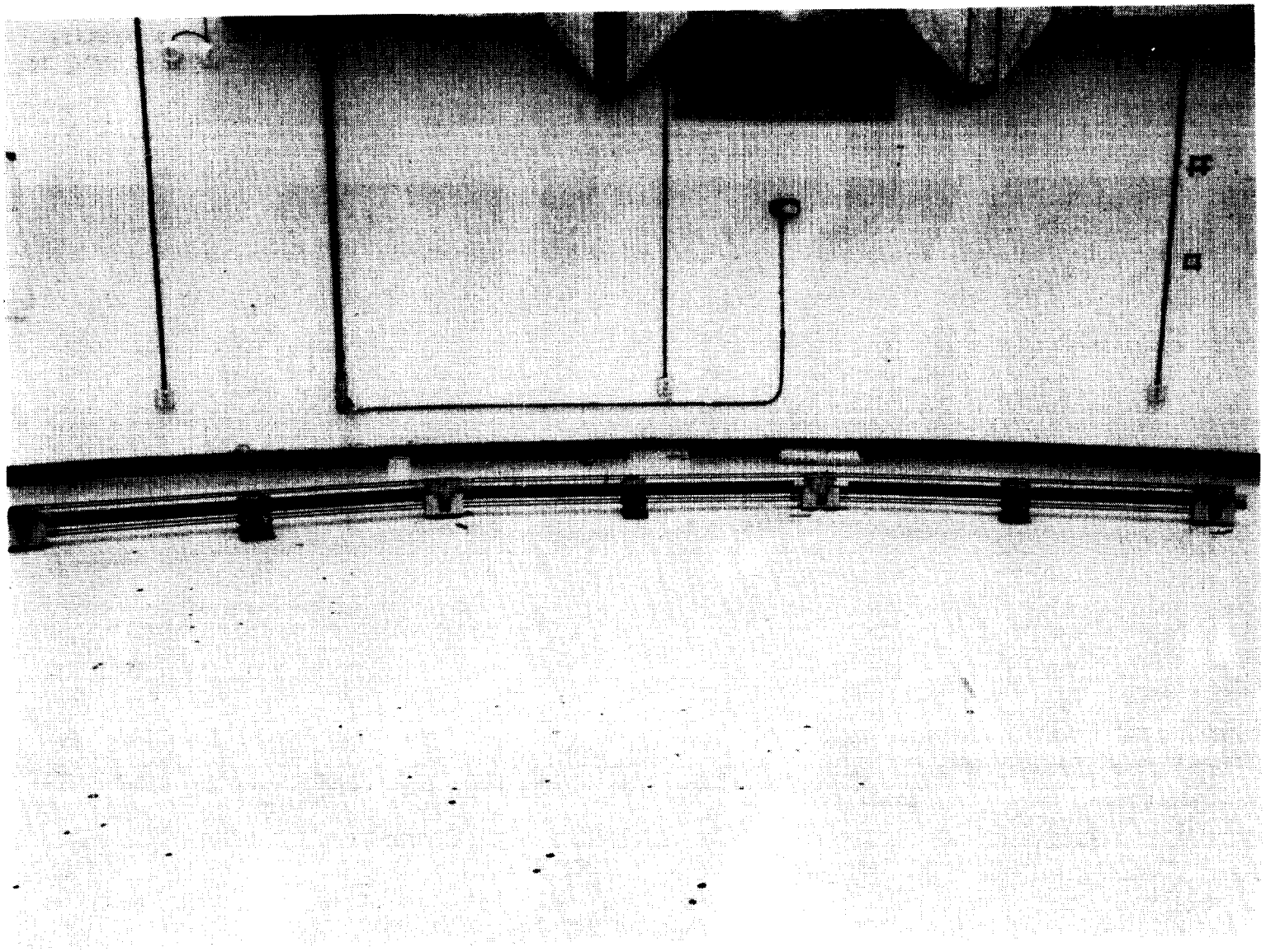

Figure 3.2-4. 83-2582CMR-3-12

To establish their proper length, the synchronization rods (4 per hoop segment) were bonded in place on the hoop hinge platforms.

Figure 3.2-5. 83-2582CMR-3-7

To prevent the synchronization rod lengths from being upset by "sagging", they were supported in a level condition during epoxy adhesive cure using scissors jacks.

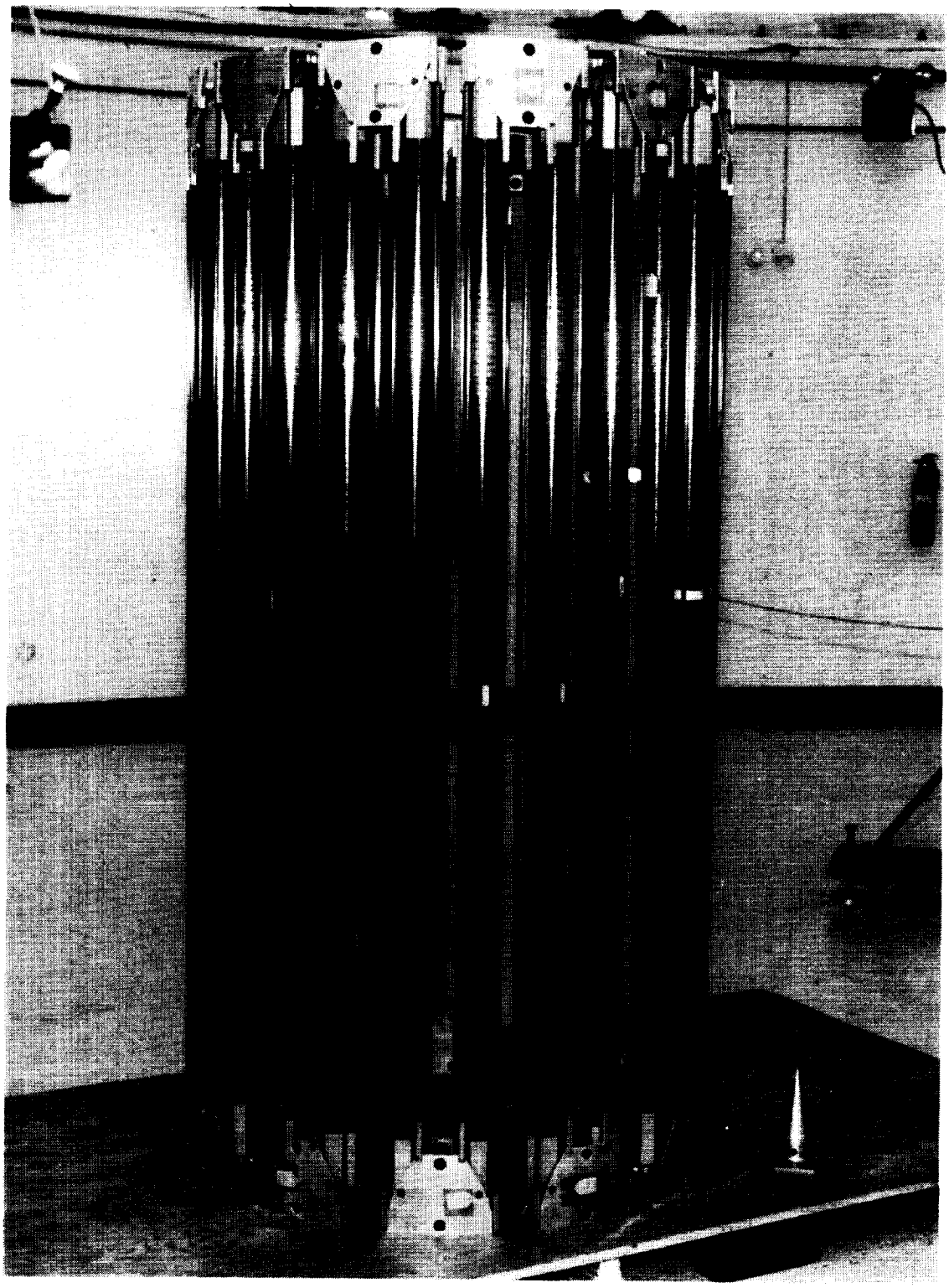

83-28720MR-2-10

Figure 3.2-6.

Integrated from eight-three segment subassemblies, the stowed hoop awaits the installation of drive motors, wiring, and column interface cones.

84-1214C

Figure 3.2-7.

Attached to the counter balance system at the mid segment fittings, the completed hoop assembly underwent a brief functional test to assess kinematics and synchronization.

HOOP CORD GEOMETRIES

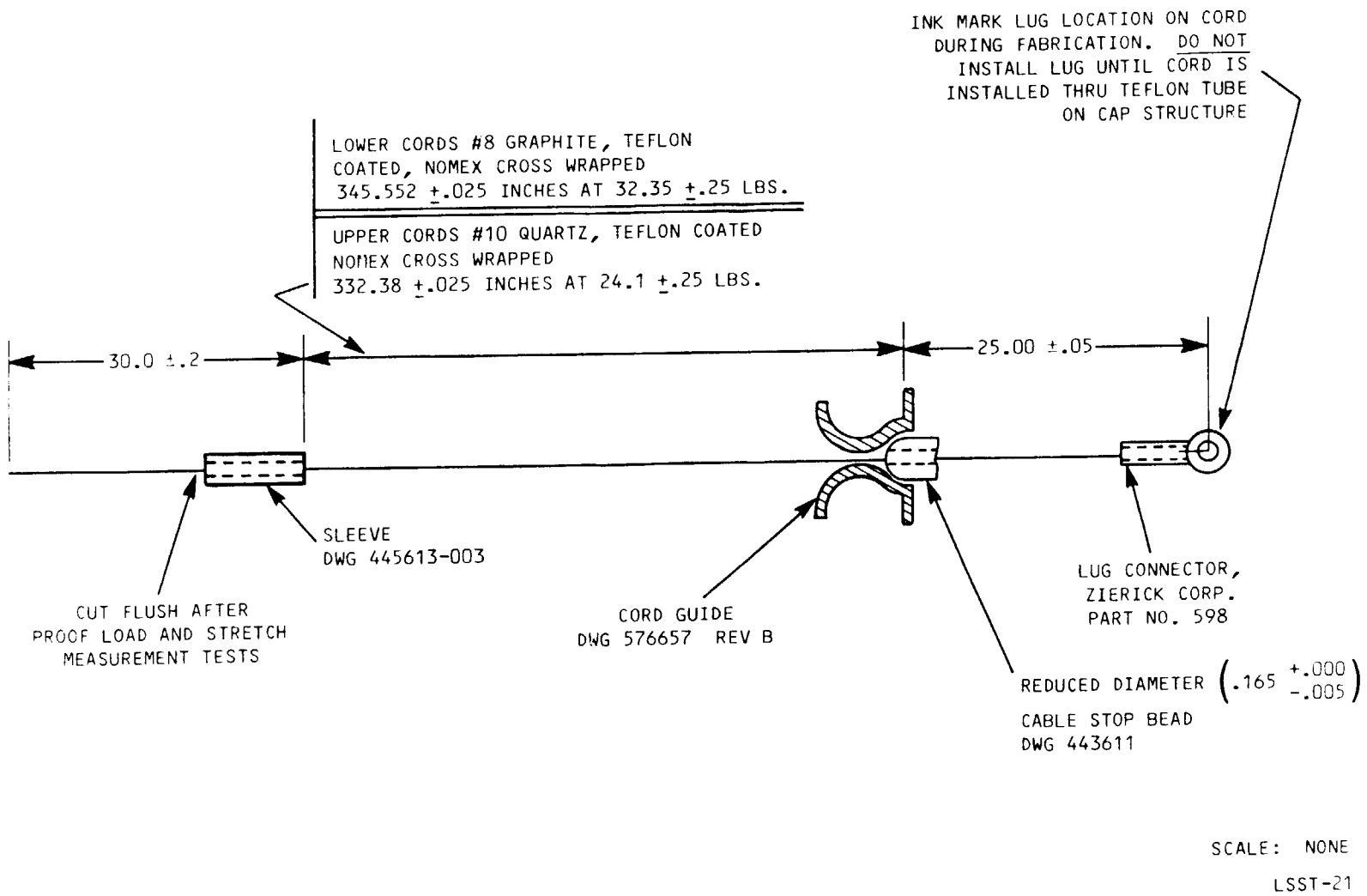

Figure 3.3-1.

The upper and lower hoop control cords were manufactured to carefully controlled load-length relationships.

structural integrity. These processes are similar, differing only in the method used to remove the teflon coating from the cords. The teflon was removed from the graphite cords by burning it off with an oxy-acetylene touch. A chemical etching process was selected for removing the teflon from the quartz cords because they could not withstand the heat generated by the torch. A typical cord preparation and bonding procedure is available in Appendix A1.

After the cords were cut to the approximate required length, the cable stop beads were bonded in place and allowed to fully cure. Next, the cord guides and sleeves were installed and the cords placed into the special fixtures shown in Figure 3.3-2. These fixtures were located on the radome annex floor using theodolites to provide the specified cord geometry within $\pm$.025 inches. After applying the fabrication load and removing the teflon, the sleeve was located, bonded, and allowed to fully cure in the fixtures.

As shown in Figure 3.3-3, each cord was proof-loaded to twice its fabrication load to verify its overall structural integrity. The cords were then returned to the original fabrication tooling to check for proof loading induced stretching or creep in the bond joints. Feeler gauges, inserted between the sleeve and its positioning tool, were used to determine the amount of growth, if any. This information was recorded so that the sleeves could be recessed the appropriate additional amount into the hoop platform fittings during installation. A total of 53 upper quartz cords and 29 lower graphite cords, including five of each type as spares, were fabricated.

3.4 Surface

The RF reflective surface of the model consists of the rear trusses, surface control cords, diagonal ties, and front cord-gores. The fabrication of these components and descriptions of their associated special processes and fixtures are discussed separately below. These discussions are followed by descriptions of the final assembly of the surface and its integration to the hoop-column structure.

HOOP CORD BONDING FIXTURES

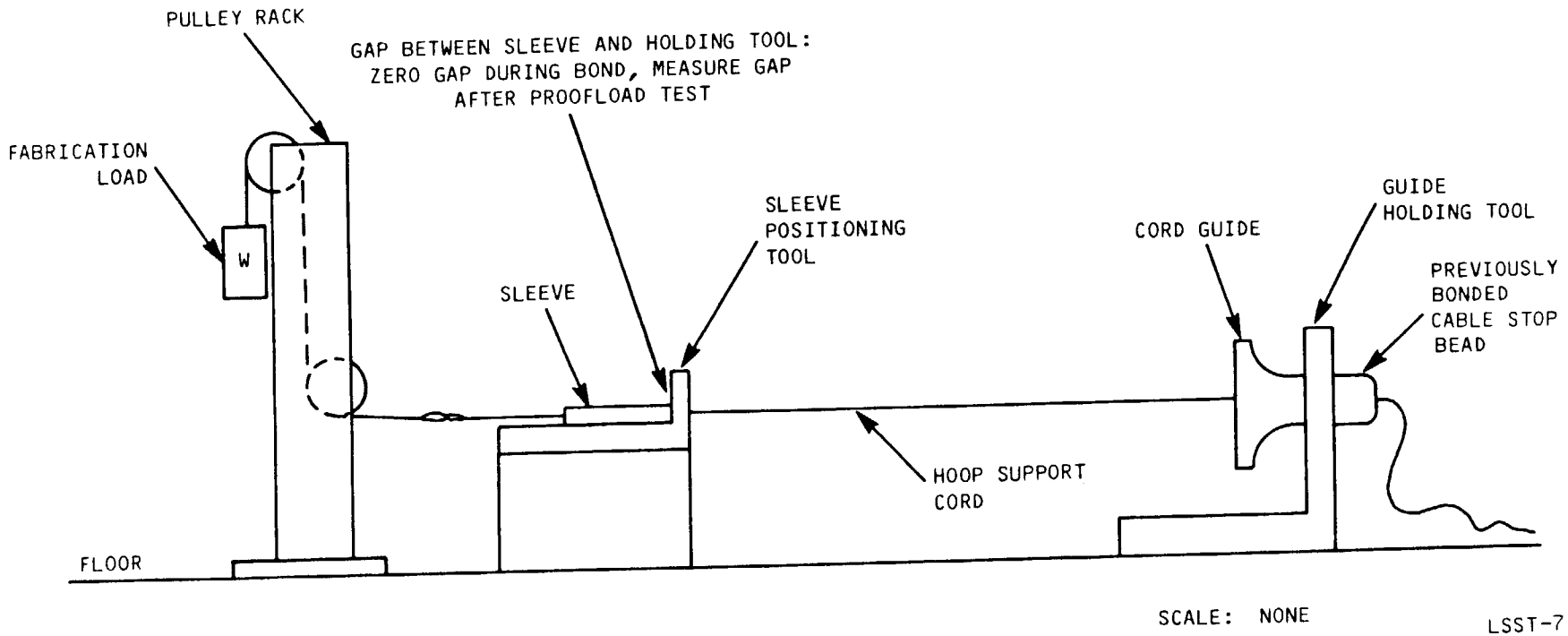

Figure 3.3-2.

The hoop support cord sleeves were bonded with the cord under load at the prescribed geometry. After proof loading, the completed cords were returned to this fixture to measure induced stretching.

HOOP CORD PROOF-LOADING

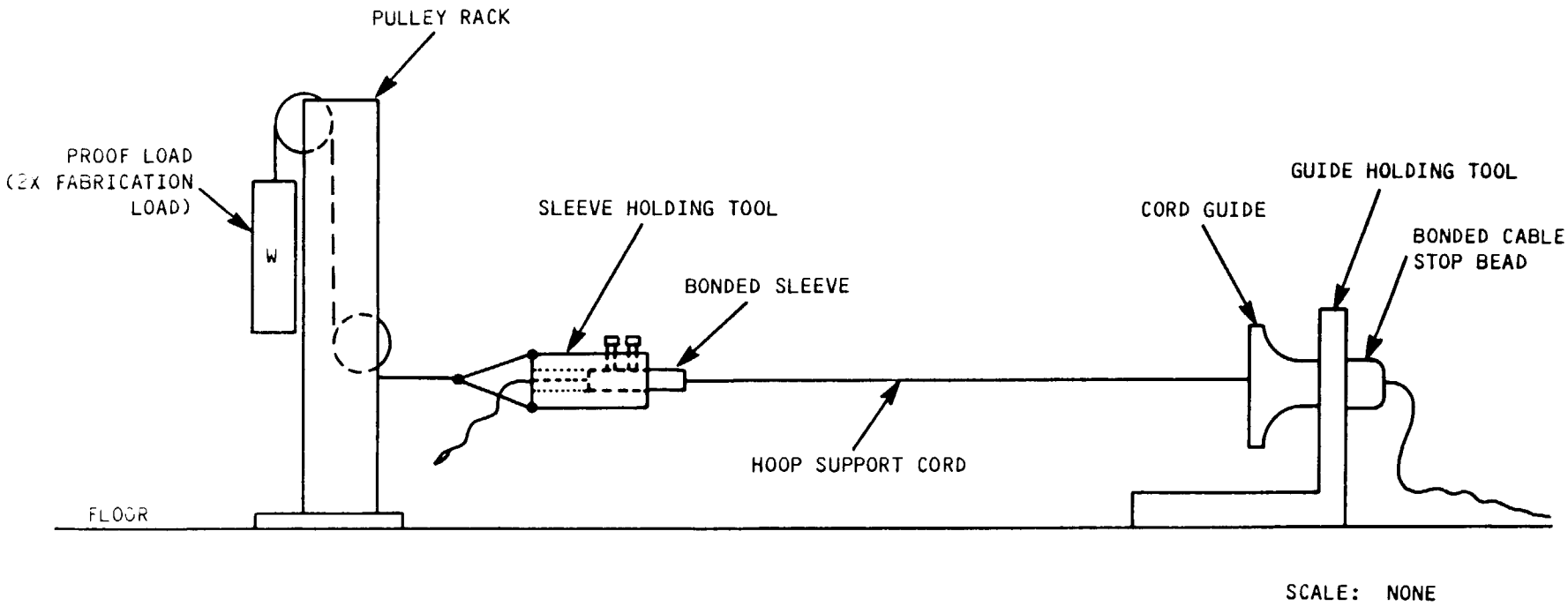

Figure 3.3-3.

Completed hoop support cords were proof loaded in the modified fabrication fixture.

3.4.1 Rear Trusses

The rear truss were manufactured on a special template. This fixture was fabricated form a single sheet (308" x 60" x 1/4") of steel. Prior to actual manufacture of the template, NASA-Langley personnel verified the accuracy of the drilling machine. Harris personnel confirmed the accuracy of the numerical control tape and monitored the actual drilling operations. After its arrival, the template was cleaned, painted, and installed in the radome annex. NASA-Langley personnel then verified the locational accuracy of the numerous holes prior to actual truss manufacture. As shown in Figure 3.4.1-1, the completed template setup included pulleys, dead weights, spring tensioners, thermometers, special junction locating fixtures, and color coded pin-stripes to differentiate between the four truss geometries. This fixturing was required to ensure that each truss was manufactured under the proper combination of length load and temperature.

Actual truss fabrication began by performing preliminary bonding of the numerous cords to the appropriate fittings. During this step, each graphite cord was cut to the approximate required length and its teflon removed on one end. Next, the prepared end was bonded into the appropriate fitting and allowed to cure, as shown in Figure 3.4.1-2. These operations were not performed on the truss template, but on an ordinary table top. These steps were taken to minimize the time required for set up and final bonding of each truss on the template.

These preliminary bonded subassemblies were then positioned on the template for final bonding by locating each fitting on dowel pins or other appropriate fixtures. The free ends of each subassembly's cords were routed to the appropriate fitting and loaded to the proper tension using either the dead weights or calibrated spring-scale tension devices. Examples of this operation are shown in Figures 3.4.1-3 and 3.4.1-4. Just prior to actual final bonding, teflon was removed from each cord using the torch and the truss setup was inspected for proper loading, configuration, cord integrity and template temperature ($70 \pm 4^{\circ}$ F).

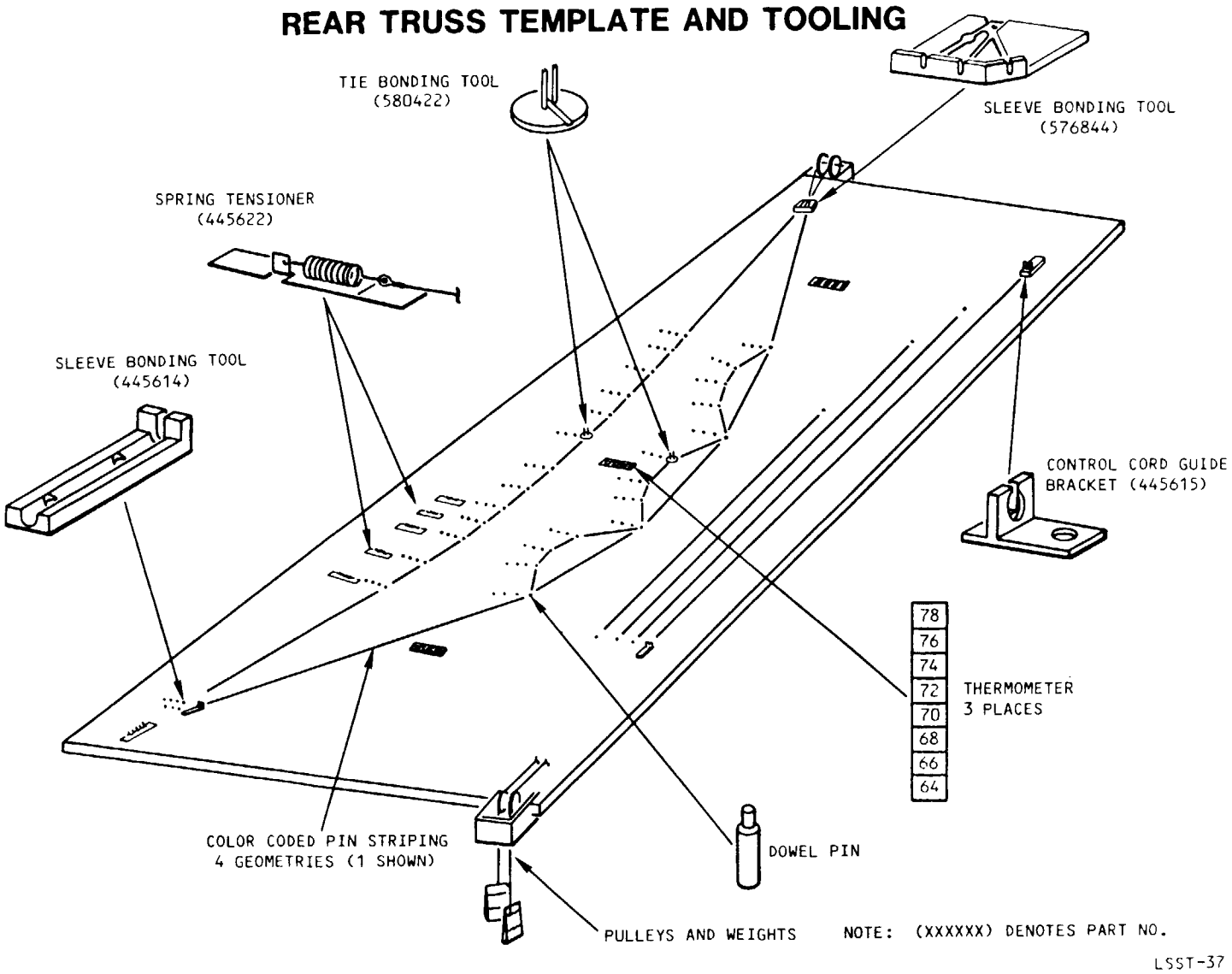

Figure 3.4.1-1.

This template and associated fixtures were used to manufacture the surface rear trusses.

TYPICAL REAR TRUSS BOND JOINTS

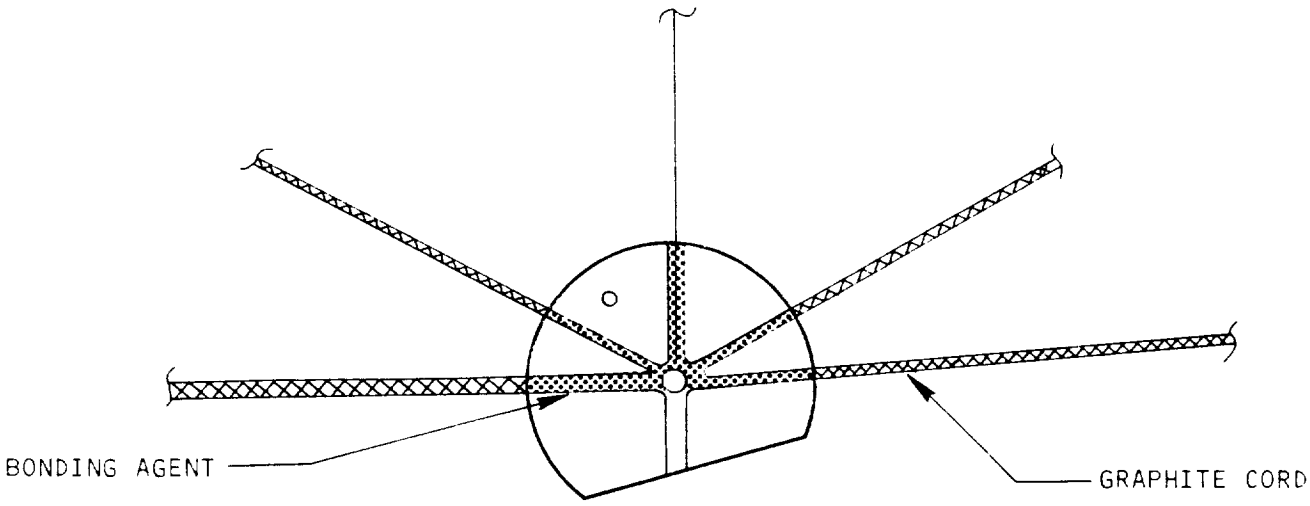

TYPICAL REAR TRUSS JUNCTION
FITTING BONDING

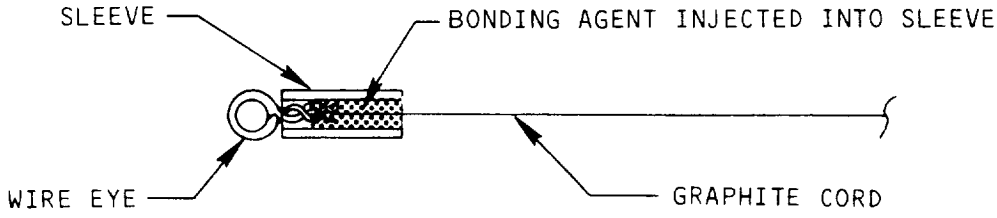

TIE BONDING

LSST-36

Figure 3.4.1-2.

During preliminary bonding operations one end of each cord is bonded to the appropriate fitting. The free end of each cord is final bonded on the template at a later step.

REAR TRUSS BONDING

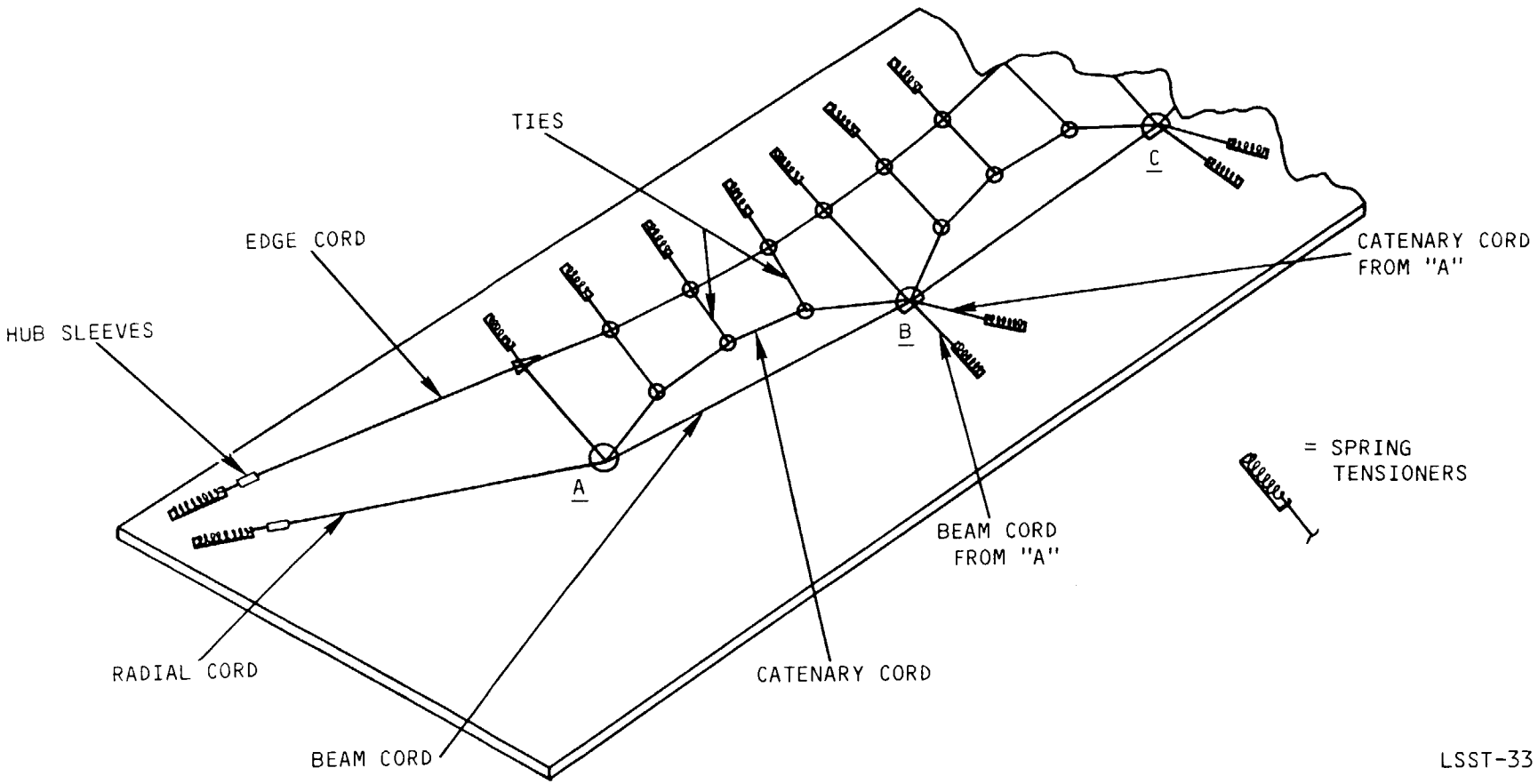

Figure 3.4.1-3.

During Truss final bonding, the radial, vertical tie, catenary and beam cords eminating from preliminary bonded fitting A are bonded under load at the hub sleeve, edge cord and fitting B. The remaining free ends of other cords (not shown) are bonded under load simultaneously.

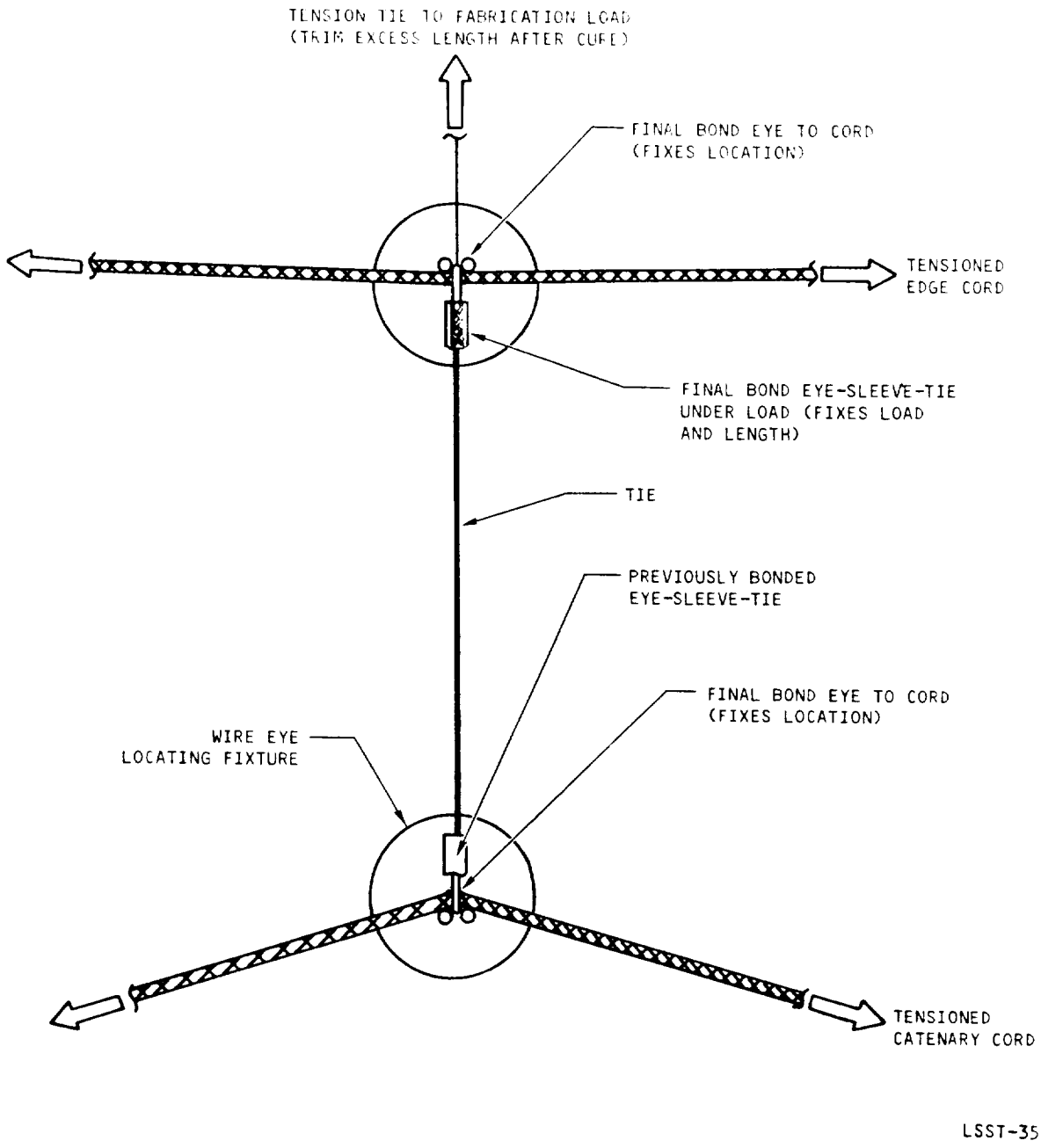

Figure 3.4.1-4.

Final bonding of truss vertical ties fixes their length, load, and location.

After a brief curing cycle, polyurethene adhesive was applied to the cord-fitting junctions to act as a strain relief, as shown in Figure 3.4.1-5. At this stage, each truss was set aside to allow the bonds to cure to full structural properties.

After a minimum bond curing cycle of 96 hours, each truss was proof loaded by applying 150 percent of the operational load to each cord. During the final stage of fabrication, each truss was enclosed in a nylon mesh snag shield as shown in Figure 3.4.1-6 and 3.4.1-7. Completed truss assemblies were then stored for use later during surface integration.

3.4.2 Surface Control Cords

The surface control cords were manufactured using the same processes used for the graphite hoop control cords previously discussed in Section 3.3. However, these cords were fabricated on the rear truss tooling template. After complete curing of the bonds, each cord was proof-loaded to twice its fabrication load to verify its structural integrity. Proof load induced stretching was measured after reinstalling each cord in the fabrication tooling. A total of 100 surface control cords were manufactured, 25 of each length with one set held in reserve as spare parts.

3.4.3 Diagonal Ties

Diagonal tie fabrication was performed on the tie tooling template and associated fixtures. This template was fabricated from a single sheet (96" x 48" x 1/4") of steel. After template painting and dowel pin installation were completed, the assembly and calibration of over 200 spring tensioners began.

As was the case for truss and control cord fabrication, the diagonal ties were fabricated under controlled conditions of load, geometry, and temperature.

The original tie design called for # 1/3 teflon coated graphite cord (1000 fibers), however, handling problems traced to defective material forced a change to a stronger #1 cord (3000 fibers). Representative tie bonding setups are

CORD STRAIN RELIEF

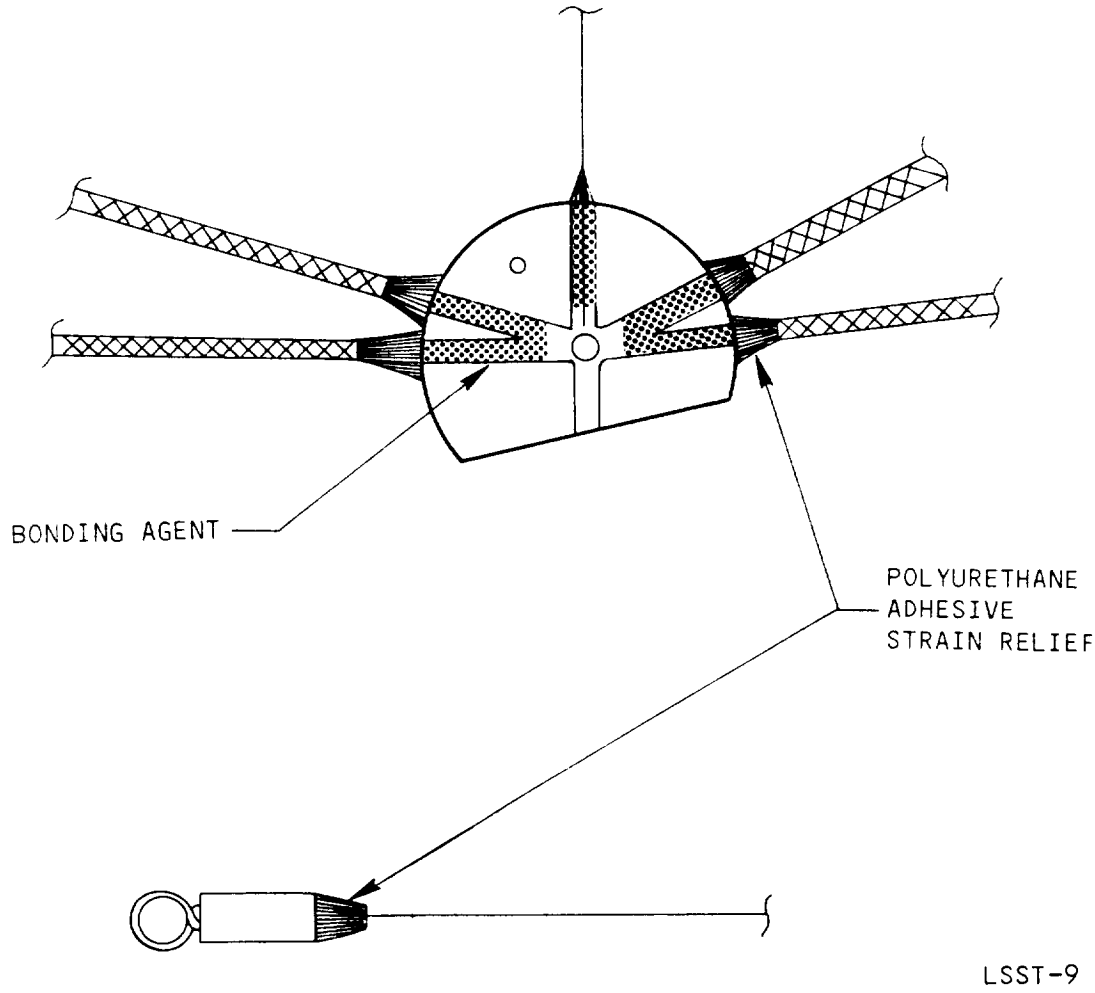

Figure 3.4.1-5.

To protect the cords near their exits from the fittings, Polyurethane adhesive was applied to the junctions to act as a strain relief.

84-22510

Figure 3.4.1-6.

A rear truss assembly is being fitted with a nylon mesh anti-snag shield. The shield will reduce the potential for entanglements of the truss on itself and other components during deployment of the completed antenna.

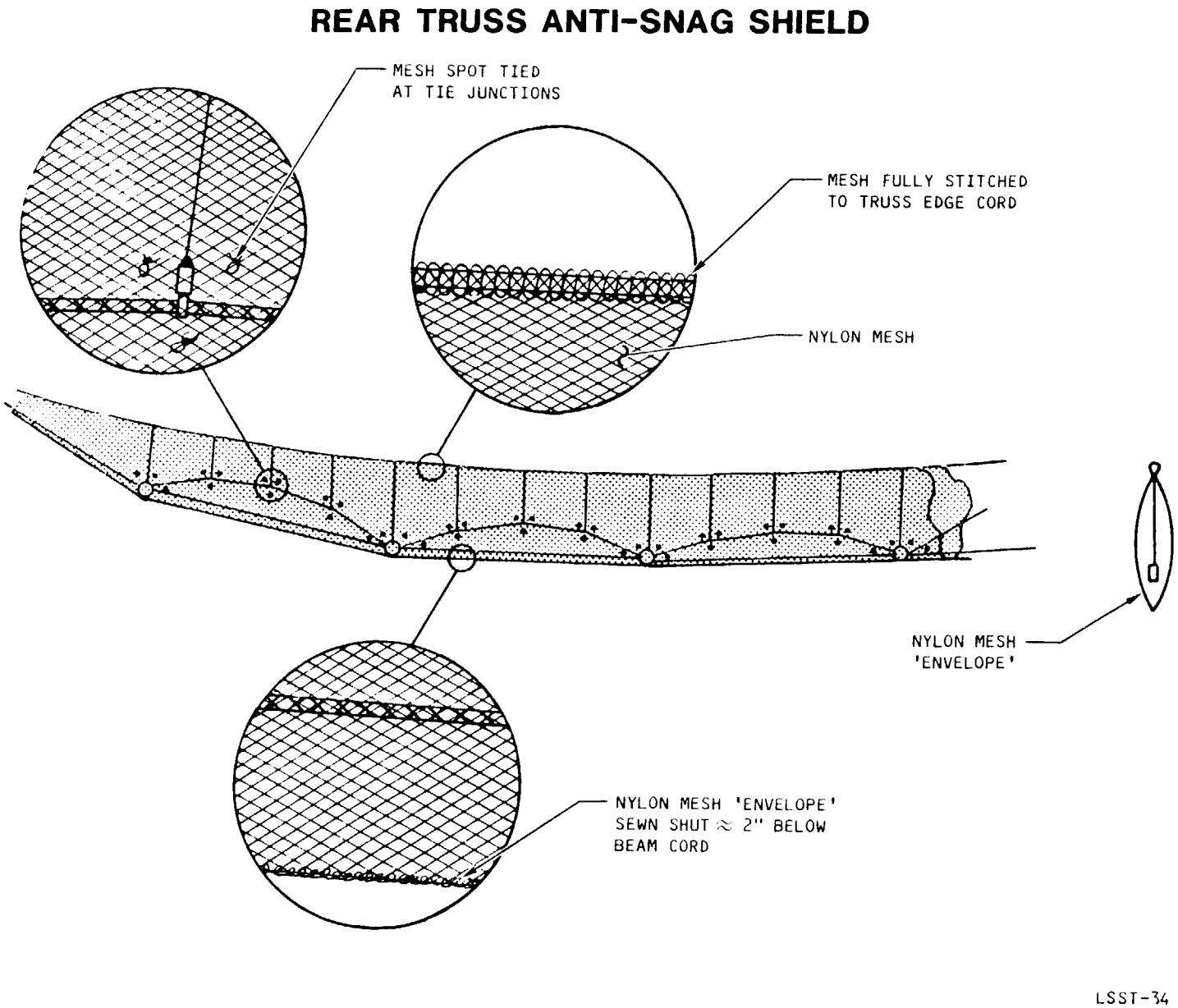

Figure 3.4.1-7.

The woven anti-snag shield forms an "envelope" ground each rear truss. By allowing the truss to float within the envelope, interaction between the truss and shield was reduced.

depicted in Figure 3.4.3-1. After bond curing, polyurethane adhesive was applied to each cord-junction interface for strain relief purposes. Each bond joint was then proof loaded to two pounds. Due to numerous bond failures of two tie configurations (Dwgs 576834 and 576836) it was determined that an improved process was needed. Experimental results indicated that the polyurethane adhesive being used for strain relief could replace the epoxy adhesive as the primary bonding agent. This eliminated the extra strain relieving step, allowing lost schedule time to be recovered.

In all, 288 diagonal ties of six configurations were completed and proofloaded. Approximately 2,000 individual bond joints were required.

3.4.4 Front Cord - Gore Assemblies

The 24 front cord-gore assemblies were manufactured using the special templates and associated fixtures depicted in Figure 3.4.4-1. Each quad aperture of the surface was assembled from six unique gores. Due to the mirror image symmetry within each aperture, only three templates were needed. That is, gores fabricated on one side of a template were the mirror image of those fabricated on the opposite side.

Each template was fabricated from a single sheet (252" X 84" X 1/4") of steel. These templates required the addition of full length stiffeners to maintain flatness and provide ease of handling. This was accomplished by bolting 4" X 4" lumber to the back sides of two templates. The third template, which exhibited more warpage, was stiffened using 8" X 2 1/4" X 6.5" "I" beams. After painting and stiffener addition were completed, NASA-Langley personnel verified the accuracy of template hole locations.

The front cord assemblies (Fig 3.4.4-1 and Fig 3.4.4-2) were fabricated using the same methods and materials used during rear truss fabrication. Preliminary bonded fittings and cords were located on the template using dowel pins. The free end of each cord was then routed to the appropriate fitting and loaded in tension using the previously calibrated tensioner and weight. Just prior to final bonding the front cord assemblies, each set up was inspected for proper loading, cord

DIAGONAL TIE FABRICATION

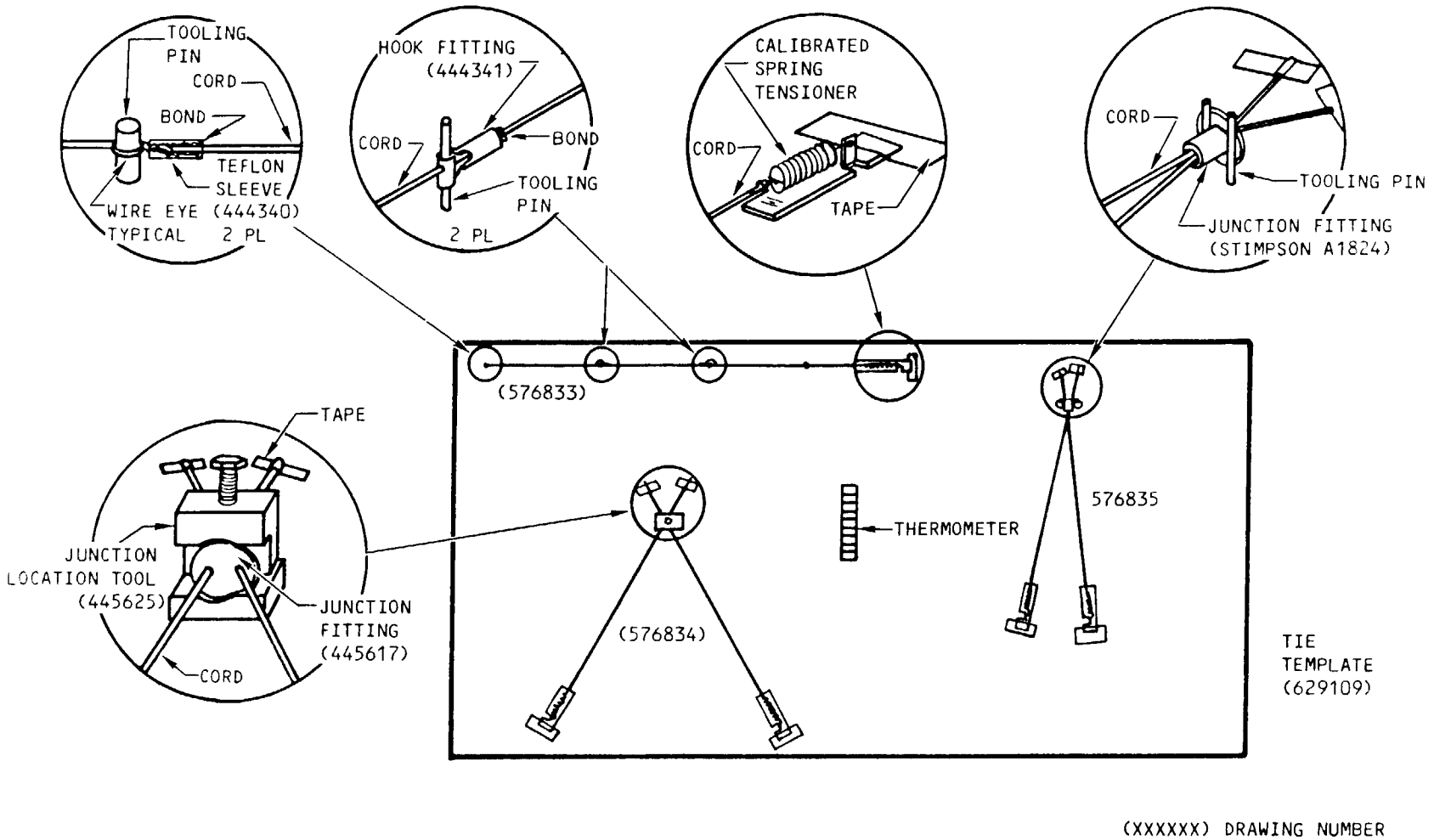

LSST-30

Figure 3.4.3-1.

Each ties junction and end fittings were located on the template using precision dowel pins. The cords were then tensioned to the appropriate fabrication load prior to bonding in place.

FRONT CORD BONDING TOOLING

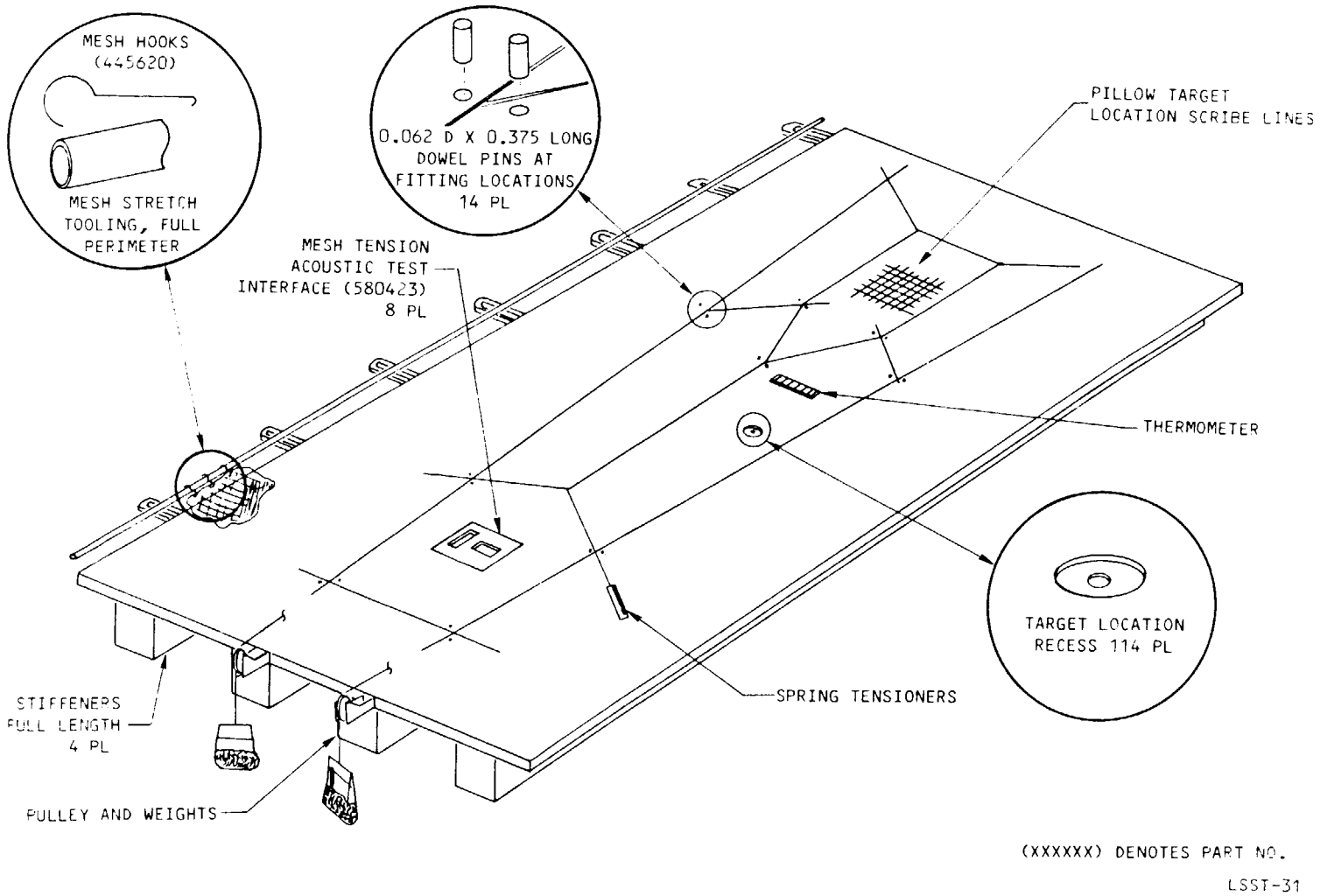

Figure 3.4.4-1.

The front cord-gore assemblies were fabricated to precise dimensions using these fixtures.

integrity and temperature. After a brief curing cycle, the front cord assembly was removed, and another set up and bonding operation began. This process was repeated until twelve front cord assemblies were produced (four assemblies from each of the three templates).

The bond joint integrity of these 12 assemblies was verified by proof loading to 150 percent of the operational load. As shown in Figure 3.4.4-2, this was a two step process. After proof loading, the front cord assemblies were returned to the template for diagonal tie installation and strain relief application. The next step was to attach the mesh.

Mesh attachment began by installing the front cord tie assembly to the template and placing the retroreflective targets adhesive side up into the counter bores. The previously cleaned mesh (bathed in Ashland brand Freon TF solvent) was then rolled out onto the template over the cord-tie assembly and hooked to the mesh stretch bracketry. This configuration is shown in Figure 3.4.4-3. Previous coupon testing of mesh samples defined the hole count pitch geometry obtained when the samples were loaded to .010 lbs/in. in the antenna radial direction and .020 lbs/in. in the antenna tangential direction. Thus, by stretching the mesh to the proper geometries, the approximate nominal tensions could be induced.

Measurements of the induced mesh tension were taken at eight locations within each gore using the Harris developed mesh tensiometer and checked against the acceptance criteria. Adjustments to the tension field were made by moving the rods holding the hooks as required to fine tune each setup. The effects of these adjustments were checked by remeasuring the tension field. This process was repeated, using the latest tension measurements to calculate the required adjustments, until compliance with the criteria was established. The algorithms, mathematical models, and theory of operation of the tensiometer, required to evaluate and adjust tensions in mesh are proprietary to Harris, and therefore not described in this report.

Upon acceptance of the tension field, plastic tape was applied over the mesh and pressed down to secure it to the template. This allowed the stitching operations to proceed without disturbing the tension field. The mesh was sewn to the cords using special glass fiber thread. All perimeter cords on the gore were tightly stitched to the mesh. The interior cords and ties were loose laced to the

FRONT CORD ASSEMBLY PROOF LOADING

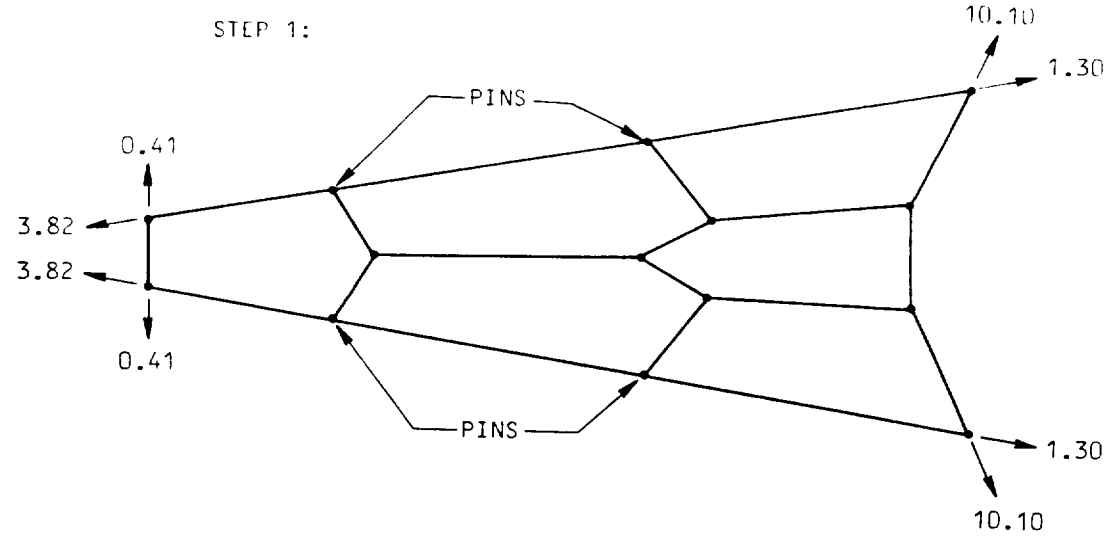

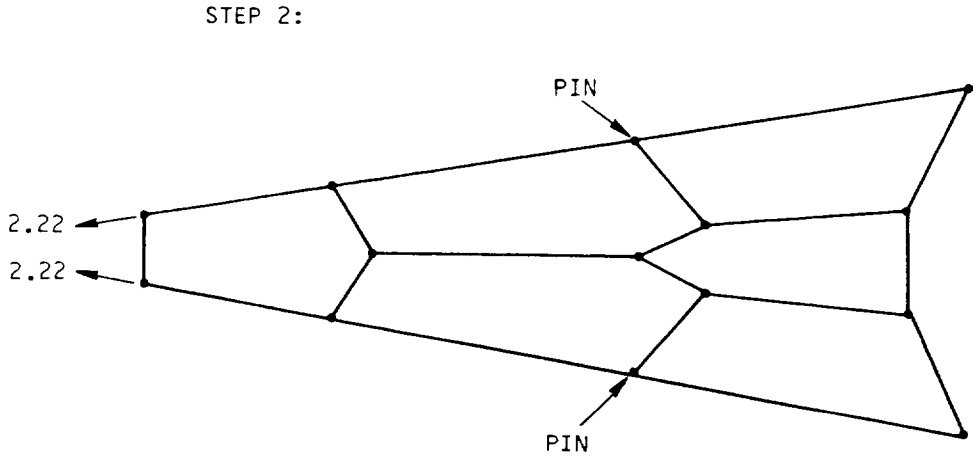

NOTE: ALL LOADS IN POUNDS,
HELD FOR FIVE MINUTES.

LSST-10

Figure 3.4.4-2.

Each front cord assembly was proofloaded to verify bond joint integrities. This process was accomplished on the tooling templates in two steps.

MESH STRETCHING

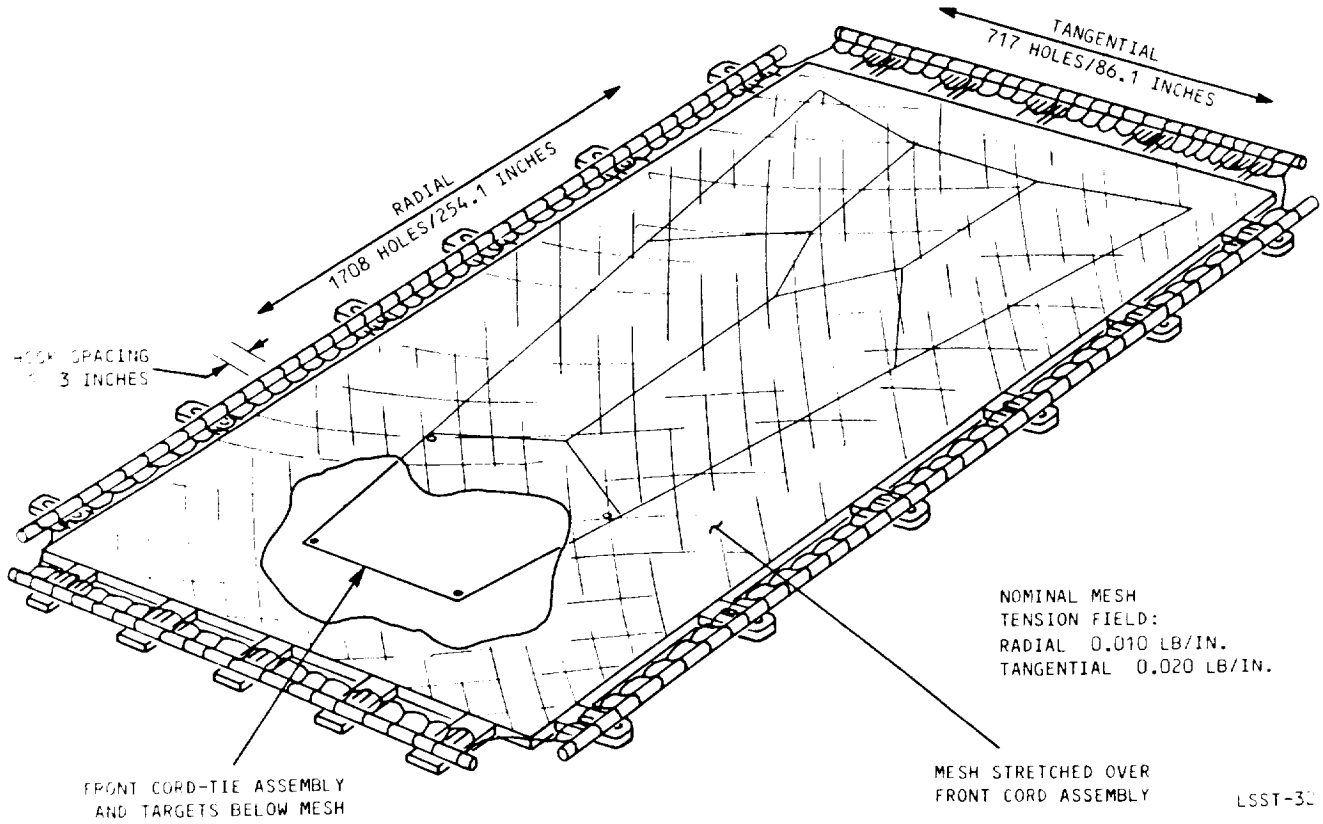

Figure 3.4.4-3.

The mesh was tensioned over the front cord assemblies by stretching to a prescribed geometry. The induced tension was verified by acoustic testing, with any required adjustments being made by moving the hook rods.

mesh by sewing over a .045 inch diameter wire rod. Upon removing the rod, the loose stitch was produced. Complete details of these operations are available in Appendix A3. Just prior to trimming the mesh along the perimeter cords, the rear side targets were installed by aligning them concentric to within .015 inches of the targets in the template counterbores.

The 1/4 inch diameter pillow targets associated with quadrant 1 were hand located on the mesh by aligning them over the scribed lines on the template. It is estimated that these targets are located within .04 inches of the requested positions. After removing the completed gore assembly from the fitting locating pins, it was proof-loaded as shown in Figure 3.4.4-4. This operation was performed to verify that the cords were not damaged during sewing operations. The diagonal ties within each gore were not proof loaded again.

These operations were repeated until four gore assemblies were produced from each of the three templates. The templates were then inverted and the stiffeners replaced on the back side. An additional 12 front cord assemblies were then bonded, proof-loaded, integrated with the diagonal ties, and stitched to the mesh as described above. These operations produced the required mirror image gores. The next step in surface manufacture was the final assembly to the previously completed rear trusses.

3.4.5 Surface Final Assembly

Final assembly of the surface gores and rear trusses were performed on a quadrant by quadrant basis. The four completed apertures were then integrated to form the total surface assembly.

The assembly of a typical aperture began by installing a rear truss into the slot of a specially designed gore final assembly fixture. This fixture, shown in Figure 3.4.5-1, was designed to hold the truss and gore edge cords in close proximity and under tension while they were sewn together. After positioning and tensioning the truss edge cord, the appropriate gores were laid onto the table tops adjacent to the truss slot. Their edge cords were tensioned and the junction fitting covers were installed as shown in Figure 3.4.5-2. Next, the truss and gore edge cords were sewn together along their entire length using a double reverse stitch. The mesh restow rings were then sewn onto the edge cord bundle at and between every rear truss vertical tie location. A tooling cord was routed

GORE ASSEMBLY PROOF LOADING

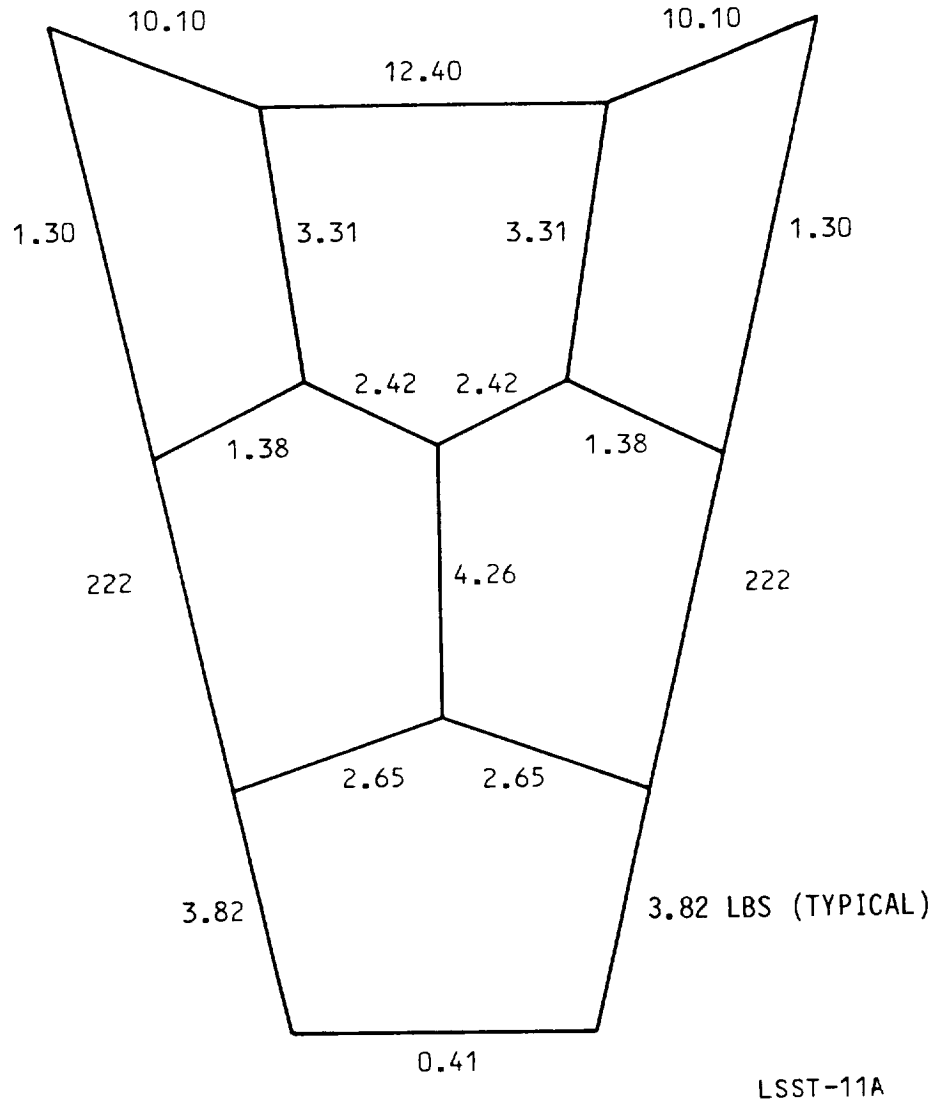

Figure 3.4.4-4.

Completed gore assemblies were proof loaded to verify their structural integrity prior to integration.

SURFACE FINAL ASSEMBLY FIXTURE

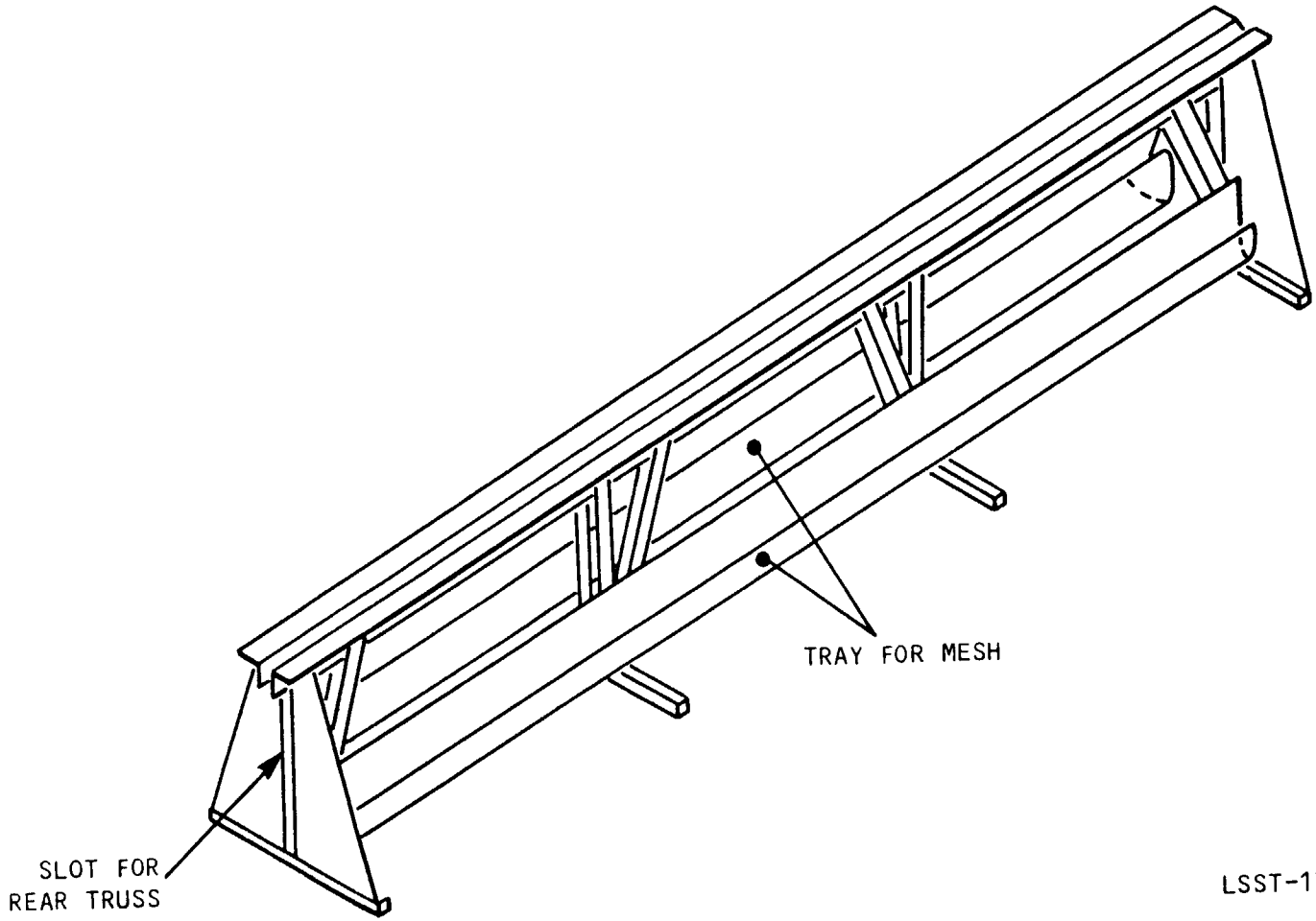

Figure 3.4.5-1.

This fixture was used to sew the gores and trusses together. A slot in the horse held the rear truss in position for sewing.

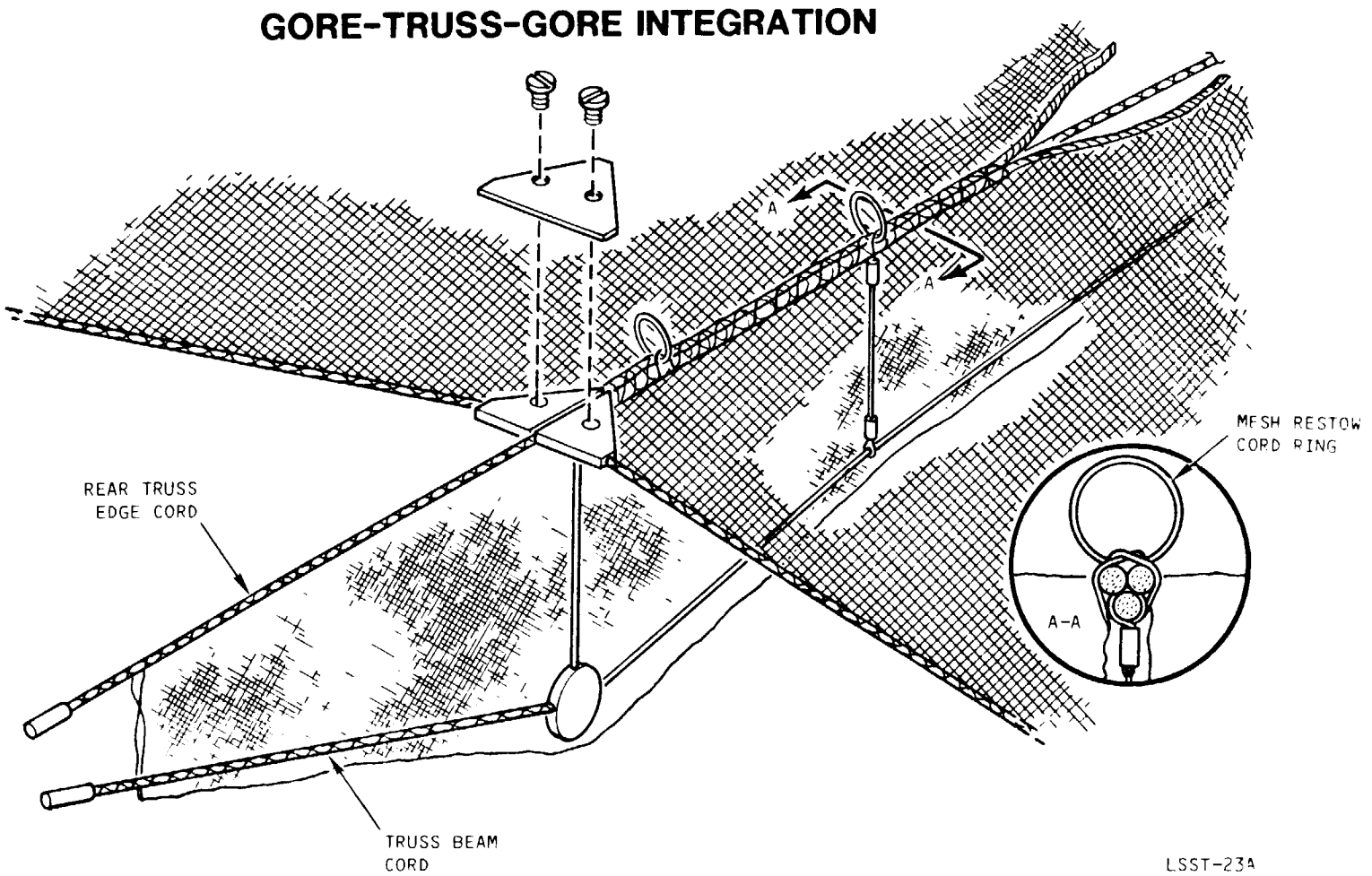

Figure 3.4.5-2.

Each rear truss was sewn between two gores using a double reverse stitch. The front cord hard points were joined with cover plates.

through these rings for later use during surface installation. After sealing all the seam knots with polyurethane adhesive, the gore-truss-gore unit was removed from the slot in the horse and placed into the tray. The next truss was placed into the slot and another gore brought into position for sewing. These operations were repeated until six gores and five trusses were sewn together, completing one aperture. After assembling the remaining three apertures, their boundary gore edges were sewn to the remaining trusses using the same methods. All but the last gore-truss-gore seam was sewn closed and the surface was stored until the structure was ready.

3.5 Preparation of Structure For Surface Installation

Prior to attaching the surface to the model, the hoop-column structure was prepared by performing modifications to the hoop and installing the anti-snag shielding.

Four additional drive joints were added to the hoop and eight new, high-torque motors were installed. Deployment and stowage testing indicated that the eight motors were not syncronized, yielding an eccentric hoop. Modifications to the wiring were suggested by NASA-Langley and implemented by Harris. Further testing determined that these modifications did not perform as desired and that an active control system would be needed. NASA-Langley then designed, installed, and tested an electronic control system that solved this problem.

To preclude entanglements between the surface and structure, anti-snag shields were installed to the column and the hoop. The stationary column hub segment was wrapped tightly in polyurethane film, and secured with transparent tape, as shown in Figure 3.5-1. Additional taping of screw heads and other potential snag areas completed preparation of the column. As shown in Figure 3.5-2, the hoop segment snag shields prevent the surface from becoming entangled with the synchronization rods and hinge platforms. These shields were fabricated from 10 mil clear mylar sheet which was bonded to a styrene support rib. Attachment to the hoop segments was with eight equally spaced nylon cable ties passing through slotted holes in the rib. The hoop platform cord interface fitting was covered using a 7 inch diameter plastic foam hemisphere, slotted to allow the cords to exit. The hoop shielding further serves to contain the surface within the stowed hoop. As the hoop segments stow, the shields overlap, forming a continuous ring between the hoop and mesh.

COLUMN ANTI-SNAG SHIELDING

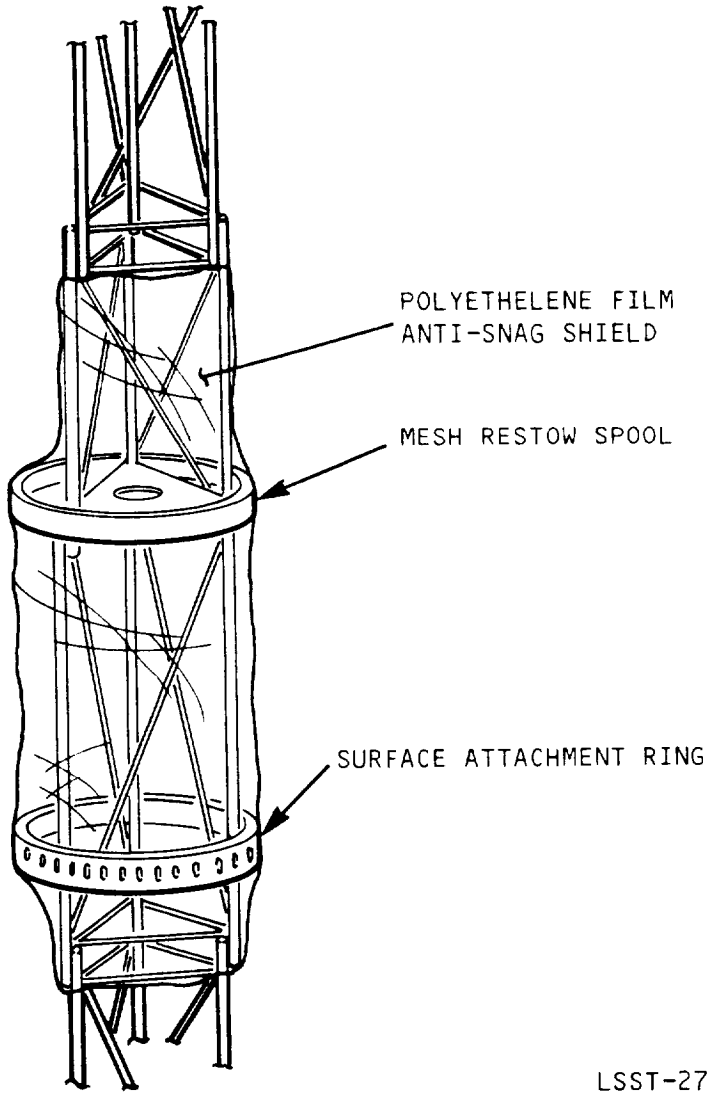

Figure 3.5-1.

The stationary column segment was covered with polyethelene film to prevent mesh and cord entanglements.

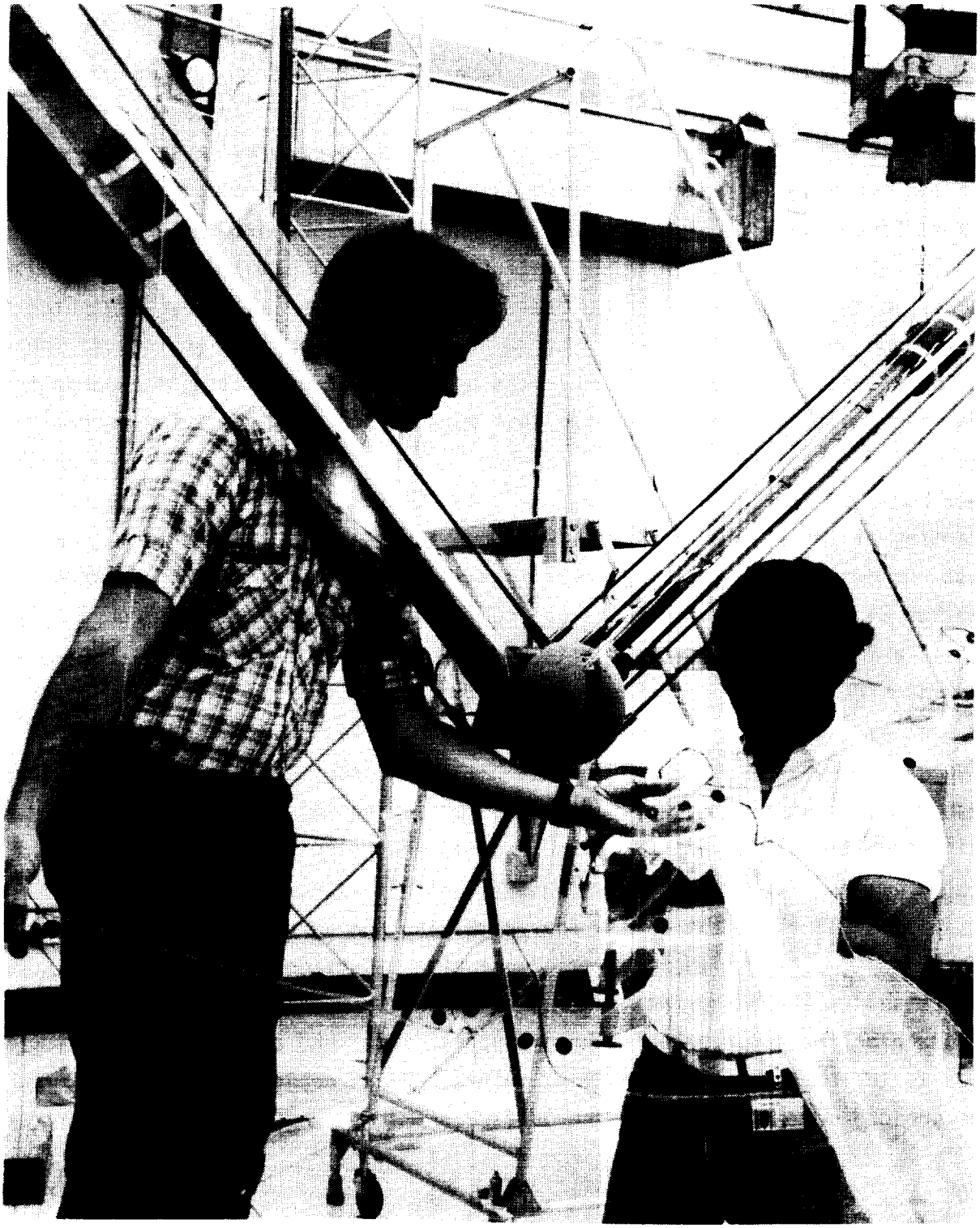

Figure 3.5-2. 85-0396CMR-1-3

The hoop segment anti-snag shields prevent entanglements between the surface and the inboard synchronization rods. These clear mylar sheets were secured to the hoop using cable ties passing through the shield support rib. The hinge platform cord interface fitting was covered with a slotted plastic foam hemisphere.

3.6 Surface Installation

Prior to installing the surface to the structure, the column and hoop were partially stowed. The radome floor was then completely covered with polyethelene film to prevent contamination of the mesh. While still connected to the counter balance system, the hoop was lowered to the floor and secured. Next, the surface assembly was placed on the floor and rolled out as shown in Figure 3.6-1. A large gap (the location of the final seam) was left to allow access to the column area without having to walk on the surface. Beginning near the column and working outward, the 23 restow cords were pulled through the rings on the previously sewn seams. This was accomplished by pulling the cords through with the tooling cables placed for this purpose during the seaming operations. The restow cords were terminated at each hoop joint platform. Then, a modified gore horse and the last rear truss were positioned to sew the final surface seam. Starting at the column, this seam was sewn shut about 24 inches at a time. The last restow cord and the rings were installed prior to continuing outward another 24 inches. This process was continued until the seam was completely closed and the restow cord was attached to the hoop joint platform. Next, working from outside the hoop, the surface was attached by installing the interface sleeves at the hoop platform fittings. The hoop was then raised approximately eight feet above the floor and held there by the counterbalance system. Then, the mesh restow system motor was energized, retrieving the restow cords onto the drum while simultaneously raising the surface to the height of the hub attachment ring. Raising the hoop an additional seven feet allowed a sixteen foot ladder to be located alongside the column for installing the surface to the negator spring blocks located within the hub attachment ring. Surface installation was completed by installing the 96 surface control cords in their rear truss fittings, reattaching the lower graphite hoop support cords, and connecting the diagonal ties to their rear truss attachment points. Final deployment of the column, hoop, and preload segment tensioned the surface.

4.0 TESTING

Testing conducted during the manufacturing process was performed on major subsystems, the integrated hoop-column structure (without surface), and the complete antenna. These tests are described separately below. Anomalies that arose during testing are mentioned here but fully described in Section 5.0.

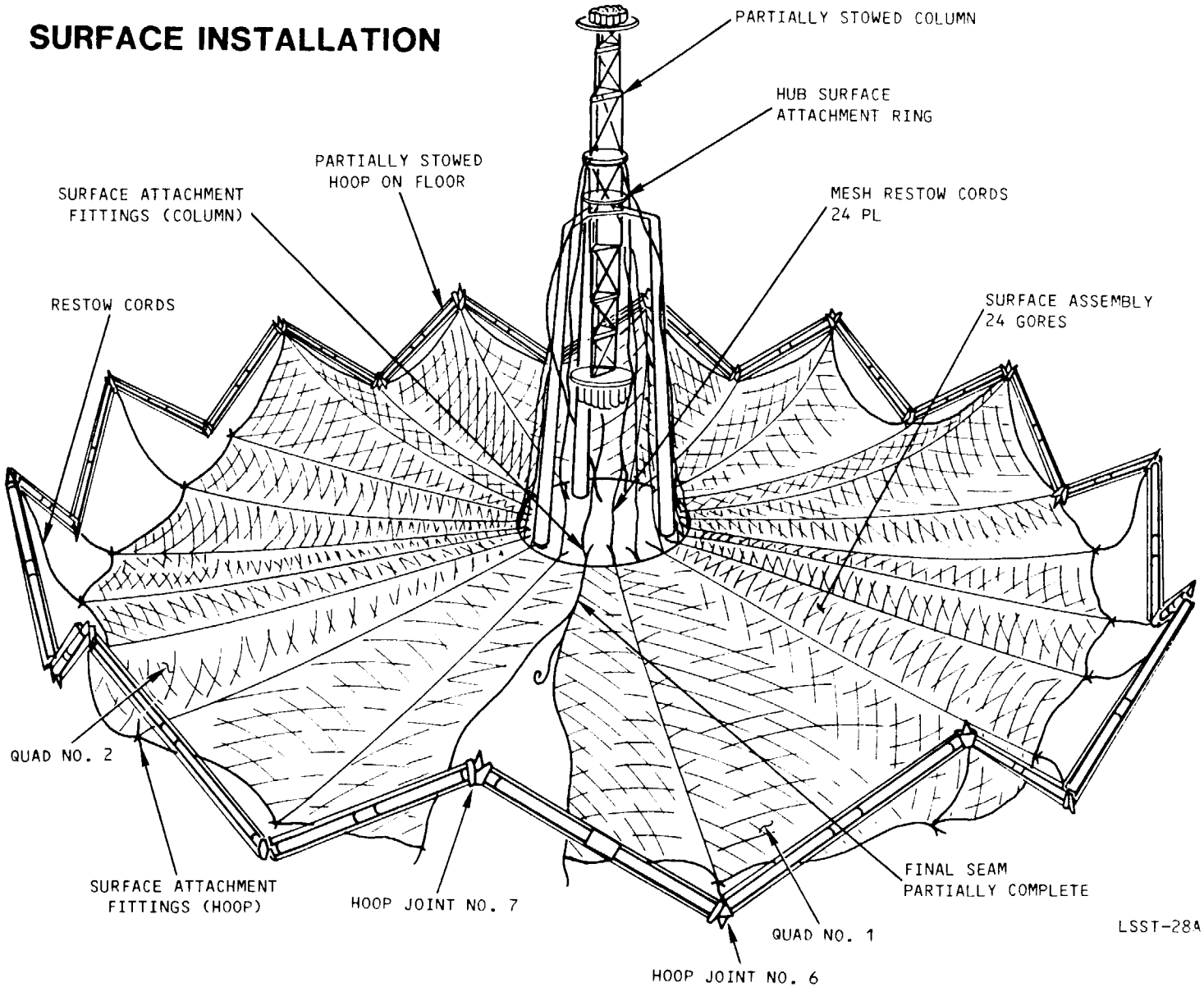

Figure 3.6-1.

After closing the final seam and attaching the surface to the hoop, the mesh restow drive was activated to pull the surface up to the hub attachment ring.

4.1 Subsystem Testing

The testing of individual subsystems included the functional checks of mechanisms and proof-loading of primary load path structural elements. In most cases these tests were performed as part of the normal fabrication sequence and are discussed fully in Section 3.0. This section describes the proof-load testing of the column, model pedestal and the counterbalance system. These tests were performed in accordance with Harris Corporation written procedures, copies of which are on file with NASA-Langley.

4.1.1 Counterbalance System Proof-loading

The counterbalance assembly (Dwg 627453) consists of a 53 foot diameter ring structure fabricated from 24 segments of six inch diameter aluminum pipe. Twenty-four radial cables connect the ring to the central hub which is supported by a winch during use. The ring assembly is supported over the antenna by eight 53 foot tall towers. This system supports the extendable column segments and the hoop during deployment and restow, and being the primary load carrying structure during these operations, required proof-loading prior to acceptance for use.

As shown in Figure 4.1.1-1 the ring assembly was restrained to the floor by being heavily weighted at each radial cable interface using lead shot bags. The central hub was connected to the overhead winch through a sling and a load gauge. By raising the hub with the winch, the tension loads in the sling and radial cables were increased in steps and correlated to the hub height above the ring by reading the scale. The initial radial cable tension, was 110$\pm$ 10 lbs with the cables level. The hub height at this position was established as zero. The hub was then raised in 100 lb increments (read on the load gauge) until the radial cable tension increased to 540 lbs. These loads were held for 15 minutes at which point the hub was lowered to 15 inches above the ring. The radial cables were then adjusted to 170 lbs nominal tension. This hub height-radial cable tension configuration was established as the maximum safe operating condition of the system. Thus, the counterbalance was proof-loaded to four times the maximum operational load.

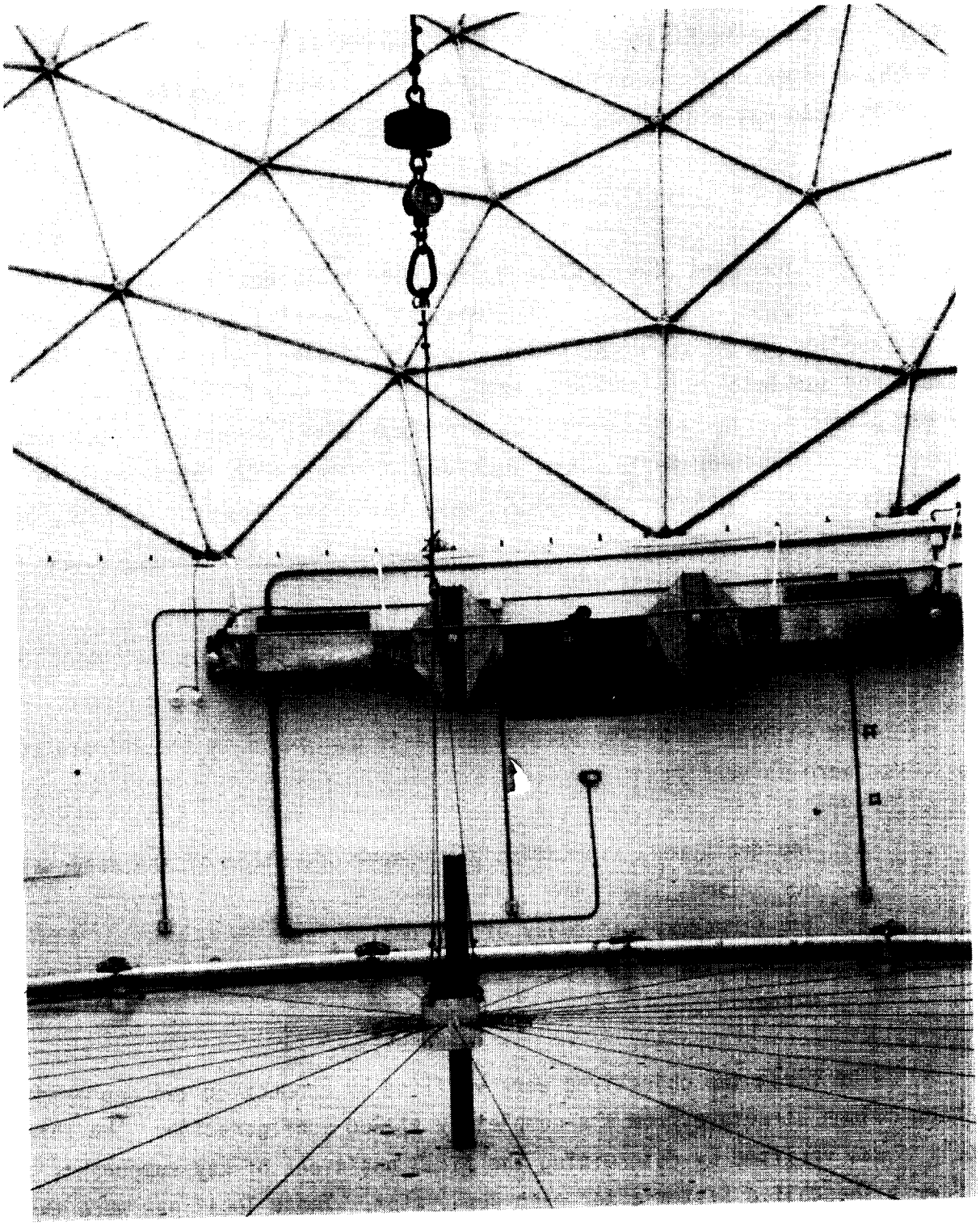

84-1116C

Figure 4.1.1-1.

The counterbalance ring and cable assembly is being proofloaded prior to installation. The central winch provides the radial loads when raised.

4.1.2 Pedestal Proof-loading

The pedestal was assembled and proof-loaded per Harris Procedure HTS-4003. As shown in Figure 4.1.2-1, the compressive load of 1550 lbs was applied by tightening a nut on the threaded rod which was anchored to the radome floor. The load was read on a gauge and held for 15 minutes.

4.1.3 Column Proof-loading

The upper and lower column halves were individually proof-loaded per Harris Procedures HPP-2003 and HPP-2004 respectfully. The compressive load of 775 lbs. was applied to the deployed lower column and preload segment using the threaded rod and load gauge shown in Figure 4.1.3-1. A scale, graduated to 10 mils was placed horizontally on the cable stowage drum platform. As the load was increased in 100 lb increments, this scale was observed with theodolites to monitor any lateral movement which could have indicated impending buckling of the column. The upper column assembly was proof-loaded in a similar manner to 1270 lbs in compression. The loads were held for 15 minutes.

4.2 Structural Testing

The objectives of the structural tests performed on the integrated hoop-column were to verify:

- The deployment kinematics and proper operation of the associated mechanisms,
- the structural adequacy of the design, and
- the ability of the structure to deploy in a repeatable, controlled manner.

The first two objectives were verified by conducting two deployments of the hoop-column structure from the completely stowed configuration. The third objective was verified by determining the final positions of key components using the Harris Theodolite System after each deployment. These locations were then compared to evaluate deployment repeatability. Deployments of the structure and the results of the theodolite measurements are discussed separately below.

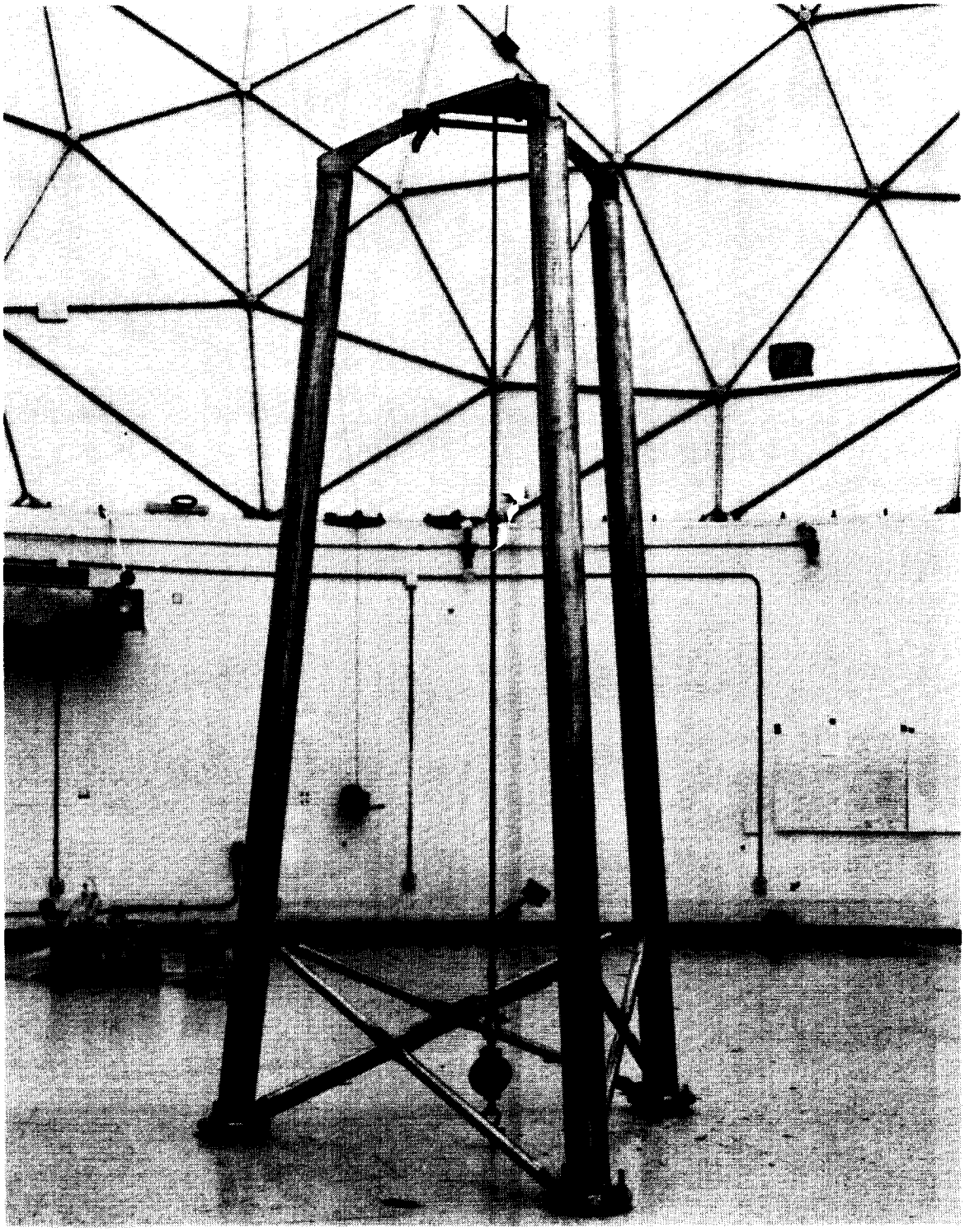

84-090

Figure 4.1.2-1.

The model pedestal was proofloaded in compression by tightening a nut on the threaded rod passing through the pedestal's centerline.

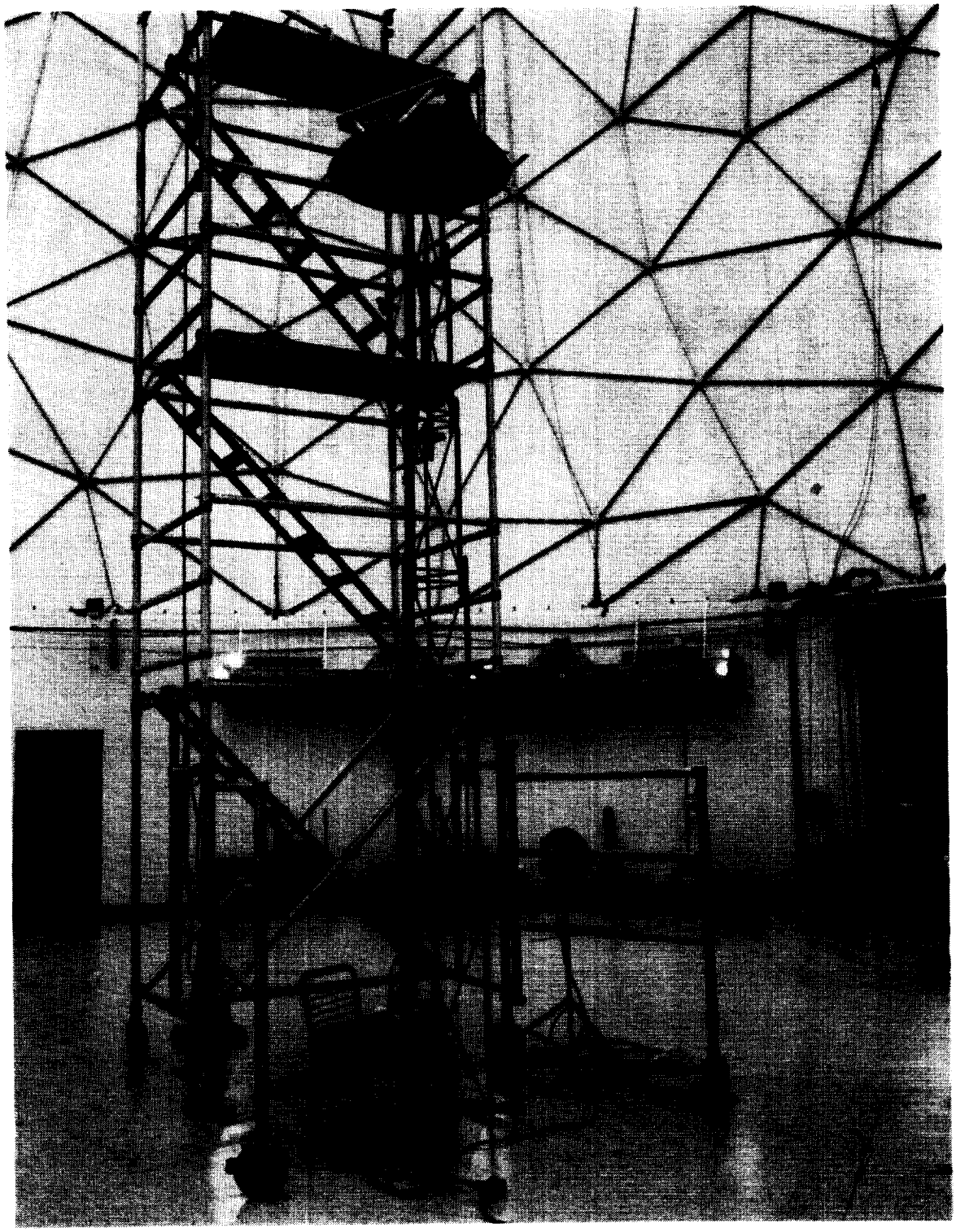

Figure 4.1.3-1. 84-1009C

The inverted lower column assembly was proofloaded in compression prior to final assembly.

4.2.1 Deployment Testing of the Hoop-Column Structure

Two deployments of the hoop-column structure were performed in accordance with the 15-Meter Hoop-Column Structural Test Plan which is on file with NASA-Langley. For these tests, the model was in its originally designed configuration, having only four motor driven hoop joints. Each deployment began from the completely stowed condition as shown in Figure 4.2.1-1.

Deployments of the column proceeded without difficulty. The column drive system motor ran smoothly during column segment latchout. One of the lower-most column latches failed to engage completely and is discussed in Section 5.0.

Hoop deployments were frequently interrupted by over-current conditions in the motors. Deployment was automatically stopped when the console sensors determined that the total current drawn by the hoop exceeded 3.0 amperes. It was determined that the "sag" in the counterbalance radial cables was greater than expected. By raising the central hub, as shown in Figure 4.2.1-2, the slope of these cables assisted the trolleys outward and reduced the inward radial load on the hoop. Although the included angles between hoop segments remained roughly equal, observation of the synchronization rods indicated that the four hoop motors were not in perfect synchronization. This was also verified by readings of the motor revolution counters. Hoop deployment continued as shown in Figures 4.2.1-3 through 4.2.1-5 until terminated by the limit switches associated with each motor driven joint.

Deployment of the preload segment was conducted in steps to allow lower hoop support cord tension measurements. Deployment of the preload segment was terminated by the limit switch. After releasing the model from the counterbalance system, structural measurements were taken.

4.2.2 Structural Measurements

The primary objective of the structural measurements was to verify absolute locations of key points on the antenna. The antenna was restowed and deployed between measurements to also assess repeatability. The first measurement occurred on August 3, 1984 and the second on August 27, 1984.

84-13.6 MR

Figure 4.2.1-1.

The stowed hoop-column structure has been prepared for its first deployment.

COUNTER BALANCE ADJUSTMENT

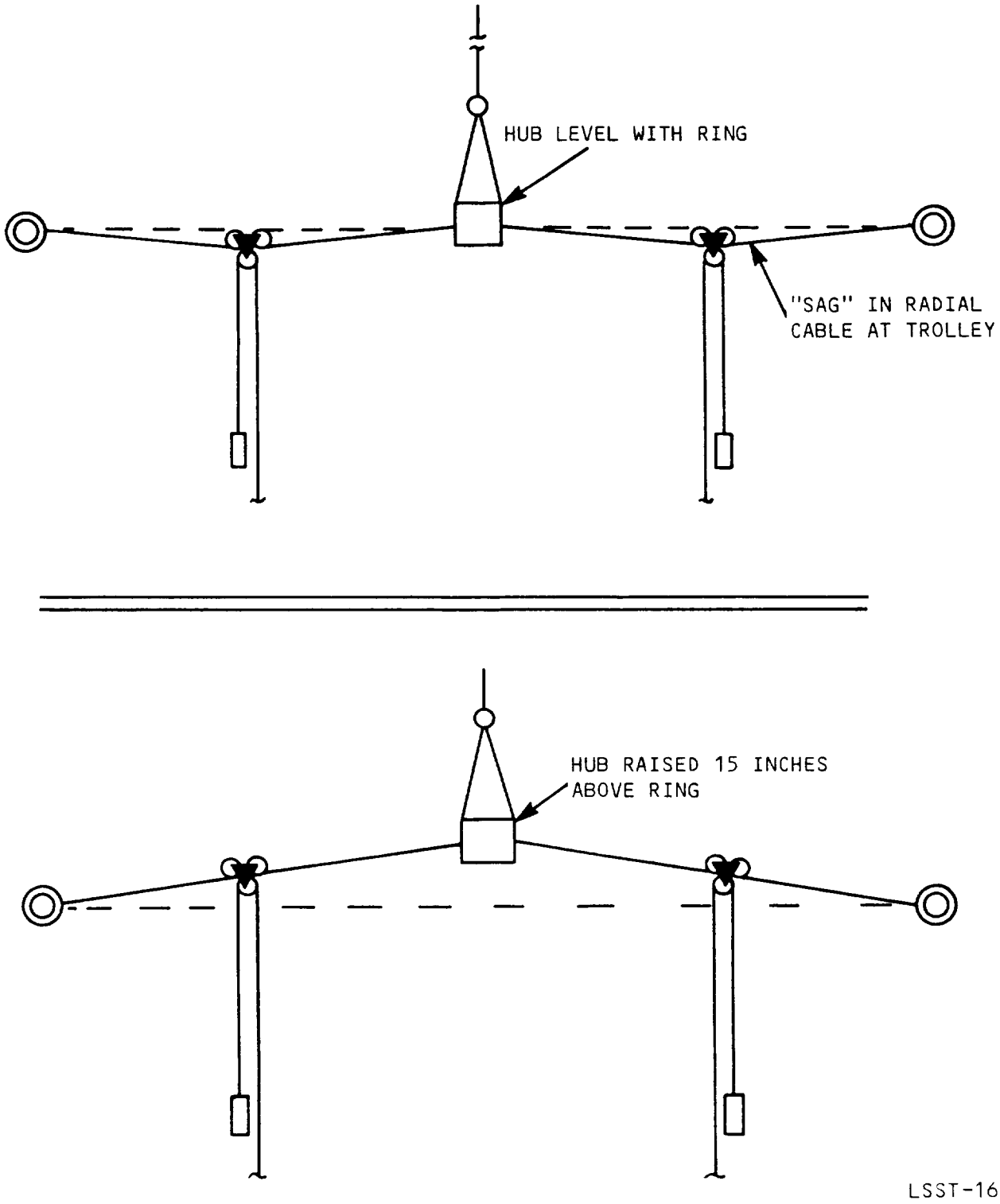

Figure 4.2.1-2.

Hoop deployments were aided by raising the central hub (below) to reduce cable "sag" (above).

C-2

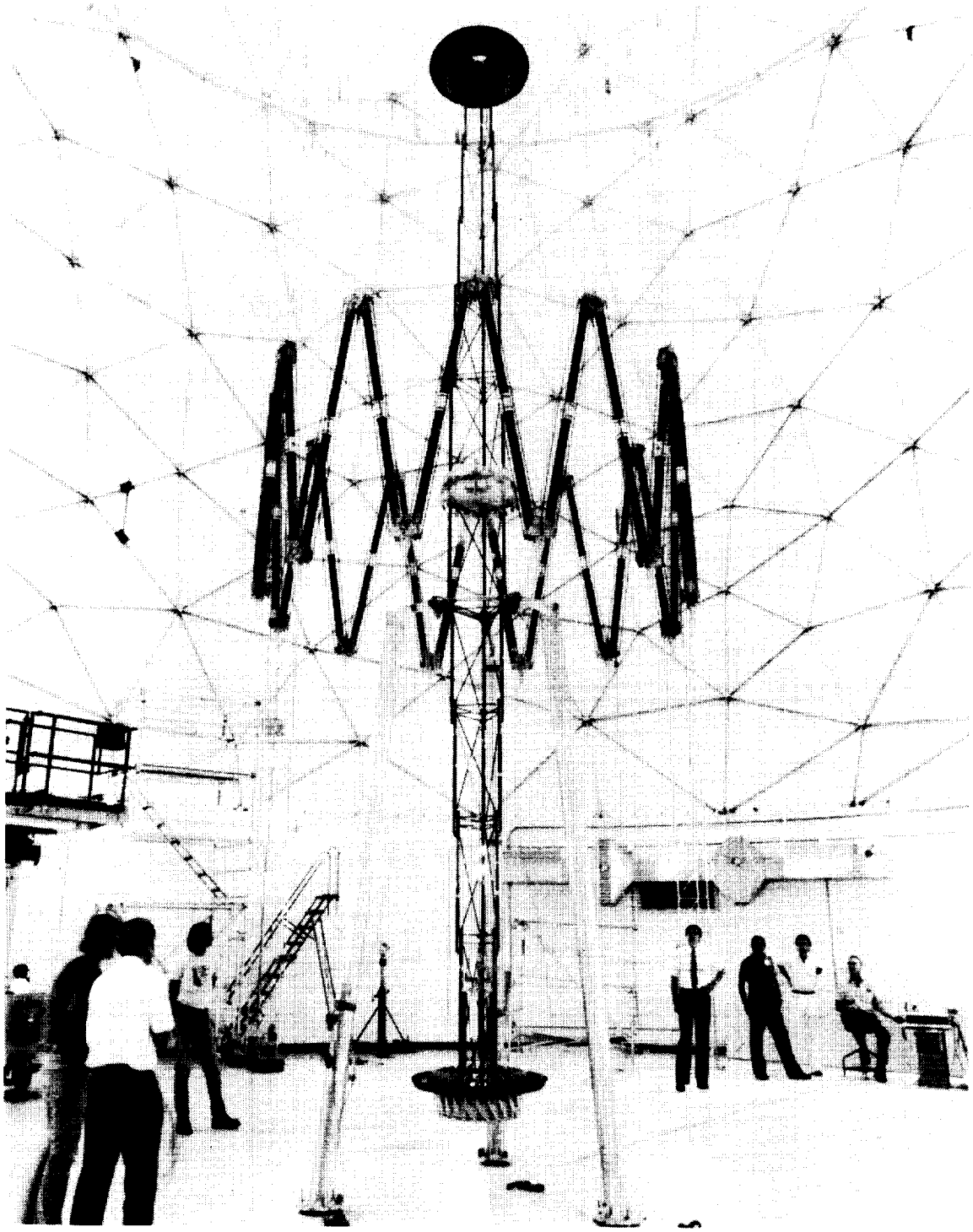

84-1610CMR-1-8

Figure 4.2.1-3.

The column has been completely extended and the hoop deployment has begun. Equal angles between the hop segments indicate a symmetrical deployment.

84-1610 MR-1-10

Figure 4.2.1-4. The hoop is approximately 75 percent deployed. Again, equal angles between the hoop segments indicate a symmetrical deployment.

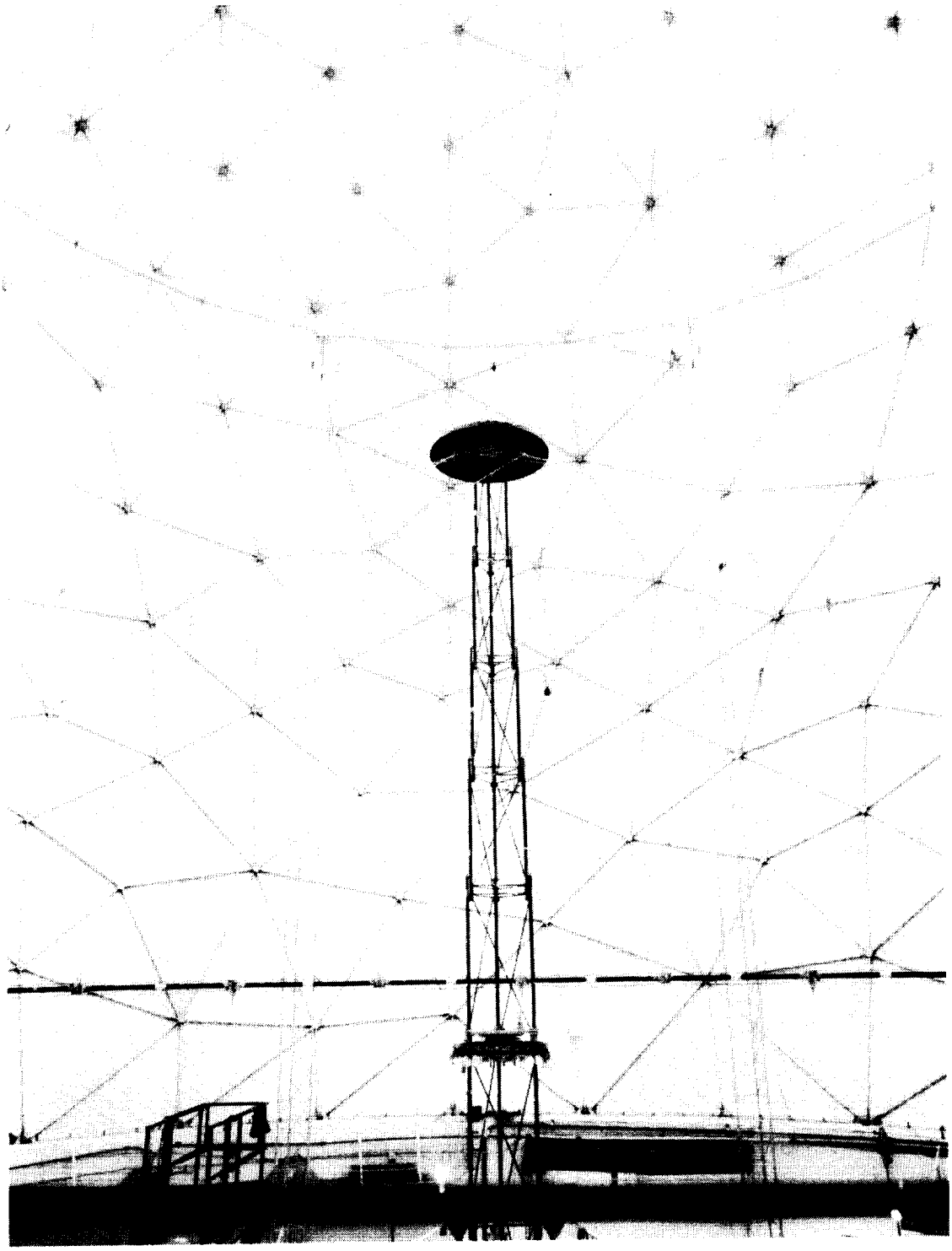

Figure 4.2.1-5. 84-1610CMR-3-10

The hoop deployment is complete. Due to its large diameter it was difficult to photograph completely.

An isometric view of the measured structure is shown in Figure 4.2.2-1. Key targets were located on the extremities of the column and at each of the hoop segment interfaces. Targets were also located on the hub restow assemblies.

The ideal locations for each of the 36 targets (in the antenna coordinate system) are shown in Table 4.2.2-1. These tolerances were accounted for in the overall surface budget also shown in this table which reflects an overall surface RMS goal of .069 inches.

The structure was measured by means of a manual theodolite system. Four theodolites were located 90° apart around the periphery of the antenna to provide a single setup for the entire measurement process. Each theodolite is accurate to within .002° of arc.

To evaluate the structural measurements, the test data were converted from an arbitrary theodolite reference system to the antenna coordinate system. A regression or "best fit" technique was used in which the error between the measured coordinates and the ideal predicted coordinates was minimized. The regression process consists of finding the set of translations and rotations required to convert the measured coordinates from the theodolite system to the antenna system such that the error between the converted coordinates and the ideal coordinates is minimized. Refer to Appendix A2 for a more detailed explanation of the regression process.

In determining the absolute locations of the targets the entire target set was used in the regression process. In resolving the repeatability errors, the August 3 hoop target set was used as a reference. It may also be noted that both data sets were converted to the antenna coordinate system prior to the repeatability regression process.

The following sections document the results of the two measurements. These sections are followed by a brief discussion of these results, and finally, conclusions based on these results.

STRUCTURE TARGET LOCATIONS

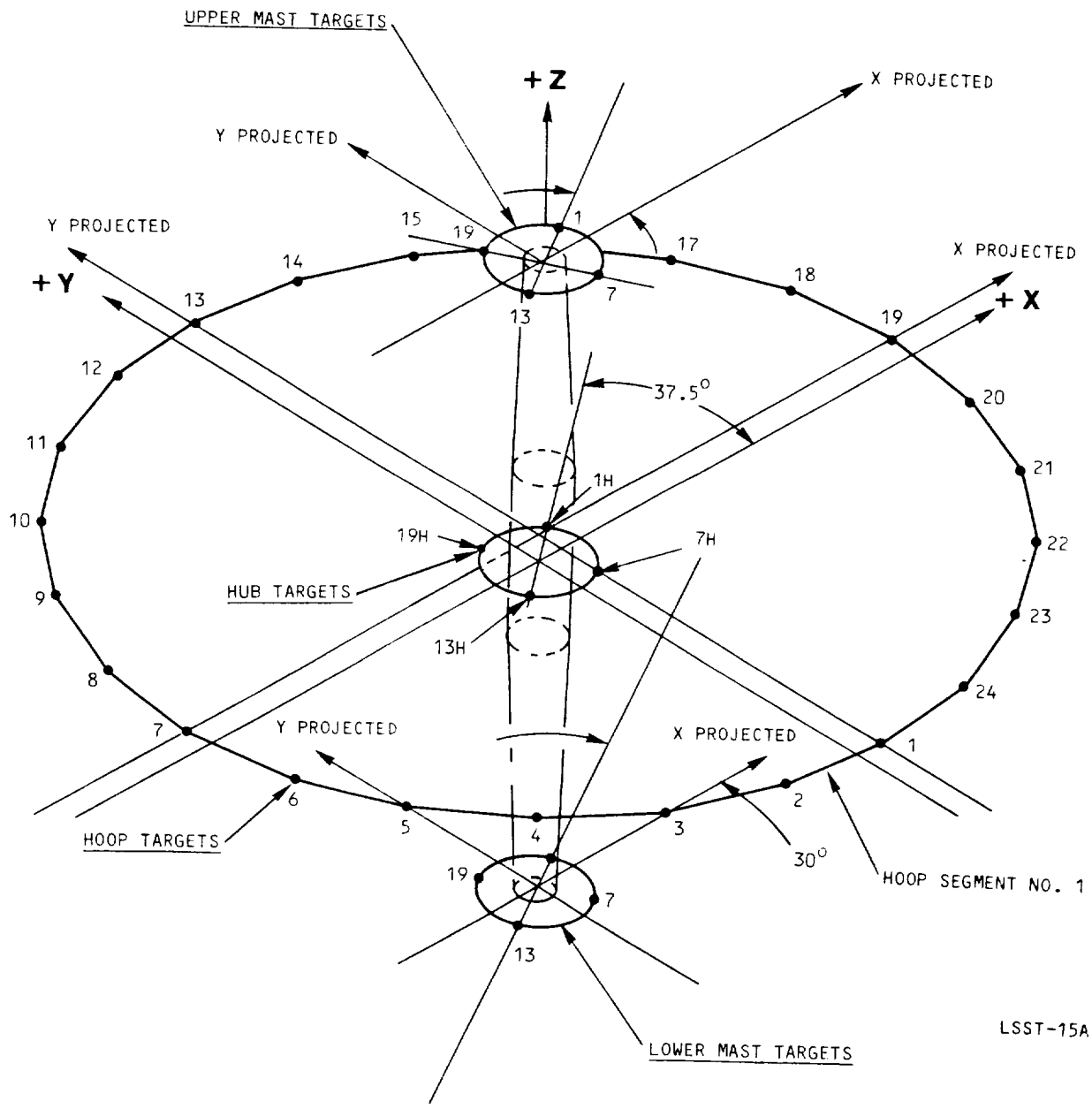

Figure 4.2.2-1.

Targets were located at key points on the structure to evaluate absolute locations and repeatability of the deployed hoop-column.

Table 4.2.2-1. Theoretical Target Locations

1. Upper Column Targets

No.	X	Y	Z
01	10.392	6.000	178.347
07	6.000	-10.392	178.347
18	-10.392	6.000	178.347
19	-6.000	10.392	178.347

2. Hub Targets

No.	X	Y	Z
01	10.286	7.383	0.000
07	7.893	-10.286	0.000
13	-7.893	10.286	0.000
19	-7.893	10.286	0.000

3. Lower Column Targets

No.	X	Y	Z
01	12.546	7.244	-193.184
07	7.244	-12.546	-193.184
13	-12.546	-7.244	-193.184
19	-7.244	12.546	-193.184

4. Hoop Targets

No.	X	Y	Z
01	0.000	-291.148	15.628
02	-75.355	-281.228	15.628
03	-145.574	-252.142	15.628
04	-205.873	-205.873	15.628
05	-252.142	-145.574	15.628
06	-281.228	-75.355	15.628
07	-291.148	0.000	15.628
08	-281.228	75.355	15.628
09	-252.142	145.574	15.628
10	-205-873	205.873	15.628
11	-145.574	252.142	15.628
12	-75.355	281.228	15.628
13	0.000	291.148	15.628
14	75.355	281.228	15.628
15	145.574	252.142	15.628
16	205.873	205.873	15.628
17	252.142	145.574	15.628
18	281.228	75.355	15.628
19	291.148	0.000	15.628
20	281.228	-75.355	15.628
21	252.142	145.574	15.628
22	205.873	-205.873	15.628
23	145.574	-252.142	15.628
24	75.355	-281.228	15.628

PREDICTED TARGET LOCATIONS

Sensitivity	Allowable Error (Inch)
Column Length Variation	0.100 (Total Length Change)
Column Eccentricity	0.250 (at each end)
Hoop Vertical Variation	0.100
Hoop Radial Variation	0.050

Budgeted Errors for a .069"RMS surface deviation

The ideal locations of the targets as well as their permissable errors for a .059"RMS surface deviation were defined prior to measurement.

4.2.2.1 Measurement #1

The first structural measurements were taken on August 3, 1984. Error components for each of the target locations are shown in Table 4.2.2.1-1. Errors of concern were in the upper column and hub where Z errors were as high as -.209 inches.

4.2.2.2 Measurement #2

The results of the second measurement which occurred on august 27, 1984 are shown in Table 4.2.2.2-1. Again, the largest errors were found in the hub region where they ranged from -.116 to +.218 inches in the Z direction and from -0.145 to +.176 inches in the Y direction.

4.2.2.3 Measurement Discussions

Table 4.2.2.3-1 contains the errors for the August 3 and august 27 deployments, expressed as X, Y, and Z RMS values. The target errors were combined for each of the four main target locations. The results of the two measurements were converted into the budgeted component directions shown in Table 4.2.2-1. Table 4.2.2.3-2 compares the actual errors with the budgeted allowables. The column length variation was calculated by summing algebraically the Z deviations and averaging the results. Column eccentricity and hoop radial variation were derived by taking the square root of the square of the RMS X and Y values for those particular areas. Hoop vertical variation is simply the RMS of the Z errors.

Table 4.2.2.3-3 shows the results of the repeatability regressions. Upon evaluation of the repeatability target errors it was determined there was possible bowing of the column from one deployment to the next, creating a relative movement between the hoop and the hub. Movement of this type was anticipated during the design phase; consequently, the surface radial cords are attached to the column hub by 48 constant-force negator spring assemblies, allowing $\pm$ 1/2 inch travel without distorting the antenna surface. The errors show up in the hub target data because, as previously mentioned the repeatability regressions were made by using the hoop targets only. In reality the hub cannot move because it is restrained by the pedestal. These data were analyzed further to ascertain whether column bowing had indeed occurred. To provide better insight, the average X, Y, and Z errors were plotted for each measurement. The results may be seen in Figure 4.2.2.3-1.

Table 4.2.2.1-1. Measured Target Locations (#1)

Target Location	Target Number	Measured Coordinates - Theolodite Reference			Regression Errors from Ideal		
		X	Y	Z	DX	DY	DZ
Upper Column	01	10.408	5.965	178.233	0.016	-0.035	-0.114
	07	6.036	-10.419	178.227	0.036	-0.027	-0.120
	13	-10.411	-6.019	178.198	-0.019	-0.019	-0.149
	19	-6.002	10.374	178.256	-0.002	-0.018	-0.091
Hub	01	10.536	7.742	-0.201	0.250	-0.151	-0.201
	07	7.840	-10.349	-0.209	-0.053	-0.063	-0.209
	13	-10.330	-7.737	-0.185	-0.044	0.156	-0.185
	19	-7.623	10.337	-0.103	0.270	0.051	0.103
Lower Column	01	12.684	7.040	-193.184	0.138	-0.204	0.000
	07	6.998	-12.632	-193.185	-0.246	-0.086	-0.001
	13	-12.693	-6.953	-193.153	-0.147	0.291	0.031
	19	-7.037	12.715	-193.161	0.207	0.169	0.023
Hoop	01	-0.025	-291.065	15.673	-0.025	0.083	0.045
	02	-75.352	-281.169	15.789	0.003	0.059	0.161
	03	-145.529	-252.055	15.581	0.045	0.087	-0.047
	04	-205.820	-205.784	15.649	0.053	0.089	0.021
	05	-252.065	-145.528	15.634	0.077	0.046	0.006
	06	-281.152	-75.279	15.625	0.076	0.076	-0.003
	07	-291.028	-0.011	15.685	0.120	-0.011	0.057
	08	-281.130	75.303	15.722	0.098	-0.052	0.094
	09	-252.092	145.570	15.718	0.050	-0.004	0.090
	10	-205.859	205.844	15.696	0.014	-0.029	0.068
	11	-145.513	251.965	15.644	0.061	-0.177	0.016
	12	-75.321	281.092	15.555	0.034	-0.136	-0.073
	13	-0.009	291.021	15.652	-0.009	-0.127	0.024
	14	75.315	281.119	15.704	-0.040	-0.109	0.076
	15	145.513	252.006	15.750	-0.061	-0.136	0.122
	16	205.699	205.798	15.687	-0.174	-0.075	0.059
	17	252.109	145.560	15.615	-0.033	-0.014	-0.013
	18	281.038	75.349	15.683	-0.190	-0.006	0.055
	19	291.069	-0.012	15.576	-0.079	-0.012	-0.052
	20	281.045	-75.276	15.652	-0.183	0.079	0.024
	21	252.021	-145.532	15.737	-0.121	0.042	0.109
	22	205.792	-205.770	15.594	-0.081	0.103	-0.034
	23	145.528	-252.089	15.824	-0.046	0.053	0.196
	24	75.360	-281.123	15.744	0.005	0.105	0.116

Table 4.2.2.2-1. Measured Target Locations (#2)

Target Location	Target Number	Measured Coordinates - Theolodite Reference			Regression Errors from Ideal		
		X	Y	Z	DX	DY	DZ
Upper Column	01	10.344	5.983	178.323	-0.048	-0.017	-0.024
	07	6.000	-10.406	178.279	0.000	-0.014	-0.068
	13	-10.378	-6.034	178.237	0.014	-0.034	-0.110
	19	-5.988	10.384	178.277	0.012	-0.008	-0.070
Hub	01	10.371	8.041	-0.191	0.085	0.148	-0.191
	07	7.969	-10.138	-0.218	0.076	0.148	-0.218
	13	-10.233	-7.720	-0.176	0.053	0.173	-0.176
	19	-7.804	10.462	-0.116	0.089	0.176	0.116
Lower Column	01	12.686	7.099	-193.200	0.140	-0.145	-0.016
	07	7.111	-12.594	-193.182	-0.133	-0.048	0.002
	13	-12.634	-7.038	-193.170	-0.088	0.206	0.014
	19	-7.071	12.658	-193.211	0.173	0.112	-0.027
Hoop	01	0.019	-291.139	15.739	0.019	0.009	0.111
	02	-75.299	-281.202	15.781	0.056	0.026	0.153
	03	-145.513	-252.092	15.563	0.061	0.050	-0.065
	04	-205.870	-205.830	15.688	0.003	0.043	0.060
	05	-252.092	-145.550	15.618	0.050	0.024	-0.010
	06	-281.168	-75.393	15.618	0.060	-0.038	-0.010
	07	-291.079	-0.030	15.720	0.069	-0.030	0.092
	08	-281.150	75.288	15.716	0.078	-0.067	0.088
	09	-252.091	145.524	15.699	0.051	-0.050	0.071
	10	-205.903	205.823	15.676	-0.030	-0.050	0.048
	11	-145.534	251.983	15.665	0.040	-0.159	0.037
	12	-75.329	281.130	15.564	0.026	-0.098	-0.064
	13	-0.023	291.090	15.664	-0.023	-0.058	0.036
	14	75.329	281.132	15.697	-0.026	-0.096	0.069
	15	145.547	251.986	15.731	-0.027	-0.156	0.103
	16	205.817	205.804	15.708	-0.056	-0.069	0.080
	17	252.096	145.564	15.563	-0.046	-0.010	-0.065
	18	281.097	75.298	15.664	-0.131	-0.057	0.036
	19	291.060	-0.028	15.579	-0.088	-0.028	-0.049
	20	281.078	-75.359	15.630	-0.150	-0.004	0.002
	21	252.013	-145.581	15.756	-0.129	-0.007	0.128
	22	205.797	-205.772	15.536	-0.076	0.101	-0.092
	23	145.544	-252.202	15.810	-0.030	-0.060	0.182
	24	75.281	-281.137	15.690	-0.074	0.091	0.062

Table 4.2.2.3-1. Structural RMS Values

August 3 Measurements:

Target Group	RMS X	RMS Y	RMS Z
Upper Column	0.022	0.026	0.120
Hub	0.187	0.116	0.180
Lower Column	0.190	0.201	0.019
Hoop	0.088	0.085	0.081

August 27 Measurements:

Target Group	RMS X	RMS Y	RMS Z
Upper Column	0.026	0.021	0.074
Hub	0.077	0.162	0.179
Lower Column	0.137	0.140	0.017
Hoop	0.069	0.071	0.083

RMS values for each of the major target areas were computed to assist in the evaluation of the structure.

Table 4.2.2.3-2.

SENSITIVITY	ALLOWABLE ERROR	AUG. 3 MEAS.	AUG. 27 MEAS.
MAST LENGTH VARIATION	.100	.106	.075
MAST ECCENTRICITY	.250	.277	.195
HOOP VERTICAL VARIATION	.100	.081	.083
HOOP RADIAL VARIATION	.050	.122	.099

A COMPARISON OF THE TWO MEASUREMENTS WITH BUDGETED VALUES SHOWS A MARKED IMPROVEMENT FOR THE AUGUST 27 MEASUERMENTS.

Table 4.2.2.3-3. Repeatability Errors

Target Location	Target Number	Regression Errors from August 3.		
		X	Y	X
Upper Column	01	-0.072	0.045	0.095
	07	-0.043	0.040	0.057
	13	0.026	0.012	0.043
	19	0.006	0.037	0.025
Hub	01	-0.166	0.325	0.015
	07	0.128	0.237	-0.004
	13	0.096	0.043	0.013
	19	-0.182	0.151	-0.009
Lower Column	01	0.008	0.084	-0.011
	07	0.120	0.063	0.008
	13	0.066	-0.060	-0.013
	19	-0.028	-0.032	-0.046
Hoop	01	0.045	-0.048	0.072
	02	0.054	-0.007	-0.005
	03	0.016	-0.012	-0.018
	04	-0.050	-0.021	0.037
	05	-0.027	0.002	-0.020
	06	-0.017	-0.090	-0.012
	07	-0.052	0.005	0.029
	08	-0.022	0.009	-0.012
	09	-0.001	-0.022	-0.024
	10	-0.047	0.004	-0.024
	11	-0.024	0.043	0.019
	12	-0.11	0.064	0.010
	13	-0.017	0.095	0.015
	14	0.011	0.040	-0.001
	15	0.031	0.007	-0.010
	16	0.115	0.034	0.033
	17	-0.015	0.032	-0.038
	18	0.057	-0.023	-0.004
	19	-0.010	0.012	0.019
	20	0.032	-0.055	-0.006
	21	-0.008	-0.021	0.034
	22	0.005	0.026	-0.045
	23	0.016	-0.086	-0.003
	24	-0.078	0.013	-0.045

By using the August 3 measurements as a reference the above repeatability errors were determined.

MAST BOWING

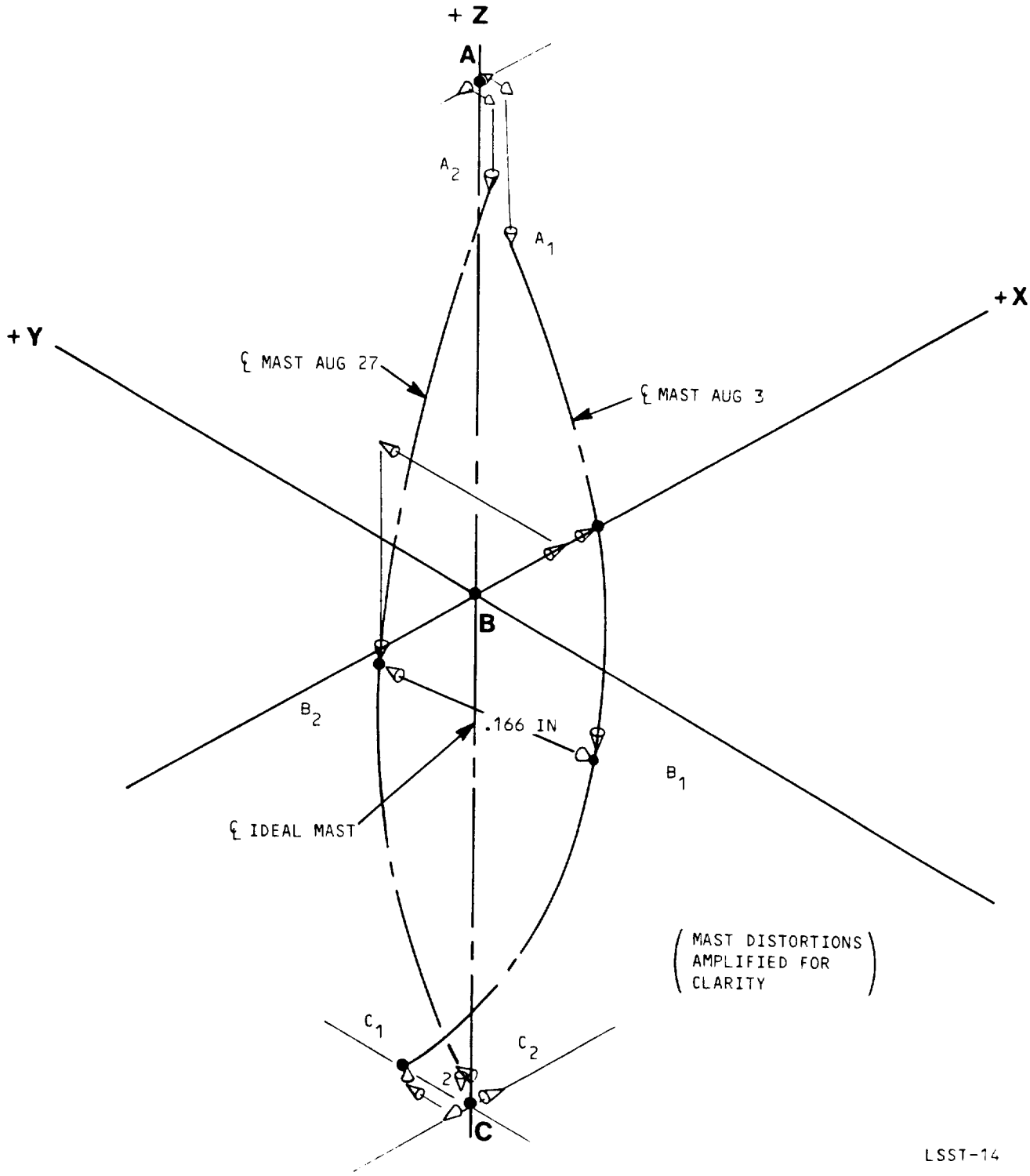

Figure 4.2.2.3-1.

Bowing of the column is shown by plotting the average deviations from the ideal case.

4.2.2.4 Conclusions

Primary areas of concern as a result of the structural measurements were:

- Column bowing
- Column length variations
- Random excessive Z errors of the hoop

Column Bowing

The antenna repeatability results indicate that the column has bowed approximately .166 inches (Figure 4.2.2.3-1) between the August 3 and August 27 deployments. This anomaly manifests itself in Table 4.2.2.3-3 where virtual hub translations ranged as high as .325 inches. The bowing was not considered a problem with regard to overall surface RMS because the surface cords were to be attached to the column by negator springs. The negator springs will maintain a constant load over a wide range of deflection thereby preventing cords and ties from becoming slack. Thus the surface will not be affected if the column is slightly out of position, however the performance of the feed may be adversely affected by this phenomena. Requirements for a feed system include remote position adjustment capability. The additional restraint due to surface and associated cords should also reduce the effects of column bowing.

The cause for bowing was not found conclusively, however the counterbalance system as well as synchronization rod rebonding discussed later in this section are likely suspects.

Column Length Variation

The column length, which was slightly over budget, was a concern because of its direct effect of the surface's attitude with respect to the hoop. Hub Z variations of .180 and .179 inch shown in Table 4.2.2.3-1 also was an area which was of concern. This anomaly was alleviated by locating the surface attach ring to the hub lower than its originally intended position.

Anomalies may be attributed to larger manufacturing errors than expected. For large antennas, ground measurements of larger subassemblies would solve this problem. For example, one half of the column could be loaded and measured to within $\pm$.005 inches prior to going to the next production phase.

Random Excessive Z Errors of the Hoop

It was noticed on both measurements that several hoop joints were out of plane as much as .182 inches. Specifically joints #1 (.111 inch), #2 (.153 inch), #15 (.103 inch), #21 (.128 inch) and #23 (.1892 inch) were candidates for investigation.

Motor joints were located at joints #1, 7, 13, and 19 so there was no correlation between motor locations and joint errors. Biases of the hoop control cords were checked and found to be correct.

One change which could have affected repeatability between the August 3 and August 27 measurements and the Z components of the hoop was the repair of the synchronization rods. Some of the bonds between the synchronization and their end fittings were broken between the two deployments. The rods were rebonded before the August 27 deployment. However, some of the rods may have been rebonded to a slightly different length as they were bonded without the aid of the original bond tooling.

While some of the budgeted allowables were exceeded as shown in Table 4.2.2.3-2, the errors at the majority of the targets were within budget. Based on the overall accuracy of the structure, no major adjustments were implemented.

4.3 System Testing

Based on the experience gained during the structural testing described in Section 4.2, the following enhancements to the model were identified and implemented prior to installation of the surface and system testing.

- The hoop counterbalance cables were lengthened to allow the weight bags to hang below the hoop. This allowed the bags to be managed from the floor without the need for special elevated personnel platforms, and eliminated cable snagging problems.

- The nylon latch-delatch rollers on the column segments were replaced with metal units fabricated by NASA-Langley, and minor latch adjustments were made.

- Four additional motor driven joints were added to the hoop, and eight higher-torque motors were installed.

- An electronic hoop motor synchronization system was designed, built, installed, and tested by NASA-Langley personnel.

Upon completion of the surface installation the model was ready for deployment, stowage, and surface accuracy testing in early March, 1985. Deployments of the antenna and the results of the structural and surface measurements are described separately below.

4.3.1 Deployment Testing of the Hoop-Column Antenna

Two deployments from the completely stowed configuration were accomplished. During deployment of the column, manual assistance of the surface control cords was required. Also, one of the top most bridle operated column latches failed to engage completely. This latch was manually engaged.

Hoop deployment, as shown in Figures 4.3.1-1 and 4.3.1-2, was smooth and symmetric. The hoop motor synchronization system performed flawlessly. Deployment of the surface was smooth and snag free.

Deployment of the preload segment was conducted in steps to allow visual inspection of the surface tensioning. Deployment was terminated normally by the limit switch and a visual inspection of the surface and structure was performed. This inspection revealed loose truss vertical ties. A top view of the deployed antenna is shown in Figure 4.3.1-3.

During stowage of the antenna for the second deployment, hands on assistance to the mesh was required to allow the hoop to close completely. During this operation the surface control cords were not allowed to stow onto their drums, but individually coiled in bundles and clipped to the truss hard point junctions. While stowing the column the upper mast restow cable failed, requiring these latches to be manually disengaged.

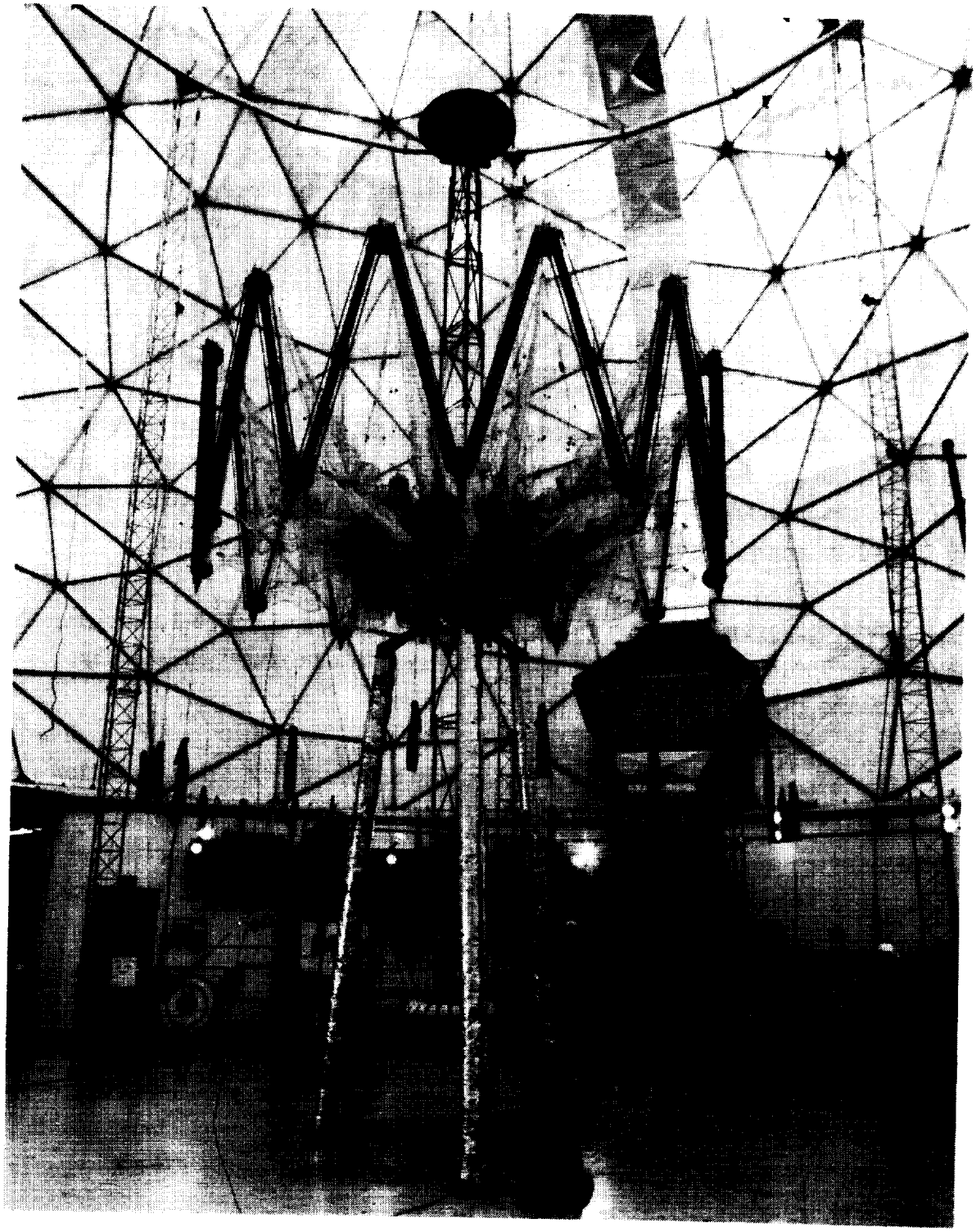

84-0519CMR-3-5

Figure 4.3.1-1.

The hoop begins its deployment from the column hub.

ORIGINAL PAGE IS
OF POOR QUALITY

Figure 4.3.1-2.

The angles between the hoop segments are kept equal by electrical and mechanical synchronization.

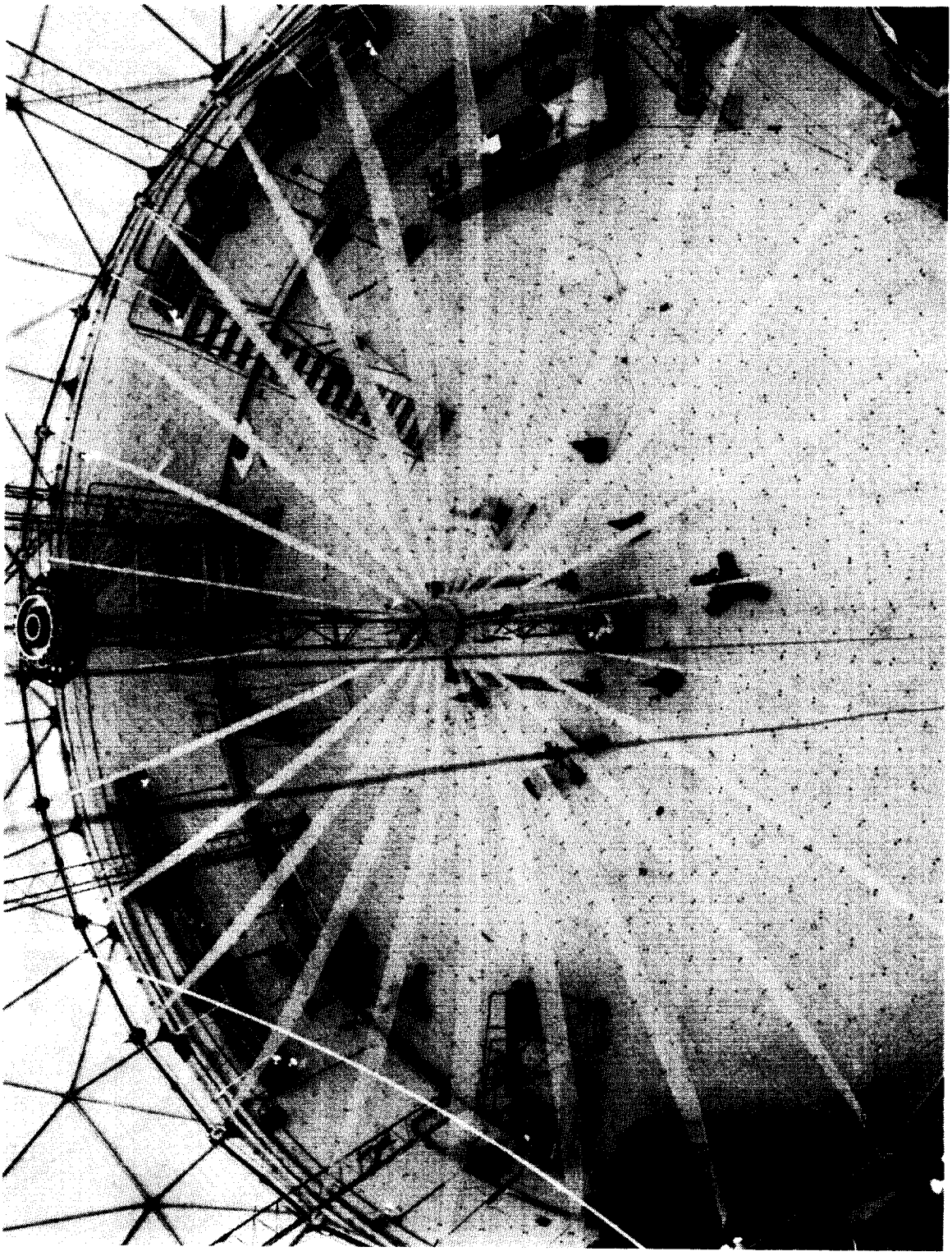

85-0519CMR-2

Figure 4.3.1-3.

The hoop nears its deployment completion.

The second deployment of the antenna was more successful. Manual assistance was required to engage the top most column latches. Hoop, surface, and preload segment deployments were completed without hands on assistance.

4.3.2 System Measurements

The primary goal of this task was to characterize the contour of the surface. A goal of .069" RMS was set.

The .069" RMS goal was determined by the following process. A one half quadrant (3 gore) finite element model was used for the analysis of the results. The model, shown in Figure 4.3.2-1 contained 570 nodes, 594 stringers, 360 membranes and 3 beams. This model was used to accomplish the sensitivity analysis which resulted in the error budget shown in Figure 4.3.2-2. As indicated in the contributor blocks, tolerances in length, loads, and stiffnesses were accounted for in the overall budget. This was accomplished by individually varying these parameters and determining the resulting RMS. These RMS values were then RSS'd to achieve the .069" RMS goal.

The surface of the completed and deployed antenna model was planned to be measured using the Harris theodolite system. The theodolite measurements were to be taken after each deployment to evaluate the repeatability of the model.

From the data obtained, a characterization of the surface could be made, and adjustments to the surface verified. A metric camera photogrammetric survey of the model was also planned by NASA to provide a backup source of surface data. The metric camera data was planned to be analyzed at a later date to determine if on future deployments only a few theodolites could adequately characterize the surface. During the measurement program, problems with calibration of the theodolite system and the inability to see all necessary targets from the floor through the "wedding veil" precluded the timely measurement of the surface targets with the theodolite system. For this reason and because the positions of all surface targets could be recorded in a short time, it was necessary to rely totally on the NASA photogrammetry for surface data. Only one surface characterization (with the metric camera) was made at Harris due to schedule constraints. Thus, no surface repeatability measurements were made at Harris.

THREE GORE FINITE ELEMENT MODEL

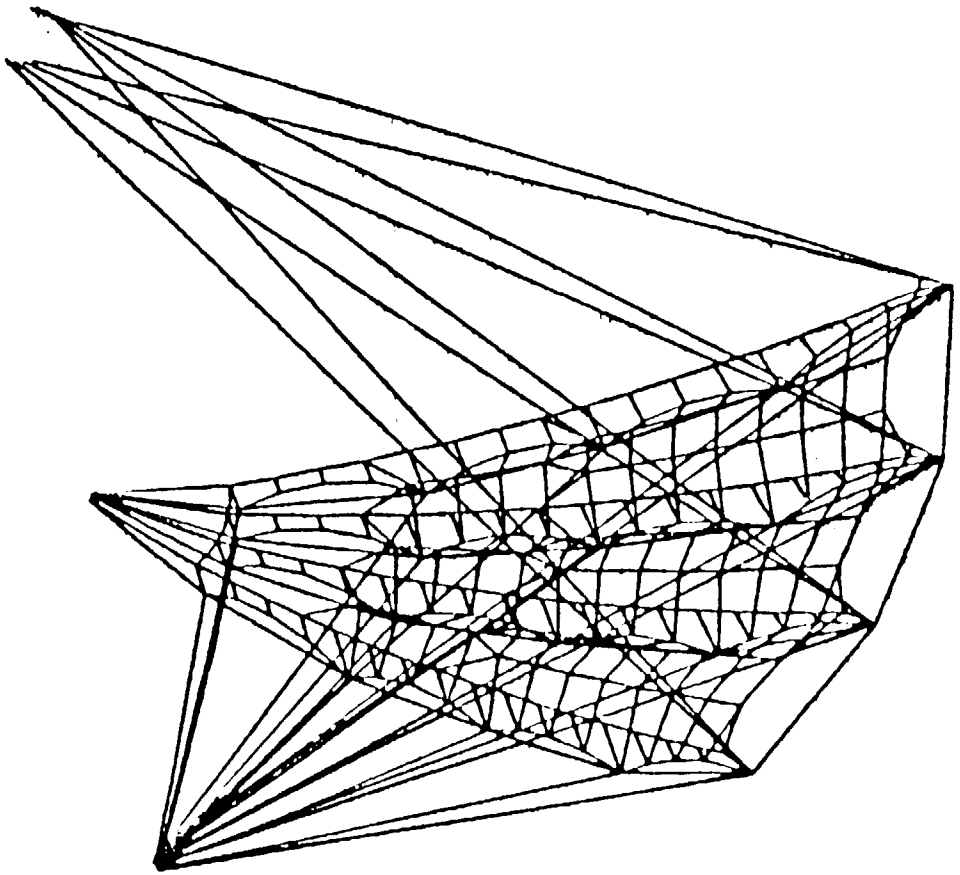

LSST-1002

Figure 4.3.2-1.

The three gore finite element model was utilized in the sensitivity analysis.

METHOD OF COMBINING BUDGET CONTRIBUTORS

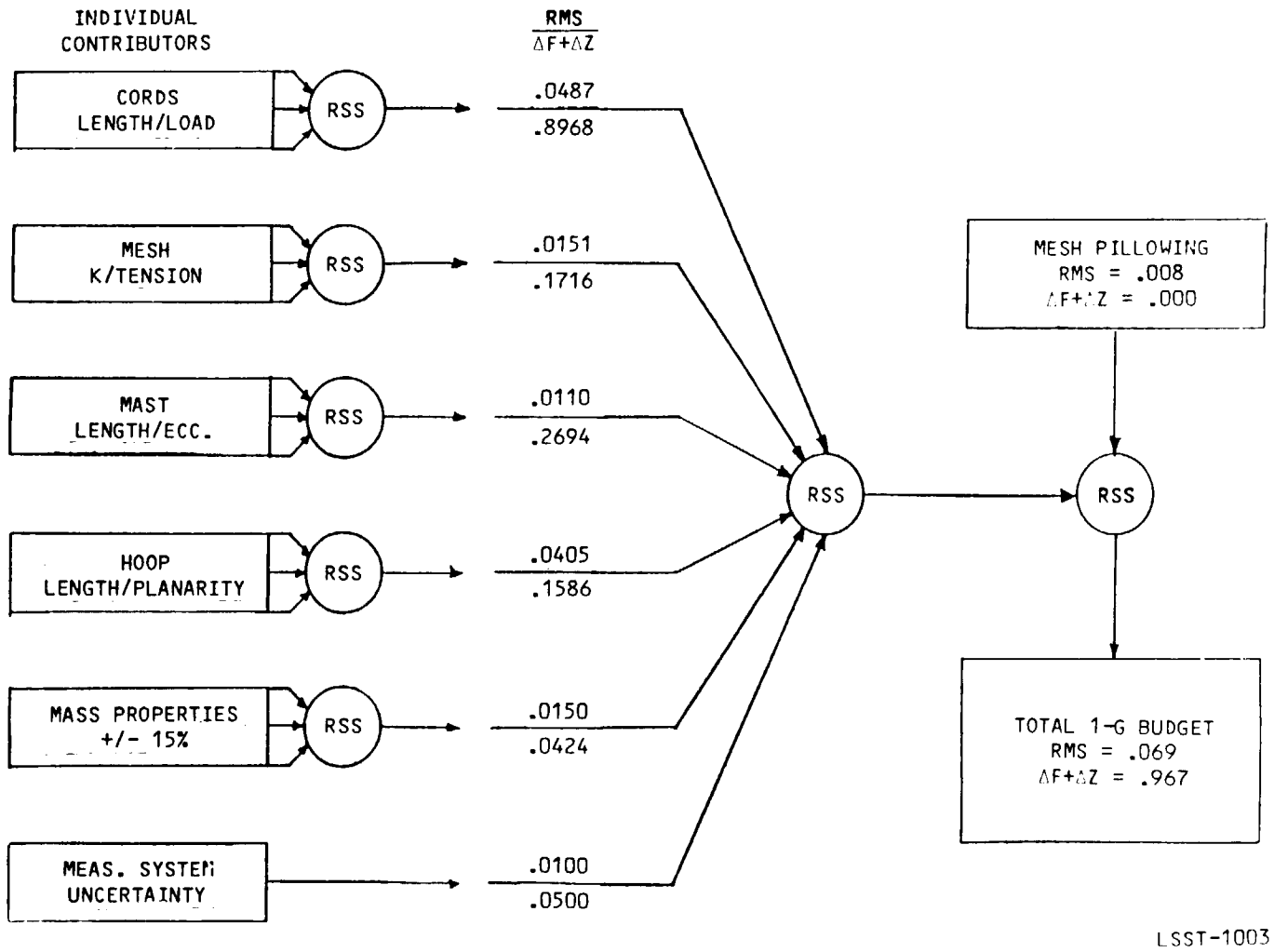

Figure 4.3.2-2.

Individual contributors and measurement uncertainties are RSS'd to arrive at the .069" RMS goal.

4.3.2.1 System Measurement and Regression

Target locations for a typical gore are shown in Figure 4.3.2.1-1. They were located primarily in the areas of the tie/surface junctions and at the cord bay centroids. On a typical gore there were 114 targets. On three atypical gores, where pillow targets were included, there were 174 targets. The targets, with special retroreflective characteristics as well as a small discernable dot in the middle, were compatible with photogrammetry cameras and theodites.

The NASA Langley Research Center used STARS (Simultaneous Triangulation and Resection System) hardware and software to measure the position of retroreflective targets of the antenna surface and other locations. One surface measurement consisted of eight full-coverage photographs of the antenna taken with a special metric camera. The photographs were taken for vantage points 21 feet above the hoop and on forty-five degree increments about the antenna. Measurements were accomplished in the early morning hours to maintain temperature stability and consequentially low thermal distortions. In addition, insulation was placed over each of the three antenna tooling pedestal legs to minimize temperature gradients.

After development of the photographs the target location and identification for each film was read. The automatic film comparator of Geodetic Services, Inc. was used for this, because manual film readup would have been much more time consuming and less accurate. After readup, standard STARS preprocessing software was used to correct for systematic comparator and film deformation errors. Then, the files were merged together, and a resection was run on the data to update the location and orientation of each camera station. The software then processed the data through a number of subroutines which determined the coordinates of each target, first with respect to an arbitrary coordinate system, and finally with respect to the antenna coordinate system. The same 888 retro-targets distributed over the reflector surface were determined to an accuracy of about .007" as estimated by STARS error propagation in the bundle adjustment.

The results of the metric camera surface measurement data were used to determine the deviations in the resulting surface from design. For this comparison, the data for each quadrant were processed by a best-fit paraboloid, and compared with the design values computed for the (x, y) value measured at

TYPICAL GORE TARGET LOCATIONS

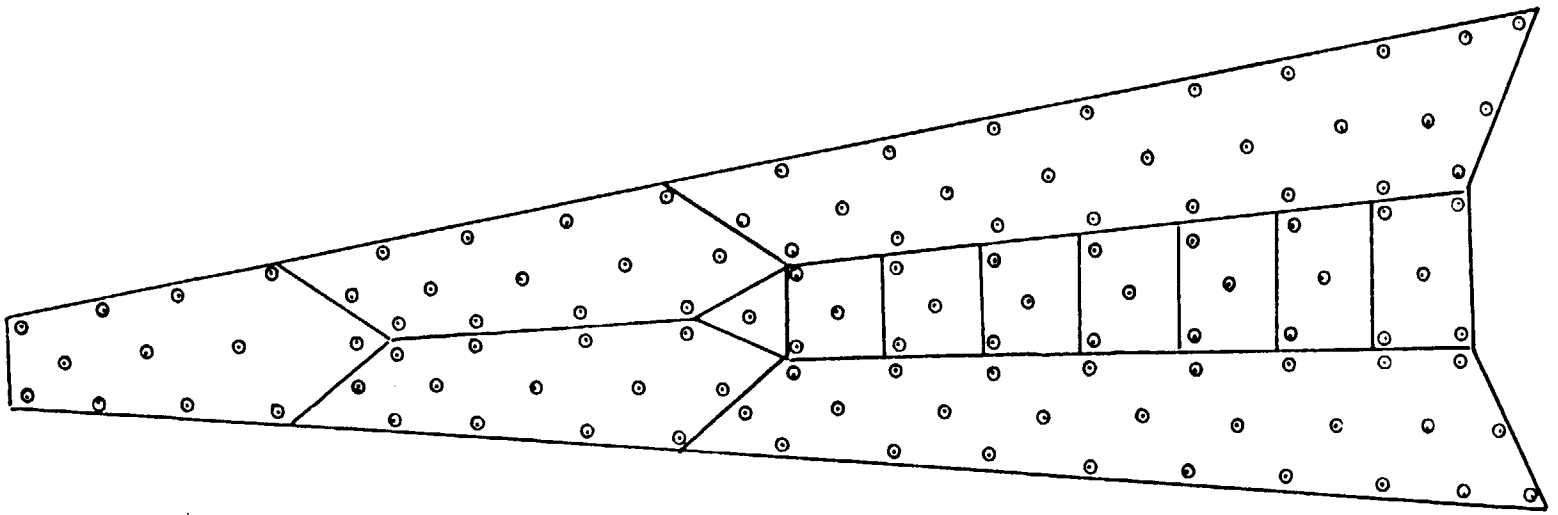

Figure 4.3.2.1-1.

Targets were located primarily at the tie/surface junction points.

each target. This activity was done by both NASA and by Harris, with correlating results.

Harris determined the as-built RMS by best-fitting the distorted surface node coordinates using the DAMS program. This program uses an iterative process to determine the characteristics of the best fit paraboloid. These fits excluded the intercostal targets, and constrained the x and y location of the vertex of the paraboloid. These intercostal targets are not shown in Figures 4.3.2.2-1 thru 4.3.2.2-4.

4.3.2.2 Measurement Results and Discussions

Figures 4.3.2.2-1 through 4.3.2.2-4 are error maps of each quadrant. Orientations of the quadrants are shown in Figure 4.3.2.2-5. The following legend should be used in discerning the mapped errors.

Map Designation	Associated Error, Inches
0	-0.6000 TO-0.5000
1	-0.5000 TO-0.4000
2	-0.4000 TO-0.3000
3	-0.3000 TO-0.2000
4	-0.2000 TO-0.1000
5	-0.1000 TO-0.0000
6	0.0000 TO 0.1000
7	0.1000 TO 0.2000
8	0.2000 TO 0.3000
9	0.3000 TO 0.4000
A	0.4000 TO 0.5000
B	0.5000 TO 0.6000

The resulting RMS values of the quadrants were .152, .138, .132, and .115 for quadrants 1 through 4, respectively.

Errors in the outboard extremity of the surface were higher than anticipated. These were due partly to the inherent discontinuity of the surface. For this reason these errors were not included in the resulting RMS's. Subsequent visual inspections revealed random cases of slack ties. Conversely, the inboard

QUADRANT NO. 1

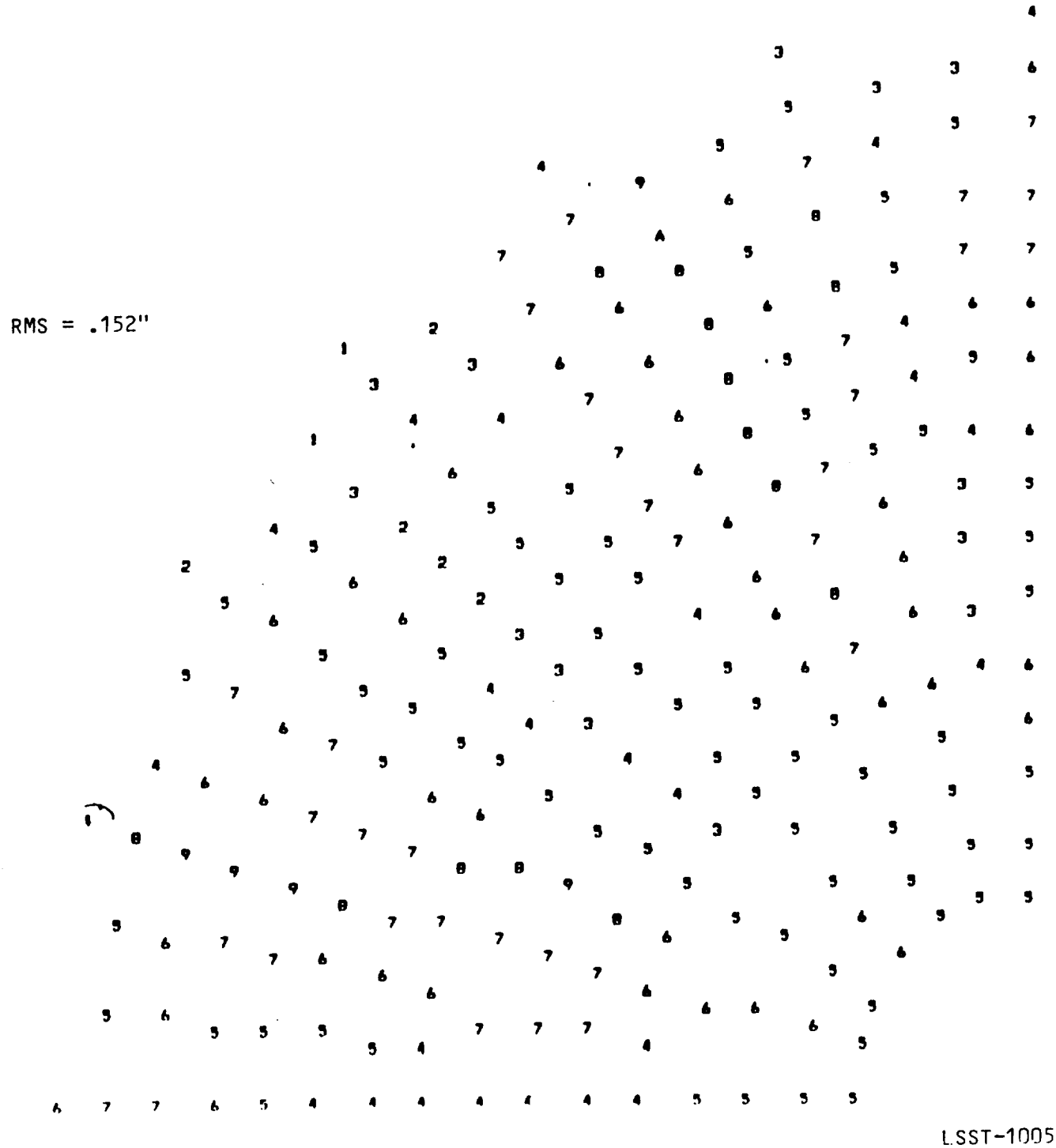

Figure 4.3.2.2-1.

QUADRANT NO. 2

RMS = .138

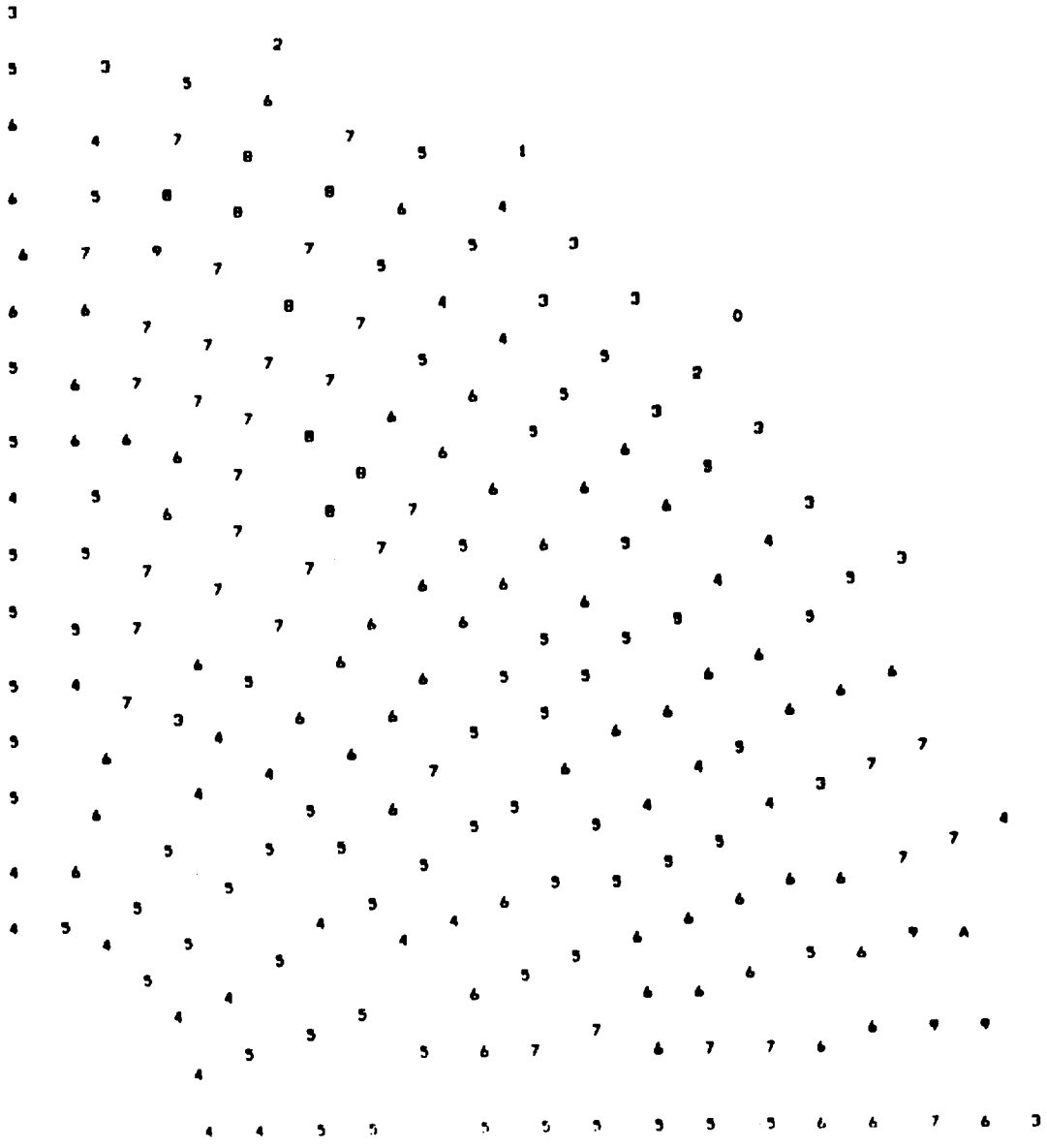

Figure 4.3.2.2-2.

QUADRANT NO. 3

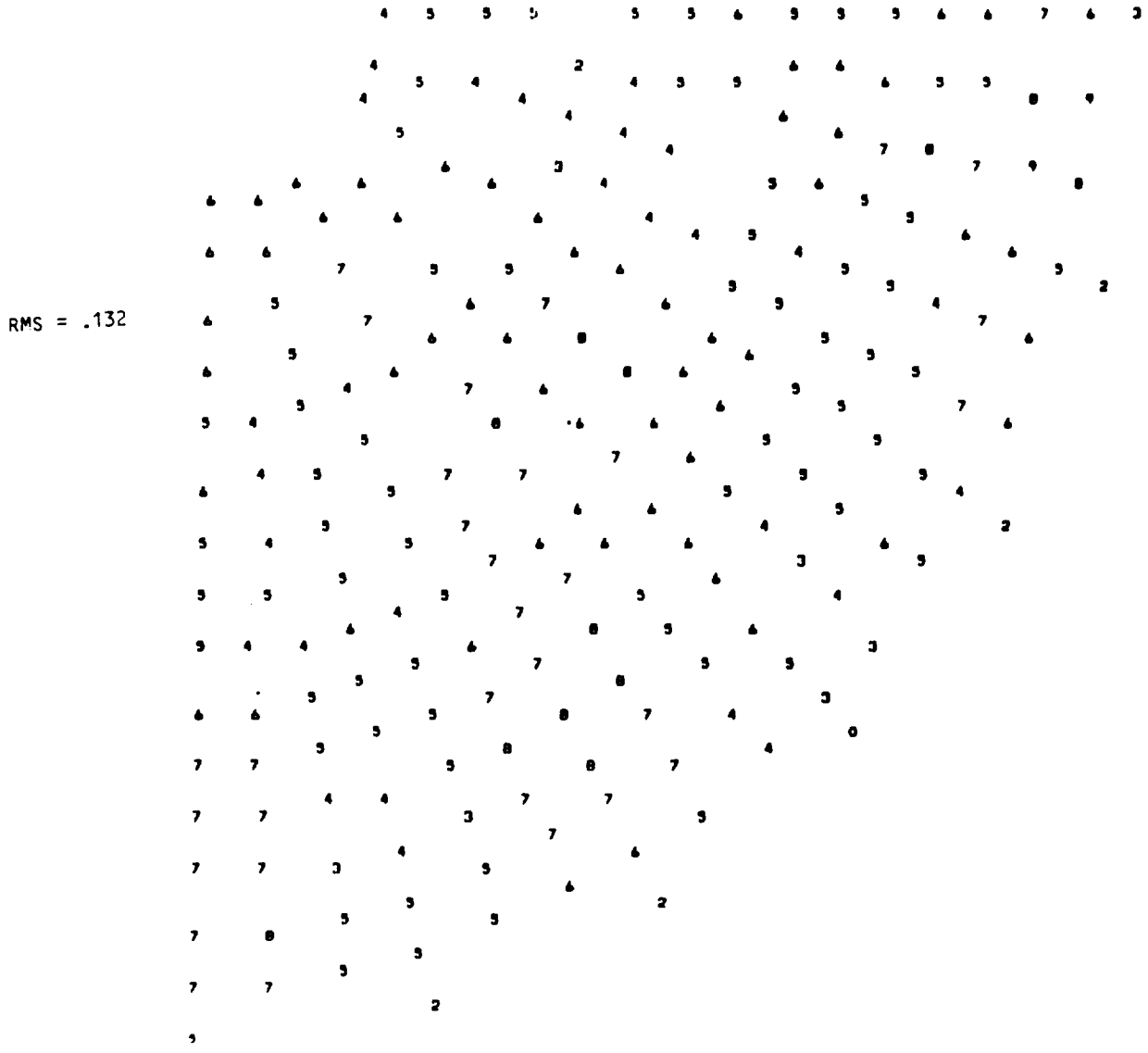

Figure 4.3.2.2-3.

QUADRANT NO. 4

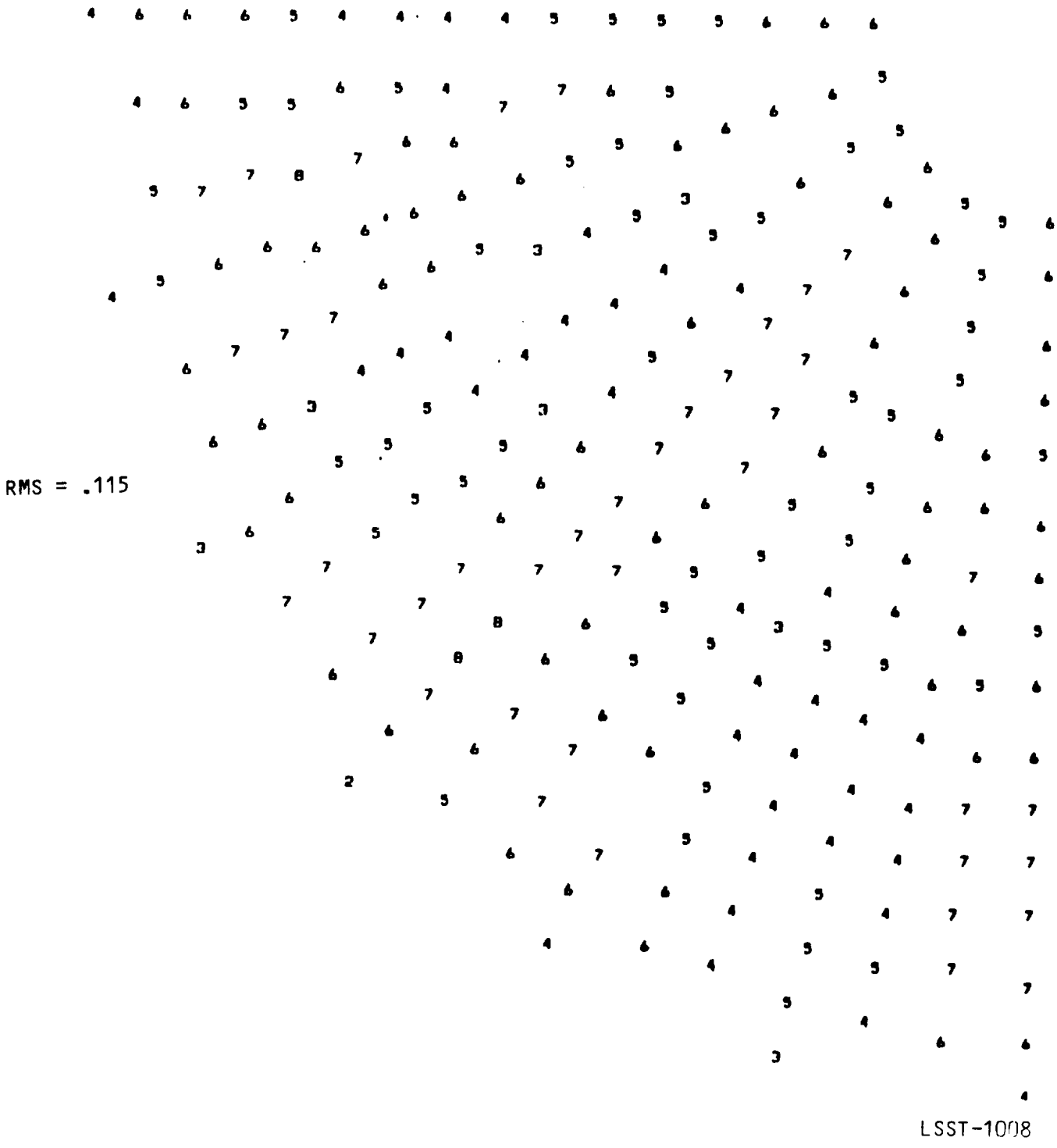

Figure 4.3.2.2-4.

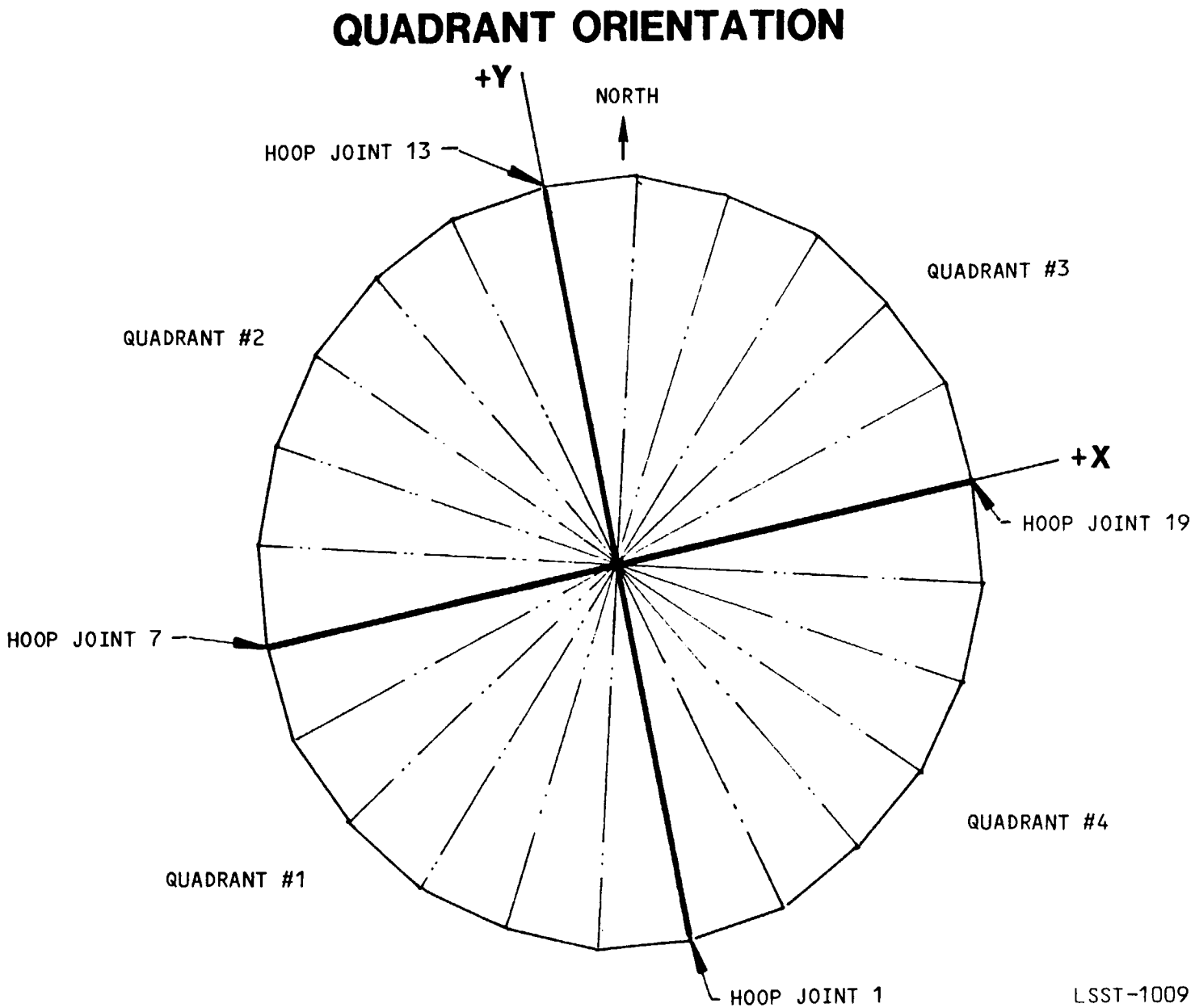

Figure 4.3.2.2-5.

The orientation of the quadrants with respect to the hoop joints and system coordinate system is shown above.

errors of the surface were acceptable, being in the 5 to 6 range. There were four particularly errant gore edge cords (one in each quadrant) which were in the 7-8 category. The feed design electronically compensated for these errors. An extensive investigation into the cause of localized errors was not accomplished due to limitations of time and money, however areas which are of suspect are:

- The Cord/Column Interface Stop Brackets
  The brackets were attached to the column by means of bolts and clearance holes. Press fits or tighter holes should be considered on future designs.
- The Surface Control Cord Biases
  Biasing of the surface control cords with respect to the truss hard points was accomplished by a special tool which was awkward at best, to use. Future designs should consider a different method of biasing or eliminate the necessity of biasing.
- The Surface Control Cord Lengths
  Manufacturing of the surface control cords is a primary area of suspect because of the cords' critical lengths. More, specific measurements of these cords are necessary to confirm the impact of length variation of the resultant surface accuracy as very minor length changes caused significant surface changes due to the low strain rate of the cord material. More accurate budgeting and more rigorous process control must be exercised in this area.
- The Hoop's Planarity
  To the extent indicated in the error budget the surface is sensitive to the Hoop's planarity. Hoop planarity could be improved by allowing more kinematic backlash in the very last portion of its deployment, thereby allowing the Hoop Control Cords to locate each of the hoop joints rather than the hoop drive system which is presently the case.
- Additional Hoop Motors - 4 motors were added to the hoop to improve hoop deployment. Since cord and surface fabrication was already well under way, the impact of the added motor weight could not be factored in to cord loads and geometry. Therefore, some distortion of the surface would be expected due to the added weight.

The antenna was subsequently delivered to the Martin Near-Field Facility in an unadjusted "as-built" condition. It may be noted that surface adjustments which had been eliminated due to funding and time constraints at the Harris Corporation could have significantly reduced the surface rms deviations. Adjustments conducted later by NASA Langley at the Martin Marietta Near Field facility reduced RMS surface deviations to 0.094", 0.061", 0.075", and 0.080" for quad apertures 1 through 4, respectively for the effective antenna surface.

4.3.2.3 Conclusions

Based on the in-house measurement results and the subsequent adjustments at the Near-Field Facility it is concluded that the overall surface shaping architecture of the quad aperture approach is correct. It may also be concluded that the surface lends itself well to substantial improvements by a relatively small number of adjustments (4 per gore). Consequently on orbit adjustment is feasible and in some cases necessary.

5.0 ANOMALIES AND CORRECTIVE ACTIONS

Table 5.0-1 is an itemized list of anomalies which occurred during the fabrication and testing of the antenna. Causes/effects and corrective actions are also discussed. Figures are included for clarification.

Table 5.0-1. Anomalies and Corrective Actions

	Anomaly	Cause and Effect	Resolution
During System Testing	[1]Structural failure of column circumferential joints	Insufficient bond area was the key factor in adhesion failure between the graphite circumferential and the striker end fitting.	This area was reinforced with internal steel rods. (see Figure 5.0-1)
During System Testing	[2]Preload segment deploy complete limit switch	Inertial momentum of the rotating elements caused switch actuator to rotate off of switch arm.	Extension of the actuator arm corrected this anomaly. (see Figure 5.0-2)
During Structural Testing	[3]Hoop "flowering" occurred at the start of deployment	An outward radial load of the C/B cables imposed deflections on the upper portion of the hoop.	The hoop was restrained by a lasso during this stage of deployment. Modification of the C/B system to allow more inboard movement will eliminate this problem. (see Figure 5.0-3)
During Structural Testing	[4]One of three lower bridle latches failed to latch	Cross wrapping of deployment cables on the cable drum caused high loads in the bridle cable (restow) preventing full latch freedom.	Cables were unwrapped and tensions in the bridle cable were reduced by turnbuckle adjustment. (see Figure 5.0-4)
During Structural Testing	[5]Hoop deployment stopped due to prematurely reaching limiting current	This malfunction occurred because higher than expected deployment loads were reached due to C/B radial loads, and more than anticipated friction in the mechanisms.	Height of central C/B hub was raised and 4 hoop motors were added to lessen this problem. Cable payout friction reduction will eliminate this anomaly.
During Structural Testing	[6]Hoop synchro rod bond failures	Backlashing restow cables during deployment caused excess radial loads on hoop synchro rods failing several bonds.	All 96 synchro rods were removed disassembled, rebonded, proofloaded and reinstalled. (see Figure 5.0-5)
During Structural Testing	[7]Hoop deployment shutdown at near deployment	Probable causes: C/B cables became wrapped around themselves imposing shutdown loads. Electrical short occurred between C/B cables and motor circuit caused current spike and consequential shutdown.	Increased length of the C/B cables to minimize wrapup. Corrected short circuit problem. Malfunction has not reoccurred.

Table 5.0-1. Anomalies and Corrective Actions (Continued)

	Anomaly	Cause and Effect	Resolution
During Structural Test	[8]Quartz cord guide disengagement	Shallow retaining ring groove caused one (of 144) cord guide to disengage from the guide fitting.	Reinforcements were retrofitted to the guide brackets to eliminate this failure. (see Figure 3.3-1)
During System Testing	[9]Surface control cord entanglement on drums	Unsymmetrical payout of surface control cords caused "backlashing" of these cords on their respective drums.	Future deployments were achieved by individually bundling these cords allowing independent payout. Mods on the payout system to allow this on future units are recommended to prevent this malfunction.
	[10]One of three upper bridle latches failed to latch	Incorrect screw length caused binding of latch pawl thereby causing malfunction.	Correct screw was installed.
	[11]Electrical short circuit on hoop system	Metallic shield allowed short circuit between the terminal and the motor case.	Shields were removed and the motor case was reoriented to solve this problem. (see Figure 5.0-6).
	[12]Rear truss shield shrinkage	Probable cause: Humidity caused polyester truss shield to shrink thereby interacting with the geometry of the rear truss.	The truss shield lower seam was cut relieving the tension field and solving this anomaly. (see Figure 5.0-7)
	[13]Hoop hinge joint planarity variations	Probable causes: Incorrect geometry on retrofitted active joints. Incorrect geometry on rebonded synchro rods. Limit switch non-repeatability.	Provide additional backlash in mechanism at final deployment to allow hoop support cords to dominate hoop hinge joint locations.
	[14]Upper mast bridle malfunction	Upper mast restow cable broke due to repeated usage and subsequent fraying, disabling the bridle.	Repair was not made due to inaccessability at the time. A manual cable was temporarily installed.

Table 5.0-1. Anomalies and Corrective Actions (Continued)

	Anomaly	Cause and Effect	Resolution
During System Testing	[15]"Insufficient" mesh stowage volume	Gravity sag of the mesh at stowage caused interference between the mesh and the hoop members.	The mesh was hand dressed on future stows to allow the hoop to close completely. Other corrections should be considered to qualify system for flight.
	[16]Hoop motor shaft failure	Incorrect heat treatment of the shaft and higher than anticipated torques caused the #7 hinge motor shaft to fail in torsion during restow.	New shafts were manufactured and heat treated per print. These will be retrofitted as needed.

COLUMN CIRCUMFERENTIAL REINFORCEMENT

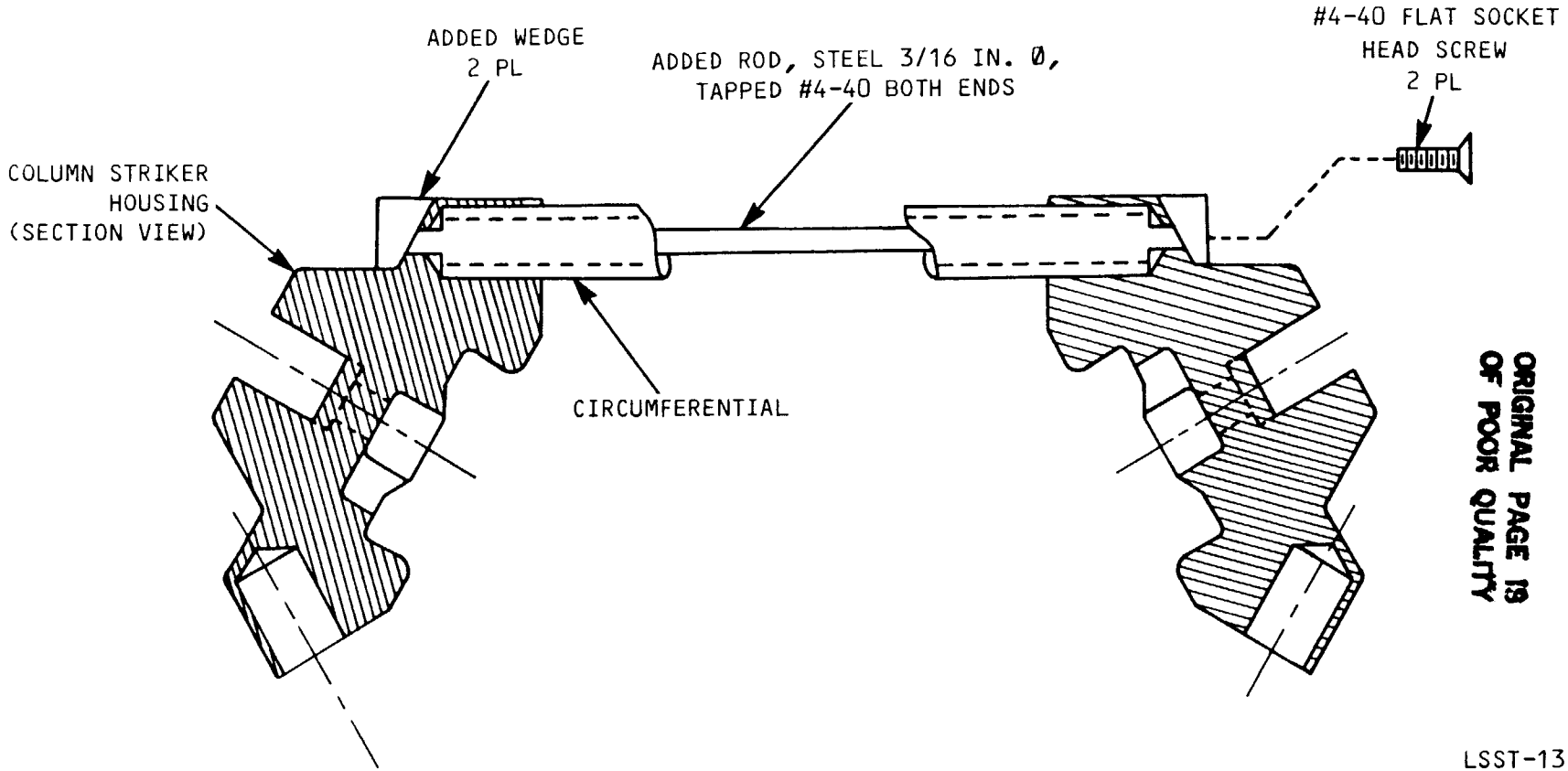

Figure 5.0-1.

Column circumferential bond joints were reinforced by installing the steel/rods inside the tubes.

PRELOAD SEGMENT LIMIT SWITCH ACTUATOR MODIFICATION

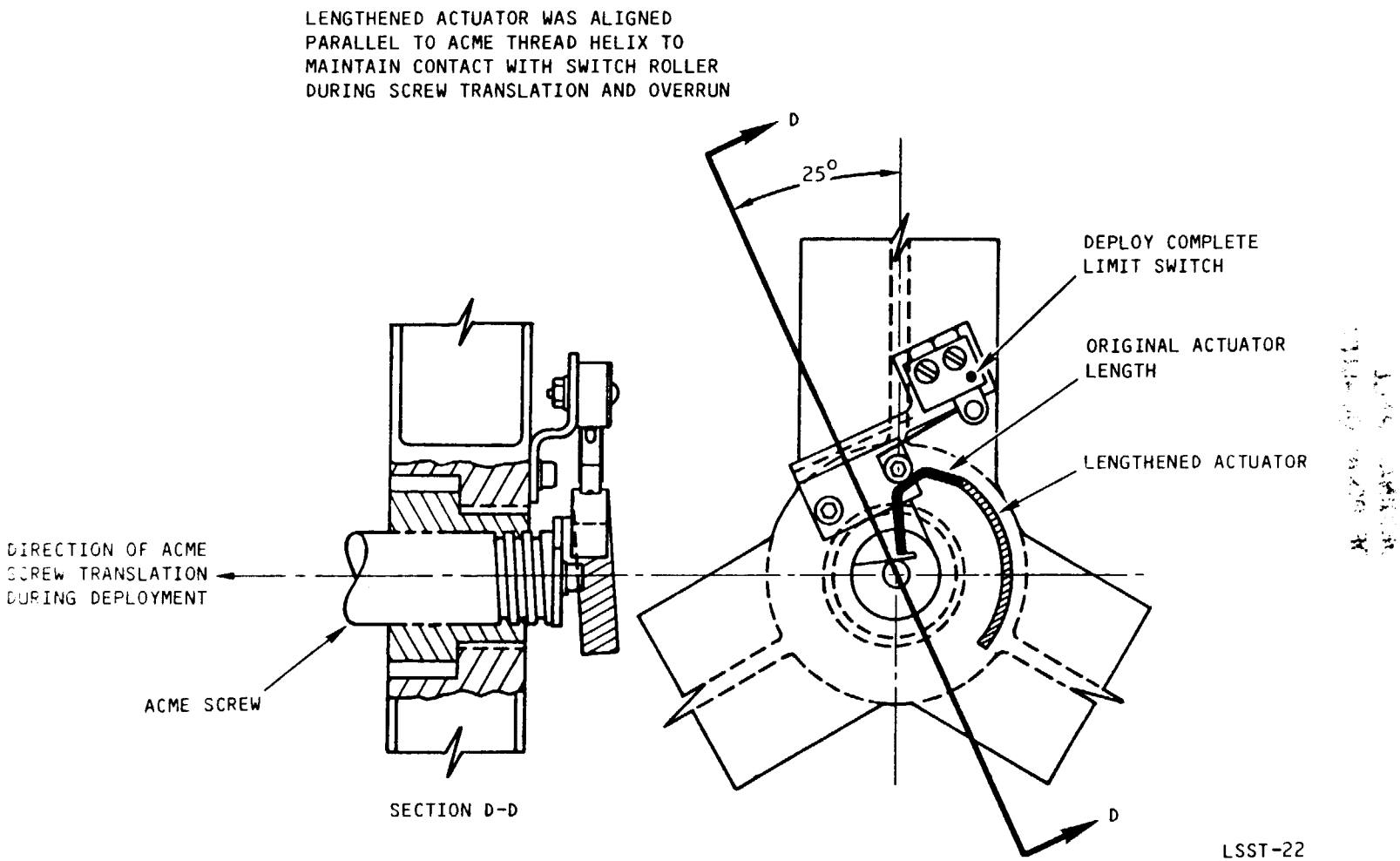

Figure 5.0-2.

Modification of the preload segment deploy complete limit switch actuator allowed proper operation.

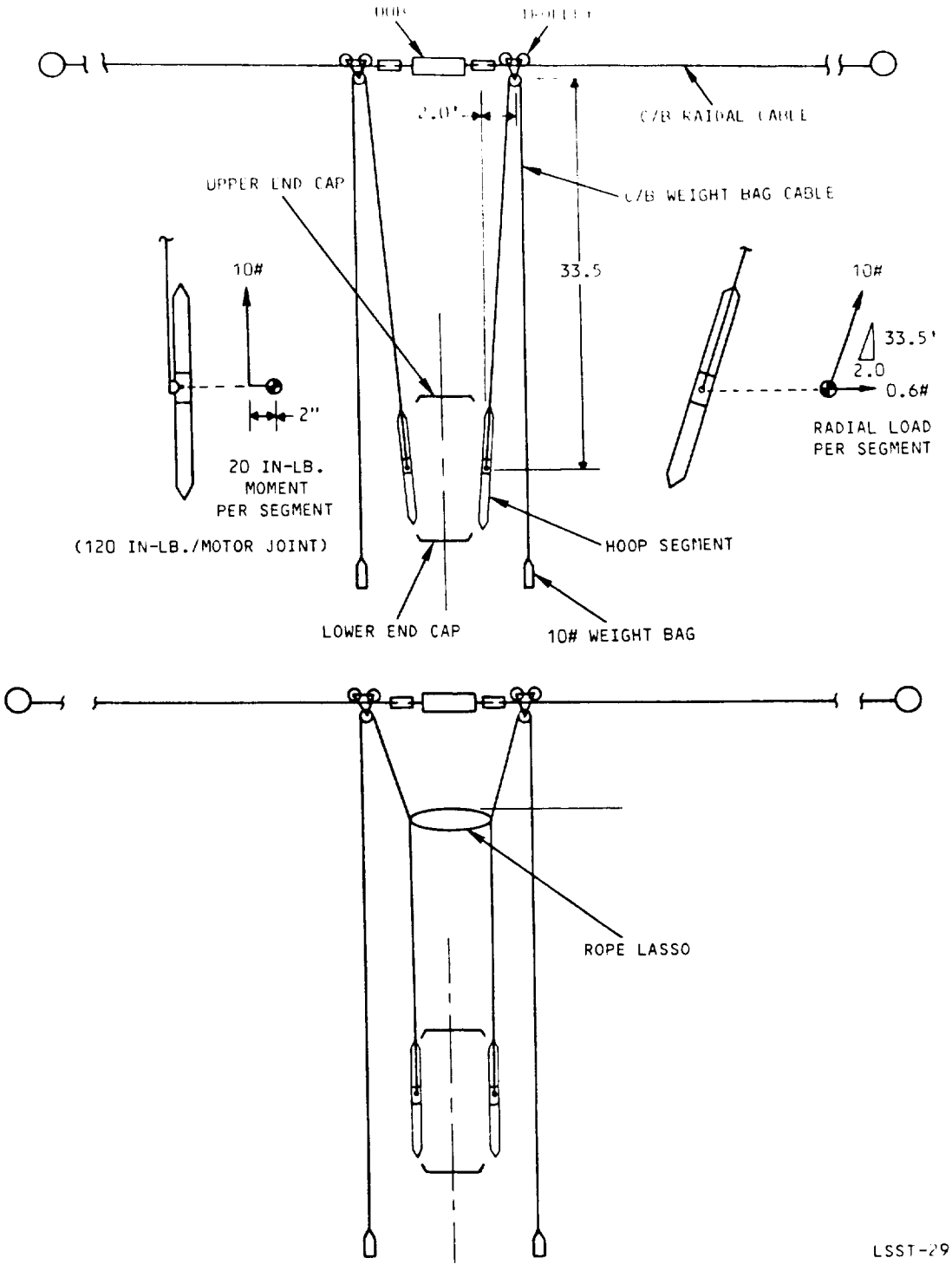

Figure 5.0-3

Hoop "flowering", shown in the top figure and free body diagrams, was prevented by restoring the counter balance cables during deployment in storage using a rope lasso.

COLUMN DEPLOYMENT CABLE CROSS-WRAPPING

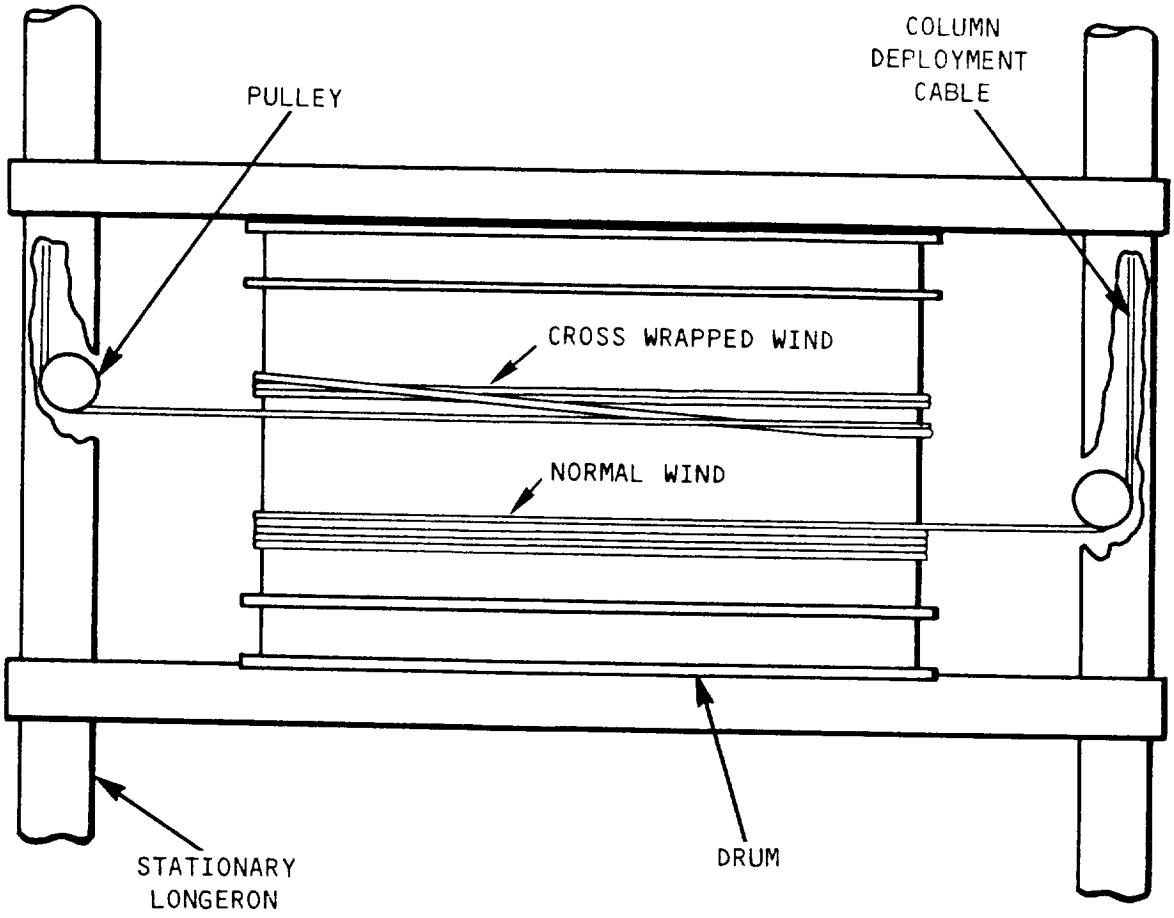

LSST-24A

Figure 5.0-4.

Oscillations of the deploying column segments caused a cable to become cross-wrapped. Normal cable winding is shown on the lower cable.

HOOP DEPLOYMENT WITH RESTOW CABLES

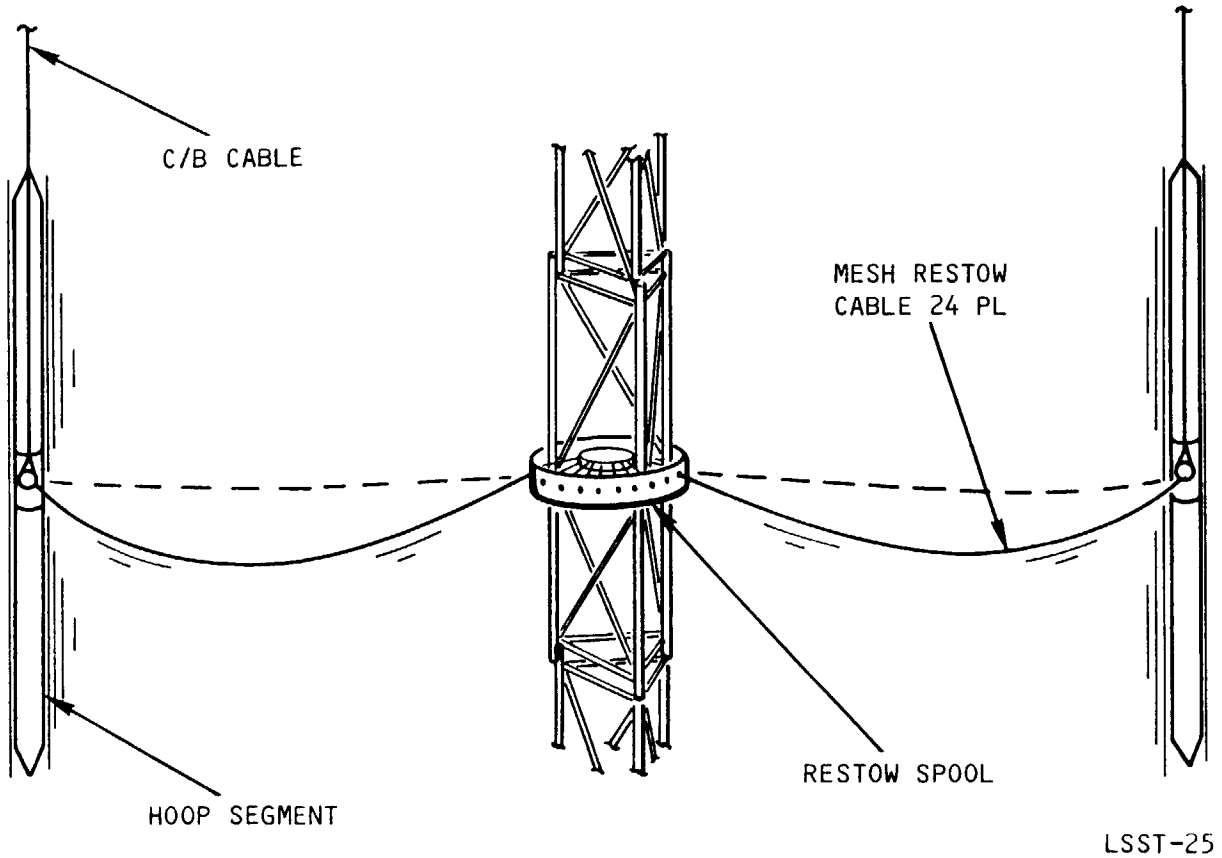

Figure 5.0-5.

As the hoop deployed and tensioned the restow cables (dashed lines) additional slack was introduced by running the restow drive motor.

HOOP MOTOR SHORT CIRCUIT

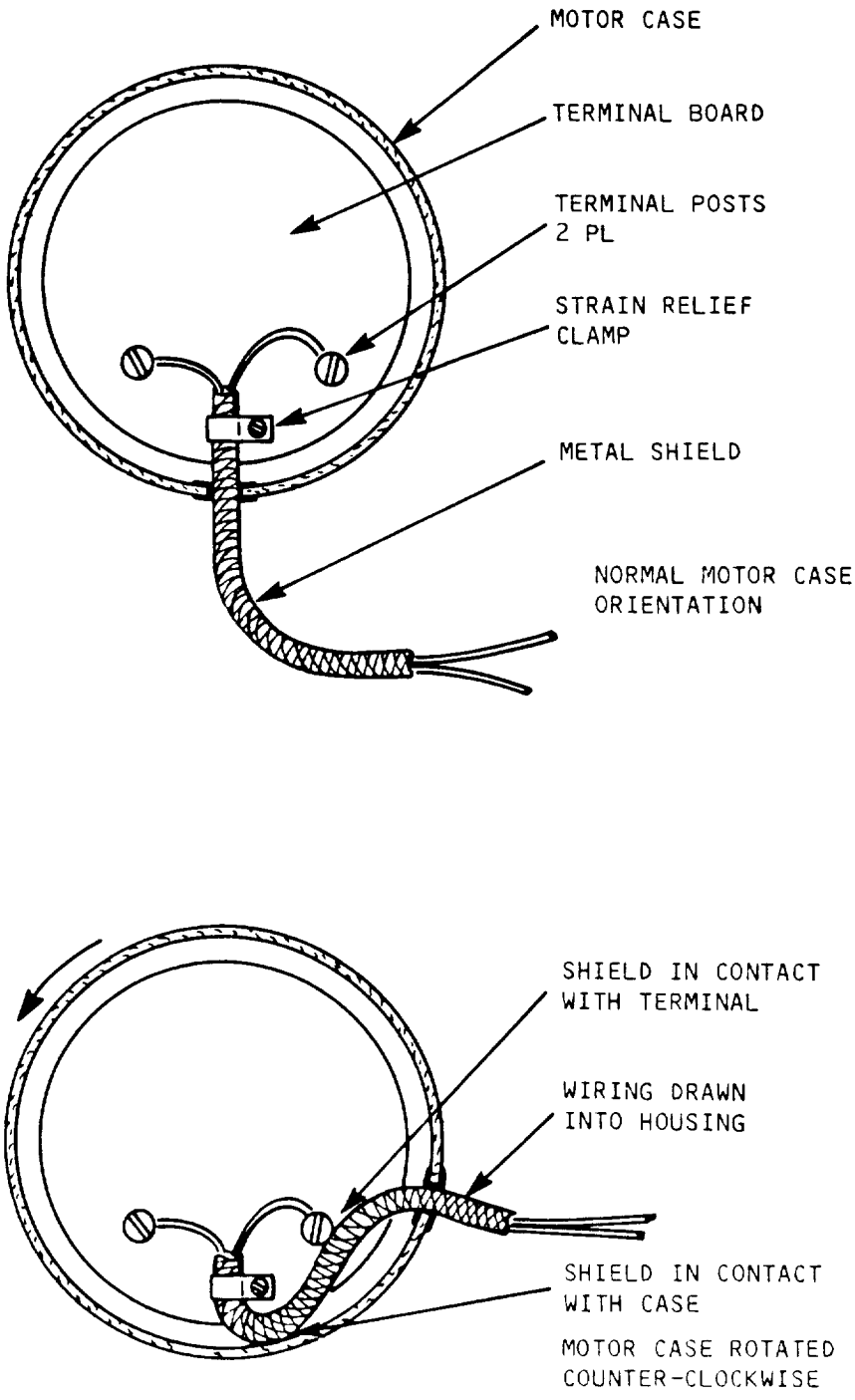

HOOP MOTOR (END VIEW WITH COVER REMOVED)

LSST-26

Figure 5.0-6.

An electrical short circuit was caused when a motor case became rotated, drawing additional shielded cable into the case.

REAR TRUSS SHIELD SHRINKAGE AND REPAIR

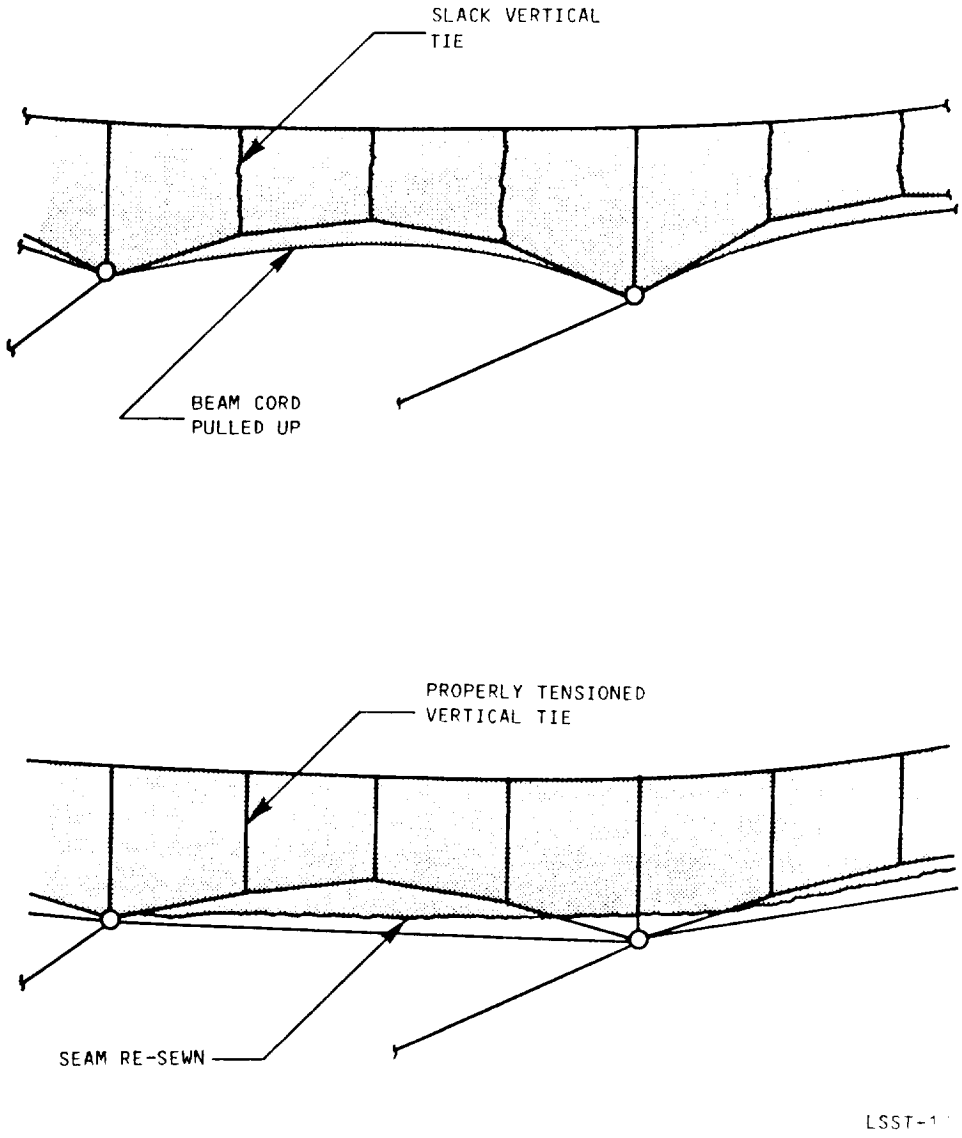

Figure 5.0-7.

Shrinkage of the nylon truss anti-snag shields (above) caused loose vertical ties and overtensioned beam cords. This problem was solved by releasing the lower seam and allowing the material to seek its own final position before re-sewing.

6.0 CONCLUSIONS

The 15-Meter Hoop Column Antenna was built with the following objectives:

- Verification of the deployment Kinematics
- Demonstration of the manufacturing techniques
- Verification of the contour analytical models

Deployment Kinematics

The overall Kinematics of the concept was verified through extensive tests accomplished at the Harris facility. Deployment testing was done with and without the mesh surface. Three deployments of the antenna without the surface were successfully completed. The last of these deployments was a "hands off" demonstration for the NASA Langley management. Following the installation of the mesh surface, two additional deployments were accomplished. These deployments required some manual assistance to avoid the long surface control cords from backlashing on the payout spool. A design modification that incorporates a positive spooling load on each cord regardless of payout symmetry would eliminate the cord payout anomaly if implemented.

Manufacturing Techniques

The manufacture of the antenna was accomplished in a submodular fashion using a "build-to-dimension" philosophy. Both the hoop and the column were final assembled in the stowed condition and tested individually prior to final installation. Theodolite measurements of the structure subsequent to its final assembly verified it to be within the overall predicted tolerance limits. Measurements of the final installed as-built (no adjustment) surface yielded .134 inches average RMS, exceeding our .069 inch goal. This is attributed largely to the manufacturing deviation of surface control cord lengths. Tighter tolerance controls or adjustment of the surface control cords will greatly enhance overall RMS values. This was substantiated by two coarse adjustments by NASA Langley at the RF near-field range which resulted in an .074 inch average RMS with the best quadrant measuring .061 inch RMS.

The .061 inch RMS quadrant demonstrates that with more time for additional adjustments, the overall surface RMS can be made better than the .069 inch goal. The rapid convergence of the RMS valves demonstrates the "as-built" accuracy of the primary surface members. Conclusively, the fabrication of a very large Hoop Column Antenna may be accomplished in a moderately sized facility and the implemented "build-to-dimension" philosophy is valid.

Contour Analytics

The determination of the surface cord sizes, loads and contour budgets were established by Harris Non-Linear Structural Analysis (NLSA) finite element models. These models were designed for cord elements which typically have non-linear structural characteristics. The surface cord loads correlated well with analytical predictions, thus validating their applicability to future large antenna applications.

The Hoop Column is applicable to large antenna missions requiring compact packaging and accurate self deploying structure. In addition, the rapid convergence of the surface RMS demonstrates the capability of the surface to be greatly enhanced by relatively few on-orbit adjustments. The program results have demonstrated the Hoop Column as a viable and versatile design for applications to radiometry, communications, and radio astronomy where large high gain devices are required.

APPENDIX A1
CORD/BEAD BONDING PROCEDURE

PROCEDURE FOR BONDING STOP BEAD TO CROSSWRAPPED TEFLON COATED CORDS
GRAPHITE CORDS ONLY

REQUIRED TOOLS AND MATERIALS

1. Crosswrapped Graphite Cord and Bead
2. Oxy/Acetylene Mini Torch
3. Heat Shield Template
4. 956 Epoxy Adhesive
5. MEK (Solvent)
6. Razor Knife

STEP 1: CLEAN BEAD

Clean the bead to be bonded with the MEK. Allow bead to dry.

STEP 2: POSITION BEAD

Slide the bead on to the crosswrapped cord past the point where the bead is to be bonded. Assure that the rounded end of the bead is toward the long portion of the cord.

STEP 3: STRIP BACK CROSSWRAP

Using the razor knife, carefully cut the Nomex crosswrap fibers in the middle of the bond location. Gently slide the crosswrap away from the bond area. Spread the fibers.

STEP 4: REMOVE TEFLON

Locate the cord so the area to have the teflon removed is located over the cut out in the lower copper heat shield. Place the upper copper heat shields over the areas on each side of the area to be bonded. Locate the shield so that one edge lines up with where the rear of the bead will be when bonded.

Use the torch to burn off the teflon in the area outlined by the templates. With a good well defined (oxidizing) flame the burn time should be less than 1-2 seconds. (Breathing of the smoke produced is not recommended).

STEP 5: APPLY ADHESIVE

Apply well mixed adhesive to the bond area. Gently work the adhesive into the graphite fibers. Try to keep the adhesive only in the bond area.

STEP 6: REPLACE CROSSWRAP

Slide the crosswrap back down into the adhesive. Apply additional adhesive to wet out the crosswrap and form a good bond joint with the bead.

STEP 7: POSITION BEAD

Slide the bead back over the crosswrap and into position in the bond area. Rotate the bead in both directions a bit to ensure even coverage of the inside of the bead with the adhesive. NOTE: Excess adhesive or wicking of the adhesive onto or into the cord in the front of the bead is not desirable. Remove excess adhesive.

STEP 8: CURE ADHESIVE

Cure the EA 956 for one (1) hour at 200 degrees F.

APPENDIX A2

TARGET COORDINATE REGRESSION PROCESS

Regressions were performed using the DAMS program. The DAMS (Data Manipulations) program is an interactive utility program which allows the user to perform any of several operations on measured coordinates. These operations include coordinate transformations, determination of the best-fit paraboloid, and the regression (or best-fit) of two coordinate sets. Algebraic operations may also be performed.

In each case, measured data was regressed to ideal data. Figure A2-1 illustrates the axis system used in the regression.

The regression algorithm is based on minimizing the error between the measured and ideal data. A set of translations and rotations are determined which can be applied to transform the data from the measured to the ideal system, using the following equation:

$$R_{IP(I)} = TIM \ R_{MP(M)} + R_{IM(I)}$$

where R_{IM} (I) defines the vector from the I (ideal) system origin to the M (measured) system origin in the I system.

R_{MP} (M) defines the position vector of a point P in the M System.

TIM is the rotation matrix defined by angles A, B, C. The matrix transforms data from the measured to the ideal system. Angles A, B, and C are positive clockwise if one looks down the axis of rotation toward the origin.

R_{IP} (I) defines the position vector of a point P in the I system.

To determine repeatability of geometry between the August 3rd and August 27th deployments, the measurement data for the two deployments were regressed together. The method used is described herein. First, the August 3rd data was regressed to the ideal coordinates given in Table 4.2.2-1. Through the regression, translations and rotations were determined which minimize the error between the measured and ideal coordinates. The translations and rotations were then applied to the August 3rd measurements to convert the coordinates from the theodolite reference to the antenna reference system.

AXIS SYSTEM

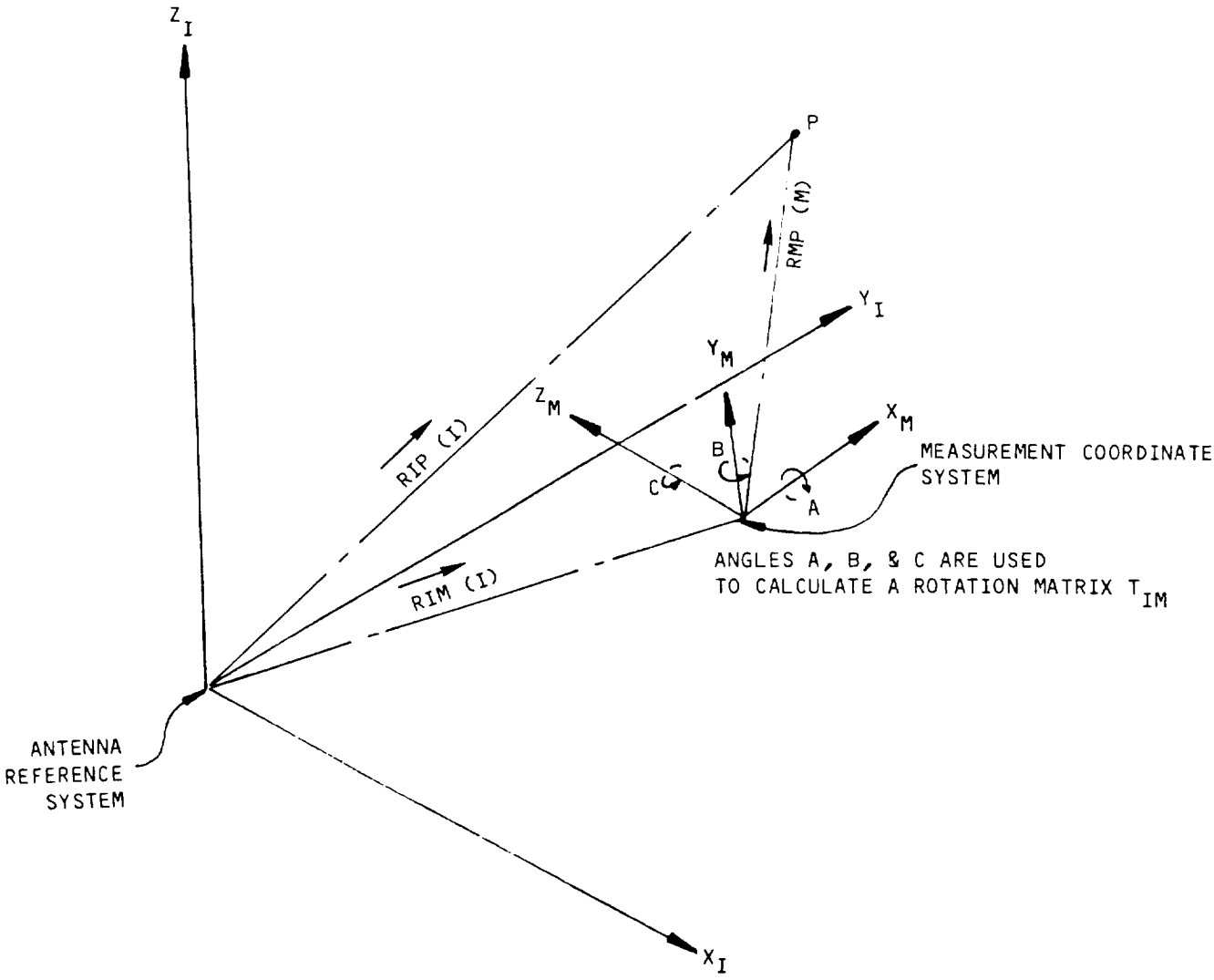

Figure A2-1.

X_I, Y_I, Z_I represent the ideal coordinate system or the antenna reference system.

X_M, Y_M, Z_M represent the measurement coordinate system.

Next, the August 27th data was regressed to the ideal coordinates and a transformation was determined. This transformation was then applied to convert the August 27th data into the antenna reference.

With both data sets converted to the antenna reference system, the August 27th data was regressed to the August 3rd data to determine a transformation which when applied would minimize the error between the data sets. The August 27th data was transformed accordingly and X, Y and Z errors were determined between the two data slots.

Several regressions as described in the preceding paragraph were performed using different targets as a reference. Using the hoop targets as a referee appeared to work best, so only the 24 hoop targets were considered in the regression. The 12 remaining mast targets were simply transformed along with the hoop targets for the error calculation. The regression errors are listed in Table 4.2.2.3-3.

APPENDIX A3
MESH SEWING PROCEDURE

PROCEDURE FOR SEWING MESH TO FRONT CORDS

1. Verify correct front cord assembly is on templates. Verify all targets are correctly placed in template counter bores. Verify mesh has been correctly tensioned over front cord assembly. Gloves to be used during all operations on mesh.
2. Check to insure that all front cord fittings are anchored via dowel pins and that all cords are laying in a straight path between fitting nodal points. Install toothpicks along outside of edge cord.
3. Using 1.0" wide Green tape, tape mesh down to table along outside of Gore. Tape should be approximately 18 inches away from outside perimeter. Roll tape on using soft tennis ball. Watch that mesh does not move. Trim excess mesh outside of tape.
4. Spot tie around perimeter ONLY of front cord assembly.
   (Note: AD-20 either before or after stitching.)
   Spot tie material: EC-12 Beta Glass
   Spot tie knot: Slightly Taut Double Double Surgeon's Knot
   Spot tie Adhesive: Mix thoroughly

CONASTIC AD-20 Part A	10.0 grams
CONASTIC AD-20 Part B	1.8 grams
DS-1831 Red Dispersion	.2 grams

   Note: No Cab-O-Sil

   Working time for AD-20 is maximum of 20 minutes. Allow 12 hours minimum cure before next step.

Sample of Spot Tie

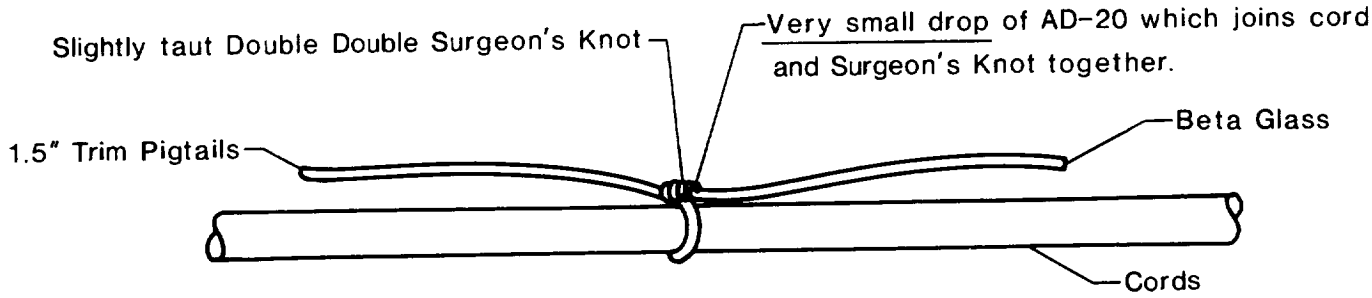

- Spot tie next to all perimeter fittings and gold curl terminals.
- Spot tie every 2.0 inches along inboard and outboard intercostals (1A → 1B and 1L → IN → 1P → IM)
- Spot tie approximately every 6.0 inches along edge cords (1A → 1C → 1F → 1L and 1B → 1D → 1G → 1M) and 1/2" from each edge cord hole.
- Spot ties to be done such that cord follows straight pathes between fitting nodal points.
- Allow 12 hours minimum for AD-20 to cure.

5. First Pass Lacing aroung perimeter of Front Cord Assembly.

   Lacing Material: EC-12 Beta Glass

   Start Knot: Double Double Surgeon's Knot

   Stop Knot: Two half hitches

   Thread overlap Technique:

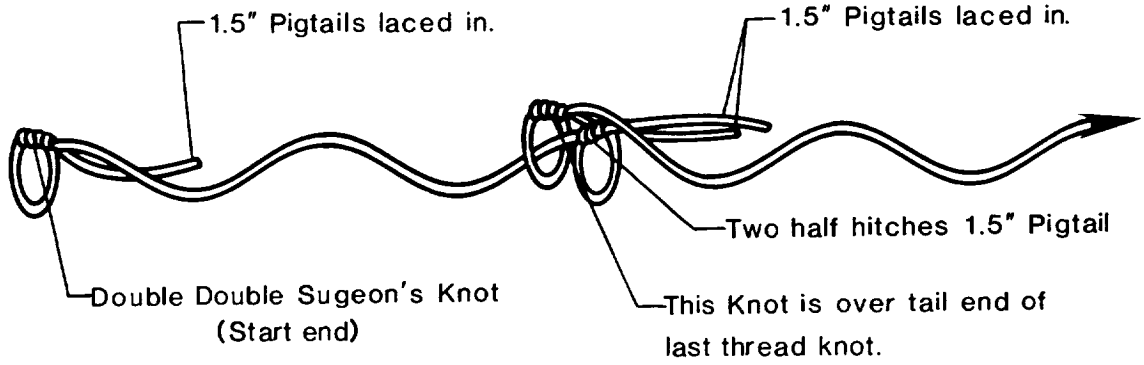

** Lacing Spacing - Every Other Diamond. Approximately .3"

** Lacing Tension - Slightly taut.

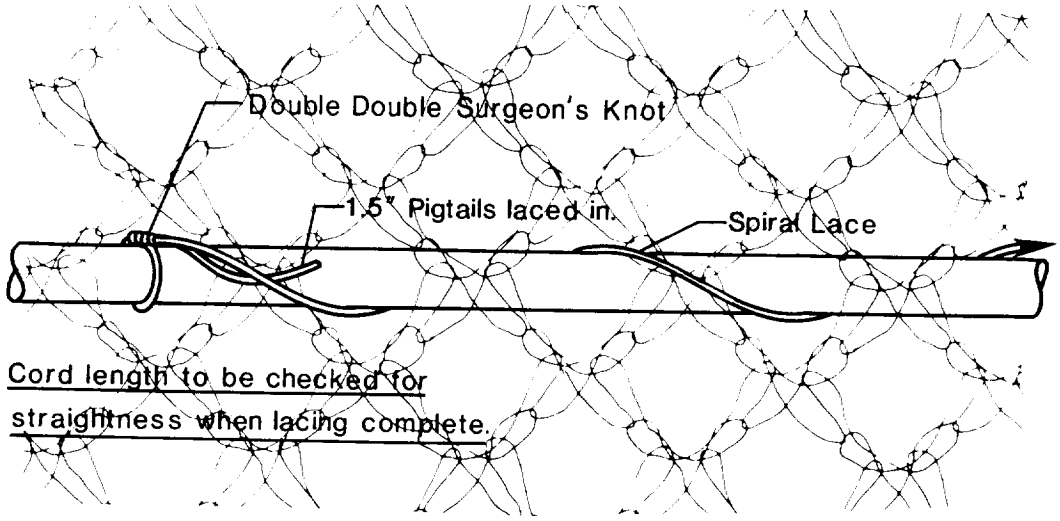

- Lacing is to be done thru diamonds directly over cord. Do not use diamonds one diamond away from cord as this will induce shear into mesh.
- First pass lacing to be done around perimeter defined by 1A → 1B → 1M → 1P → 1N → 1L → 1A.

6. Loose Lacing Interior Cords.

   Lacing Material: EC-12 Beta Glass

   Start Knot: Double Double Surgeon's Knot.

   Stop Knot: Two 1/2 hitches

   Knot over .045 Dia. rod.

Thread Overlap Technique:

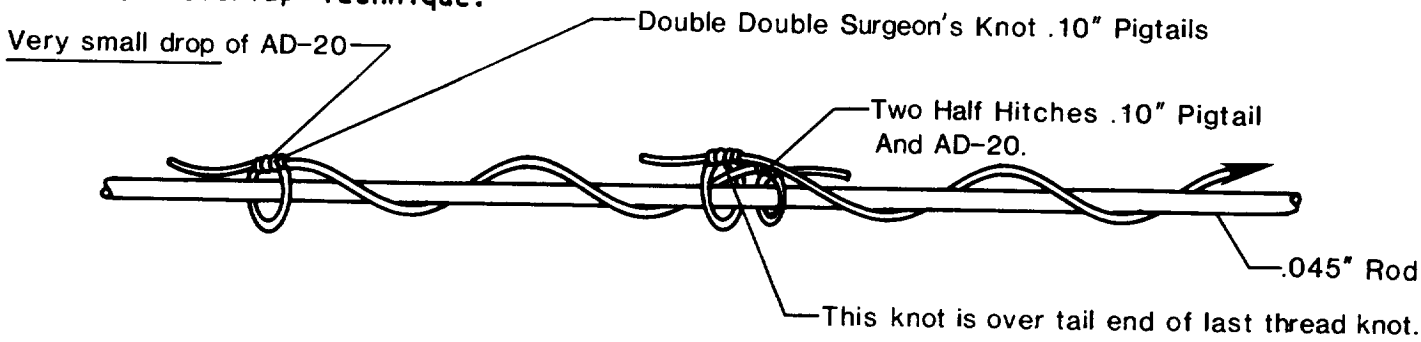

** Lacing Spacing - Two open diamonds along lacing path.

** Lacing Tension - Loose: use .045 inch Diameter Spacer Rod

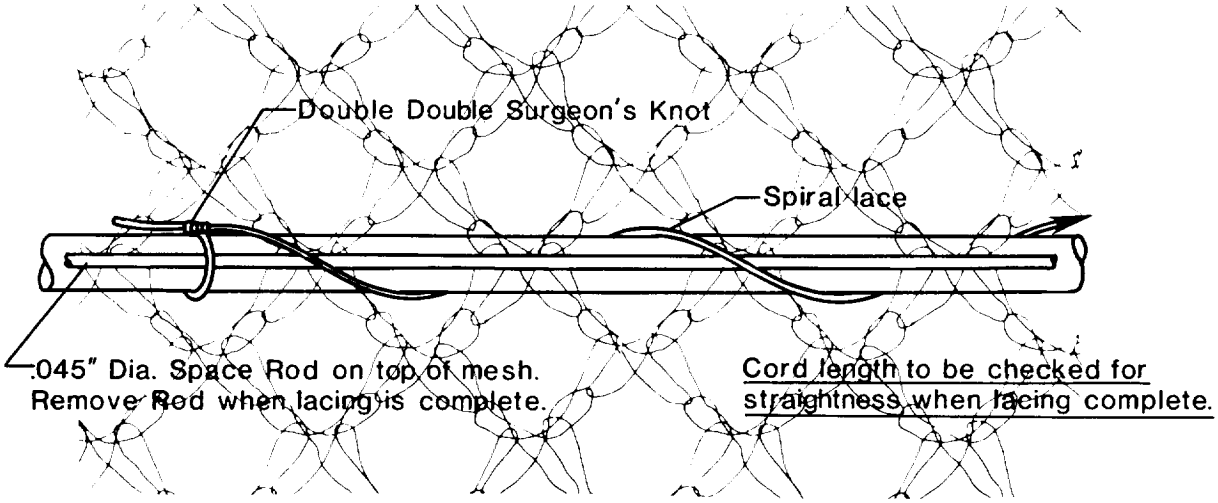

- Lacing is to be done thru diamonds directly over cord.
- Loose lacing to be done on all interior cords and on all surface ties which are in sections E-E, F-F, G-G, H-H, J-J, K-K, & L-L.

7. Install top and bottom targets to mesh. Insure targets are installed concentric.
8. Unpin all except one side. (1A - 1C - 1F - 1L)
9. Cut mesh around perimeter of panel leaving at .25" to .35" outside margin.

10. **Second Pass Lacing** on intercostals **of Front Cord Assembly**
(1A → 1B and 1L → 1N → 1P → 1M)
Curl mesh as shown around perimeter cords:

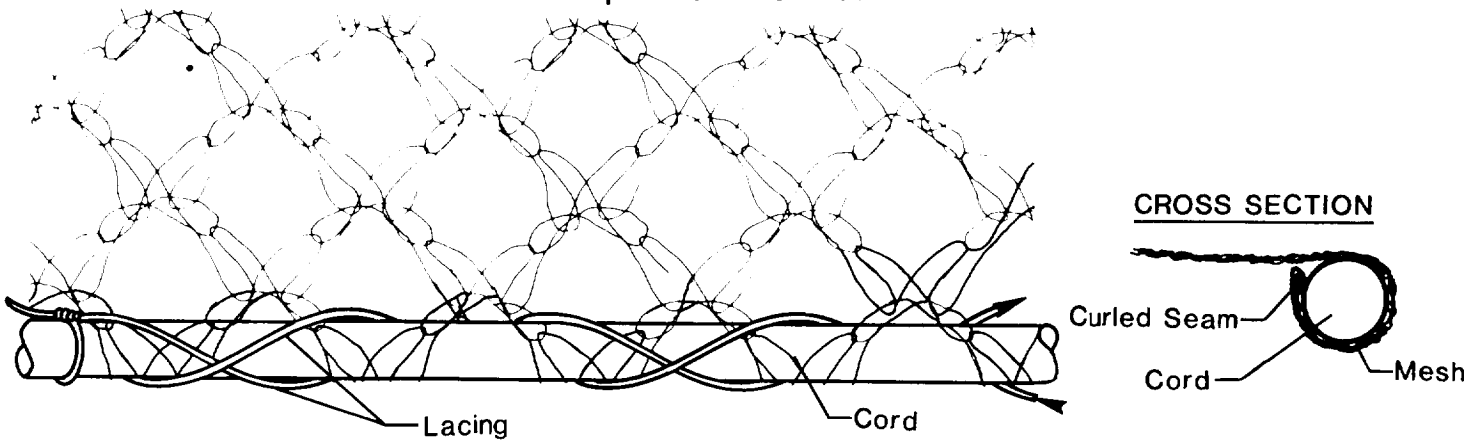

APPENDIX A4
CORD TENSIONS

The following data was gathered by NASA Langley at the Martin RF Near-Field facility in May/June of 1985.* Figures A4-1 and A4-2 describe the locations of the six basic cord families. Figure A4-3 summarizes data taken at different points in time to ascertain load stability as a result of hoop deployments. Figure A4-4 examines mean cord loads with the design specification loads.

*Personal Communications: "Report on Cord Tension Data and Hoop Positioning Repeatability at Martin Marietta Aerospace, Denver CO." Memo from: Elvin Ahl, NASA Langley Research Center, Hampton, VA 23665

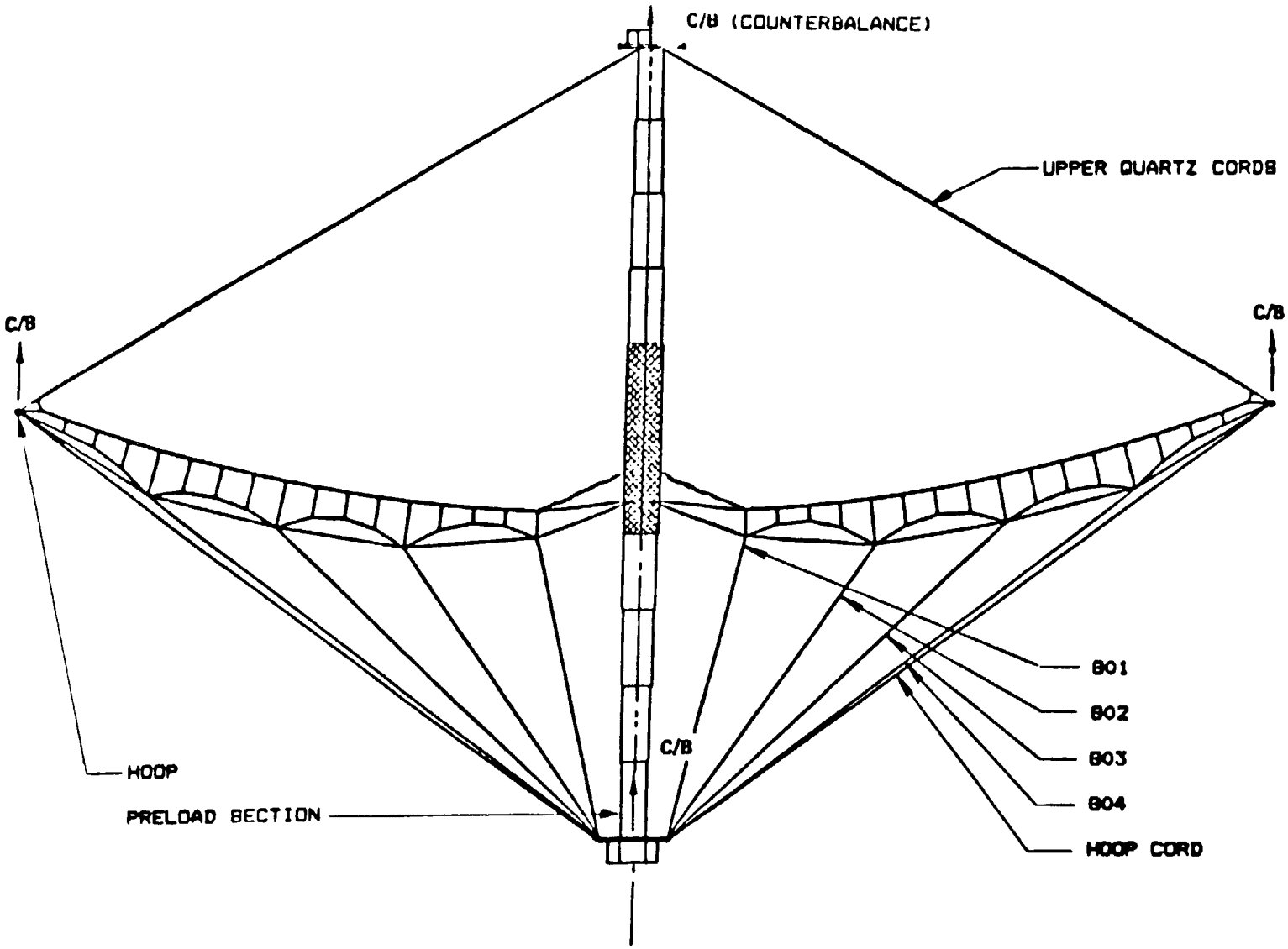

Figure A4-1.

LSST-1016

Lower graphite cords.

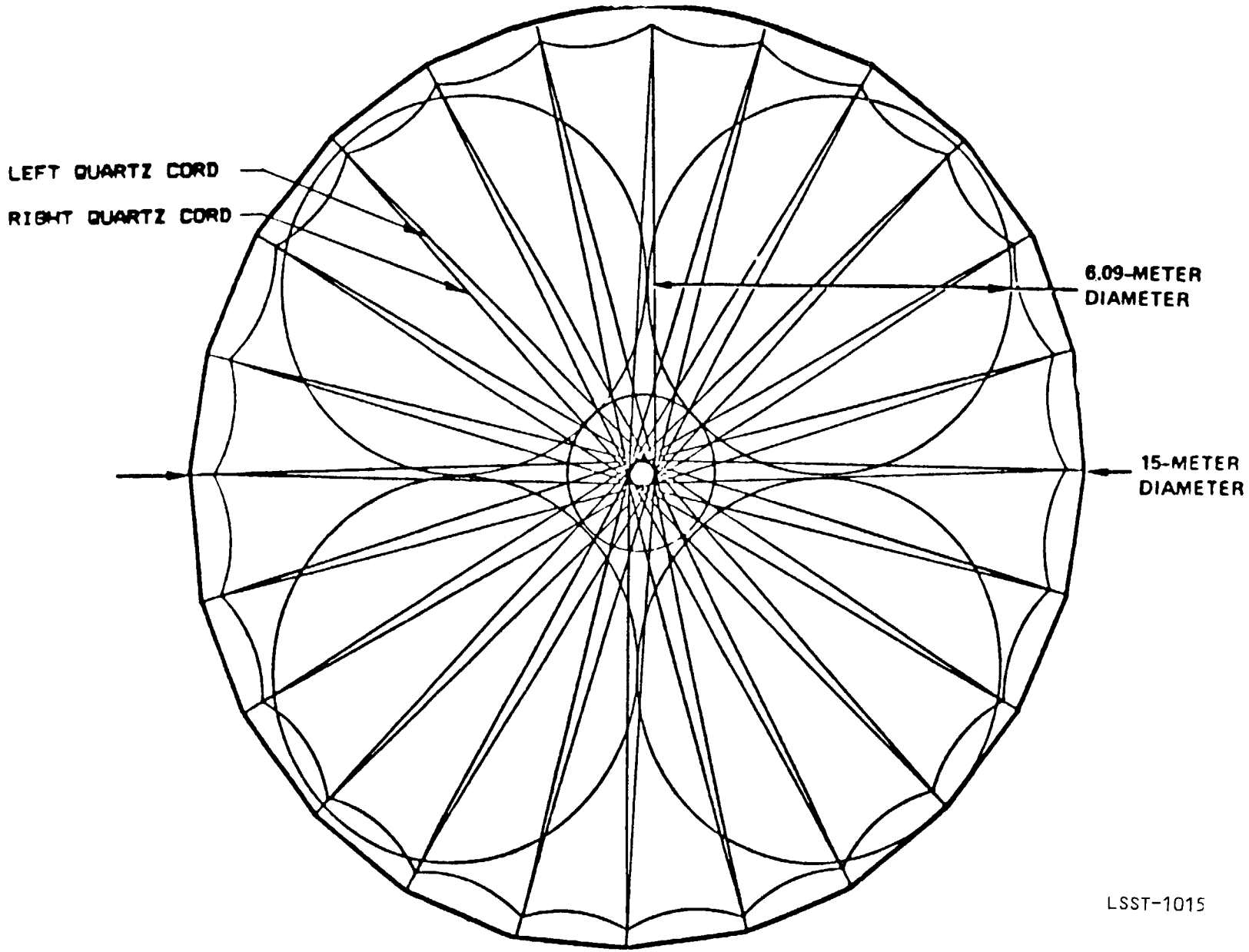

Figure A4-2.

Upper quartz cords.

CORD TENSION DATA

	G01 (LB.)	G02 (LB.)	G03 (LB.)	G04 (LB.)	HOOP CORDS (LB.)	QUARTZ CORDS LEFT (LB.)	QUARTZ CORDS RIGHT (LB.)
DATE 5/14/85 TIME 9:00 AM							
MEAN				11.17	5.87		
STD. DEV.				1.02	1.99		
RANGE				9.75-13.17	1.27-11.09		
DATE 5/14/85 TIME 4:00 PM							
MEAN				11.44	5.83		
STD. DEV.				1.04	1.92		
RANGE				9.89-13.65	1.35-10.81		
DATE 5/14/85 TIME 5:00 PM							
MEAN				11.4	5.85		
STD. DEV.				1.07	1.96		
RANGE				10.4-13.39	1.15-11.24		
DATE 5/14/85 TIME 6:00 PM							
MEAN				11.6	5.92		
STD. DEV.				1.06	1.92		
RANGE				10.1-13.73	1.32-11.04		
DATE 5/15/85							
MEAN				11.3	6.10		
STD. DEV.				1.12	2.43		
RANGE				9.87-13.48	1.1-11.64		
DATE 5/24/85 TIME 8:00AM							
MEAN	1.46	1.37	1.72	9.78	4.47		
STD. DEV.	.11	.15	.16	.67	1.63		
RANGE	1.17-1.71	1.06-1.64	1.37-2.07	7.95-10.77	1.66-8.49		

LSST-1017

Figure A4-3.

CORD TENSION DATA

	G01 (LB.)	G02 (LB.)	G03 (LB.)	G04 (LB.)	HOOP CORDS (LB.)	QUARTZ CORDS LEFT (LB.)	QUARTZ CORDS RIGHT (LB.)
DATE 6/6/85 TIME 9:00 AM							
MEAN	1.45	1.37	1.67	11.28	5.81		
STD. DEV.	.08	.11	.14	.625	2.80		
RANGE	1.29-1.65	1.18-1.54	1.37-1.94	9.79-12.39	0.0-12.22		
DATE 5/15/85							
MEAN						27.5	27.8
STD. DEV.						2.7	2.16
RANGE						22.4-33	23.8-31.1
CORD TENSION SPECIFICATIONS							
MEAN	1.33	1.06	1.15	11.12	13.12	30.15	30.15
STD. DEV.	.042	.089	.118	.79	.32	.34	.34
RANGE	1.28-1.37	.94-1.15	.99-1.25	10.1-11.8	12.9-13.6	29.8-30.6	29.8-30.6

LSST-1014

Figure A4-4.

Standard Bibliographic Page

1. Report No.	2. Government Accession No.	3. Recipient's Catalog No.
NASA CR-4038		

4. Title and Subtitle	5. Report Date
Development of the 15 Meter Diameter Hoop Column Antenna - A Final Report	December 1986
	6. Performing Organization Code
7. Author(s)	8. Performing Organization Report No.
9. Performing Organization Name and Address Harris Corporation P.O. Box 94000 Melbourne, FL 32902	10. Work Unit No.
	11. Contract or Grant No. NAS1-15763
12. Sponsoring Agency Name and Address National Aeronautics and Space Administration Washington, D.C. 20546	13. Type of Report and Period Covered Contractor Report
	14. Sponsoring Agency Code 506-43-51-04

15. Supplementary Notes

Technical Monitor - Lyle C. Schroeder NASA Langley Research Center
Hampton, VA 23665-5225

16. Abstract

This report describes the building of a deployable 15-meter engineering model of the 100 meter antenna based on the point-design of an earlier task of this contract, complete with an RF-capable surface. The 15 meter diameter was selected so that the model could be tested in existing manufacturing, near-field RF, thermal vacuum, and structural dynamics facilities. The antenna was designed with four offset paraboloidal reflector surfaces with a focal length of 366.85 in and a primary surface accuracy goal of .069 in rms. Surface adjustment capability was provided by manually resetting the length of 96 surface control cords which emanated from the lower column extermity. This report gives a detailed description of the 15-meter Hoop/Column Antenna, major subassemblies, and a history of its fabrication, assembly, deployment testing, and verification measurements. The deviation for one aperture surface (except the outboard extremity) was measured after adjustments in follow-on tests at the Martin Marietta Near-field Facility to be .061 in; thus the primary surface goal was achieved.

17. Key Words (Suggested by Authors(s))	18. Distribution Statement
Large Space Deployable Antenna Cable Stiffened Hoop/Column Quad Aperture, Offset Feeds Mesh Antenna Reflector	Unclassified - Unlimited Subject Category: 15

19. Security Classif.(of this report)	20. Security Classif.(of this page)	21. No. of Pages	22. Price
Unclassified	Unclassified	162	A08

For sale by the National Technical Information Service, Springfield, Virginia 22161